UC Riverside

UC Riverside Electronic Theses and Dissertations

Title

Development of FRET-based Technologies for Dynamic and Quantitative Measurement of Protein-protein Interactions and High-throughput Screening of Small Chemical Inhibitors of the SUMO Pathway

Permalink

https://escholarship.org/uc/item/4t69w279

Author

Song, Yang

Publication Date

2011

Peer reviewed|Thesis/dissertation

eScholarship.org Powered by the California Digital Library
University of California

UNIVERSITY OF CALIFORNIA
RIVERSIDE

Development of FRET-based Technologies for Dynamic and Quantitative Measurement of Protein-protein Interactions and High-throughput Screening of Small Chemical Inhibitors of the SUMO Pathway

A Dissertation submitted in partial satisfaction
of the requirements for the degree of

Doctor of Philosophy

in

Bioengineering

by

Yang Song

August 2011

Dissertation Committee:
Dr. Jiayu Liao, Chair
Dr. Victor G.J. Rodgers
Dr. B. Hyle Park

Copyright by
Yang Song
2011

The Dissertation of Yang Song is approved:

_____

_____

_____

Committee Chairperson

University of California, Riverside

Acknowledgements

I would like to thank Dr. Jiayu Liao for his great support in my PhD training, and Dr. Jerome Schultz, Dr. Victor Rodgers and Dr. Hyle Park for their helpful advice. Dr. Xuemei Chen, Dr. David Carter and Dr. Glenn Hicks offered a lot of help on HPLC and screening instrumentation. I also thank all the members in Liao's group for their collaborative work and helpful discussion. The work is supported by funding from University of California, Riverside and National Institute of Health.

The text of this dissertation, in part, is a reprint of the material as is appeared in *Ann Biomed Eng*. 2011 Apr; 39(4):1224-34. Listed in that publication, Dr. Jiayu Liao supervised the research which forms the basis for this dissertation, and Vipul Madahar provided technical help during the research.

Dedication

I would like to dedicate this dissertation to my wife and parents for their constant support and encouragement throughout my PhD study.

Abstract of the Dissertation

Development of FRET-based Technologies for Dynamic and Quantitative Measurement of Protein-protein Interactions and High-throughput Screening of Small Chemical Inhibitors of the SUMO Pathway

by

Yang Song

Doctor of Philosophy, Graduate Program in Bioengineering
University of California, Riverside, August 2011
Dr. Jiayu Liao, Chairperson

SUMOylation is an important post-translational protein modification mechanism which plays important roles in a variety of biological processes. Conjugation and deconjugation of SUMO is a cascade event requiring multiple protein-protein interactions between SUMO, SUMO E1-E3 enzymes and SUMO substrates. The nature of the SUMOylation network indicates a great potential for small chemical inhibitors to be used in the investigation and manipulation of this important pathway. FRET is an energy transfer phenomenon which occurs between two spectrum-overlapping fluorophores in close proximity. The efficiency of FRET is highly dependent on the distance between the donor and acceptor fluorophores, which makes FRET very powerful in the detection of molecular interactions. The goal of my research is to develop FRET-based techniques to study protein-protein interactions in the SUMOylation network and to identify bioactive chemical compounds which can inhibit the activity of this pathway. Using engineered fluorescent proteins to modify protein components involved in the SUMOylation

pathway, I set up a FRET-based assay and developed mathematical algorithms to determine the binding affinity of non-covalent protein-protein interactions. I then developed this FRET-based assay into high-throughput screening platforms to look for small chemical inhibitors which can disrupt the interaction of SUMO1 and its E2 enzyme, Ubc9. I further used FRET-based strategy to set up a whole-pathway screening assay to identify SUMOylation/deSUMOylation inhibitors. Over 200,000 compounds were screened and the positive hits were characterized for their activities *in vitro* and in cells. Finally, I was able to use FRET to detect the formation of intermediate protein complex during SUMOylation reactions, and used the assay to map the targets of the SUMOylation inhibitors identified from the high-throughput screening. These FRET-based applications provide powerful tools for the study of the SUMOylation pathway and can be used in the investigation of protein-protein interactions in other biological pathways.

Table of contents

List of Figures

List of Tables

List of Abbreviations

SUMO: small ubiquitin-like modifier

FRET: Förster resonance energy transfer

SMT3: Suppressor of Mif Two 3

SENP: Sentrin/SUMO-specific protease

PIAS: protein inhibitor of activated STAT

STAT: signal transducers and activators of transcription

SPR: surface plasmon resonance

ITC: isothermal titration calorimetry

CFP/YFP: cyan/yellow fluorescent protein

SD: standard deviation

IC_{50}: half maximal inhibitory concentration

INTRODUCTION

SUMO: Machinery of post-translational modification

Post-translational modifications are general mechanisms to alter the localization and function of proteins after they are translated from messenger RNAs in the cells. While post-translational modification can be either reversible or irreversible, enzymatic catalysis is required for efficient modification in most cases. Examples of protein modifiers are small chemical moieties such as phosphate, acetyl or methyl groups, which play key roles in many cellular events including signaling transduction, protein turnover, DNA repair and transcriptional regulation (1-4). Besides those small chemical moieties, small peptides can also function as protein modifiers. One well known example is ubiquitin, a 76-residue peptide which can be covalently linked to many proteins and results in proteasome-mediated degradation (5). SUMO, known as Small Ubiquitin-related MOdifier, has emerged as an important protein modifier in recent years. SUMO is expressed in all eukaryotes but is absent from bacterium (6). In human beings, SUMO represents a family of four closely related small proteins with sizes around 100 amino acids. Human SUMO1 was first discovered in 1996 by homology studies of yeast SMT3 (Suppressor of Mif Two 3) protein and shown to share sequence homology with human ubiquitin protein (7, 8). SUMO1 is conjugated to the Ran-GTPase-activating protein RanGAP1 in a reversible manner, which results in its translocation from the cytoplasm to nuclear pore complex (9, 10). SUMO2 and SUMO3 were identified shortly after the discovery of SUMO1 (11, 12), and SUMO4 was not cloned until 2004 (13). So far more than 1000 proteins have been identified as the targets of SUMO, and SUMO modification has been implicated to play important roles in the regulation of many biological processes, including transcription, intracellular transport, DNA repair and chromosome maintenance (14).

The mechanism of SUMOylation and deSUMOylation

Protein modification by SUMO is a highly dynamic and reversible process. Generally the term SUMOylation is used to describe the conjugation of SUMO to its targets, and deSUMOylation refers to the deconjugation of SUMO from target proteins. The whole SUMOylation/ deSUMOylation cascade is briefly summarized in Figure 1. Pre-SUMO is translated from messenger RNA as a precursor protein. Pre-SUMO is then recognized by SUMO-specific proteases (SENPs) and its C-terminal residues were cleaved to generate mature SUMO with a C-terminal Gly-Gly motif (6, 15). The Aos1 subunit of the E1 activating enzyme, which is a heterodimer of Aos1 and Uba2 proteins, functions as an adenylating enzyme and activates SUMO using the energy from ATP hydrolysis. The SUMO-E1 complex then undergoes a conformational change and transfers adenylated SUMO from the binding pocket of Aos1 to the cysteine active site of Uba2, where the carboxyl group of the C-terminal glycine of SUMO forms a thioester bond with the cysteine residue of Uba2 (16). In the next step, the E2 conjugating enzyme Ubc9 non-covalently binds to SUMO-E1 complex and SUMO is transferred from E1 to the cysteine active site of Ubc9. Catalyzed by SUMO E3 ligases, SUMO is finally transferred from Ubc9 to the lysine residue of target proteins. SUMOylated proteins may then be recognized by SENPs and free SUMO is cleaved off and used for the modification of other proteins (17).

SUMOylation is a multi-step reaction and involves many enzymes with different specificities (Table 1). While only one isoform of E1 and E2 exist in human beings, a number of E3 ligases have been identified. There are three major families of E3 ligases: the PIAS (protein inhibitor of activated STAT) family (18), the polycomb group protein Pc2 (19) and the nuclear pore complex protein RanBP2 (10). These E3 ligases function as a scaffold to recruit substrates to SUMO-E2 complex and facilitate SUMOylation (20). E3 ligases also control the specificity of SUMO conjugation to different target proteins (6, 14). In term of the deSUMOylation process, six SENPs

have been identified: SENP1-3 and SENP5-7 (17). These SENP enzymes catalyze the processing of pre-SUMO proteins as well as the deconjugation of SUMO from target proteins with different specificities, and they also have strong preference for different SUMO isoforms (21).

SUMO	E1	E2	E3	SENP	Substrates
SUMO1 SUMO2 SUMO3 SUMO4	Aos1-Uba2	Ubc9	PIAS1 PIAS3 PIASx PIASy RanBP2 Pc2	SENP1 SENP2 SENP3 SENP5 SENP6 SENP7	STAT1, p53, Mdm2, IκBα, GLUT1, GLUT4, Histones, RanGAP, CtBP, etc.

Table 1. Summary of human proteins involved in the SUMO pathway. Some E3 ligases and substrates are listed as examples.

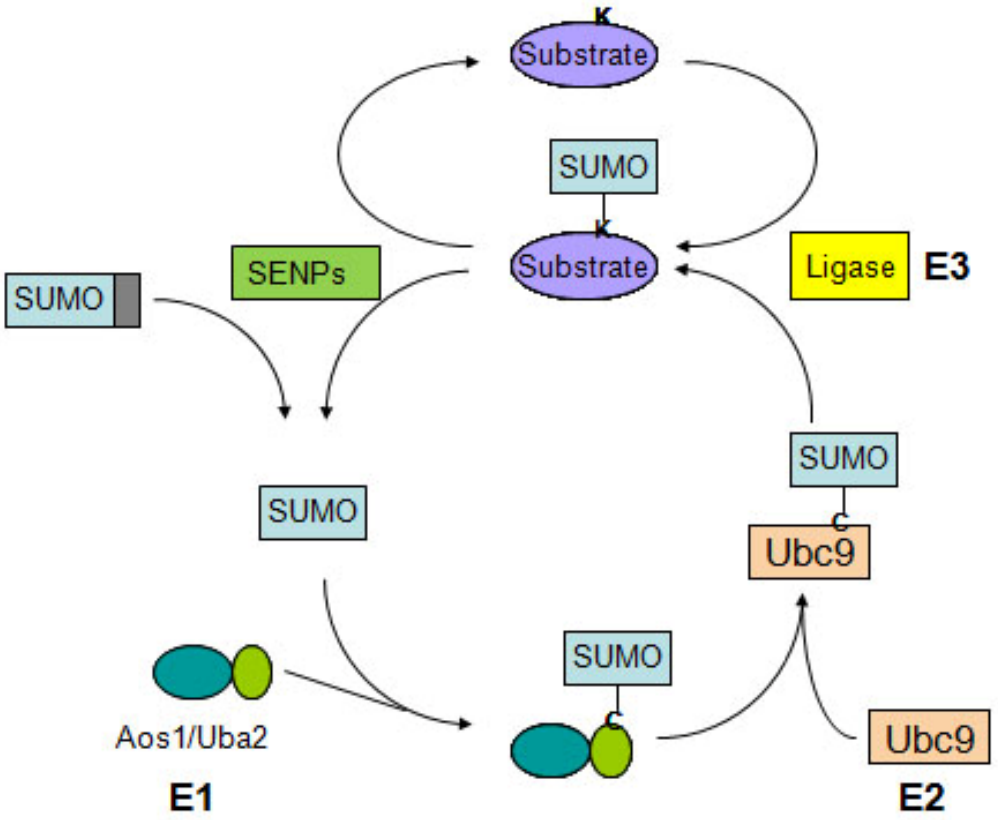

Figure 1. The SUMO cycle. Precursor SUMO is processed by SENPs and activated by E1 heterodimer (Aos1/Uba2). Activated SUMO forms a thioester bond with a cysteine residue of Uba2. After being transferred to the cysteine residue of E2 (Ubc9), SUMO is conjugated to the lysine residue of substrate proteins with the help of E3 ligases. SUMO can then be cleaved from the substrate with the action of SENPs.

Function of SUMO and roles in various diseases

While the 3-dimensional structures of SUMO and ubiquitin are highly similar, the functional consequences of SUMO conjugation are quite different from those from Ubiquitin (15). The effect of SUMO modification is highly target-specific. SUMOylation has been implicated to repress the activity of many transcription factors, including p53, STAT-1, Elk-1 and the androgen receptor (22-25). In these examples, mutation which prevents SUMO conjugation results in increased transcription from responsive promoters, which is consistent with the negative role of SUMO in gene expression (26). SUMOylation can also create new binding interface to facilitate protein-protein interactions. A well-characterized example is the PML nuclear body, whose assembly requires SUMOylation of many subunits (27). Modification of SUMO can control the subcellular localization of target proteins. RanGAP1 is the first identified SUMO target, and its SUMOylation cycle mediates the constant shuttling between the cytoplasm and nuclear membrane (9). Finally, in contrast to ubiquitin whose conjugation results in proteasome-mediated degradation, SUMO can also compete with ubiquitin for the same lysine residue and prevents the target protein from degradation. One example is IκB, a regulatory protein in the NFκB pathway whose SUMOylation results in resistance to signal-induced degradation and persistent inhibition of its downstream signaling (28).

Given the large number of SUMO targets and its importance in the regulation of many physiological processes, it is not surprising that misregulation of the SUMO pathway is involved in many diseases (Figure 2). The relationship between SUMO and cancer has been implicated in many cases (29). Increased level of Ubc9, the SUMO E2 enzyme, has been found in several types of human cancer, and overexpression of Ubc9 can also promote the growth of cancer cells (30, 31). Upregulation of other SUMO enzymes such as SENP1 and the E3 ligase PIAS3 has also been observed in certain cancers (32, 33). Besides cancer, the roles of SUMO in neuronal

disorders have also been extensively studied. Many key proteins involved in Huntington's, Alzheimer's and Parkinson's diseases can be modified by SUMO, such as Huntington, Tau and Amyloid-β (34-36). Interestingly, SUMOylation of these proteins seems to have diverse effects on the fate of neuronal cells. Expression of SUMO rescues neuronal cells from degeneration in case of Amyloid-β in Alzheimer's disease (36), whereas it enhances cell death in Huntington's disease (34). Other than cancer and neurodegenerative diseases, mutants which are unable to be SUMOylated have been associated with heart disease and diabetes (37, 38). While these results showed that SUMO may serve as a potential target for therapeutic applications, the detailed mechanism of how misregulation of the SUMO pathway leads to pathogenesis still requires further investigation.

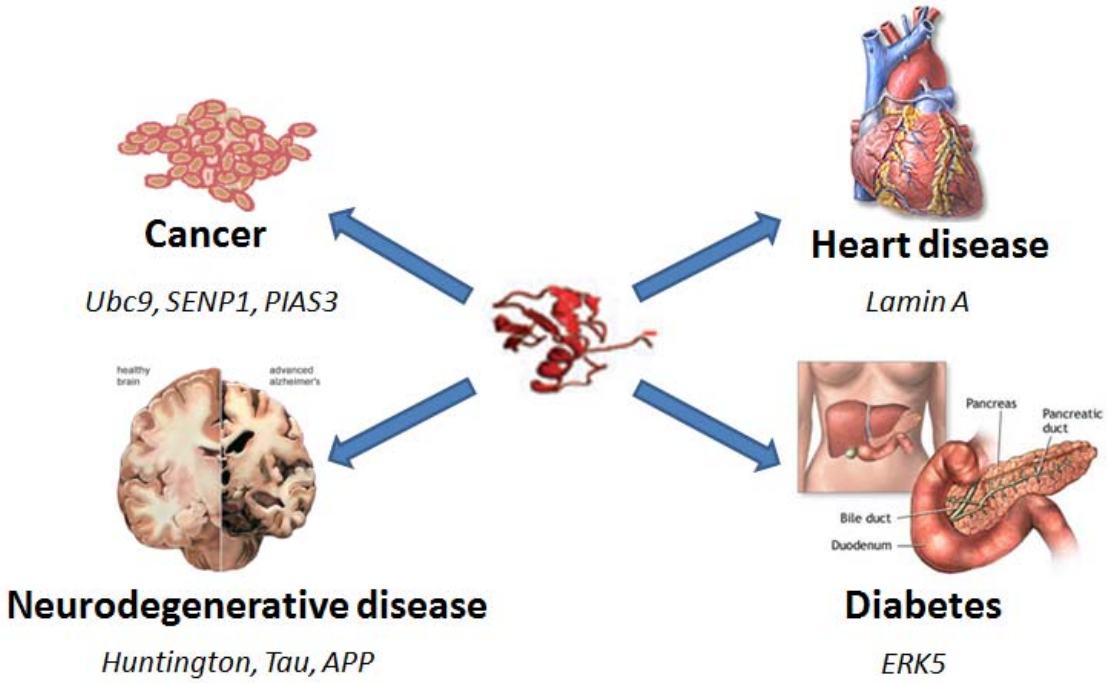

Figure 2. Misregulation of the SUMO pathway has been associated with many diseases including cancer, heart diseases, diabetes and neurodegenerative diseases. Listed are some of SUMO-related proteins whose mutation or overexpression has a positive relationship with pathogenesis.

Small chemical compounds can serve as useful tools to control SUMO pathway

SUMO plays an important role in many biological processes including regulation of immune signal transduction, stabilization of target proteins and maintenance of chromosomal integrity, yet investigation of the SUMO pathway has many challenges. Conjugation and deconjugation of SUMO is a highly dynamic process and SUMO can be quickly removed upon cell lysis unless cells are lysed in denaturing conditions or in the presence of SENP inhibitors (6). Furthermore, given the important roles they play, knockout of genes involved in SUMOylation can have serious effects and may even kill the transgenic animals, which makes genetic studies quite difficult. Depletion of SUMO1 or the E2 enzyme in mice is embryonically lethal (39, 40). Mice embryos that are deficient of the E3 ligase PIAS1 also exhibit a lower survival rate than wide type embryos (41). To overcome these difficulties, new tools besides the traditional biochemical and genetic approaches are needed to study the SUMO pathway.

Among a variety of techniques for biological research, small chemical compounds stand as unique tools to control the activity of biological processes. Compared with other biological approaches, bioactive small chemical compounds not only offer better spatial and temporal control of biological processes but can also be used to investigate the biological function of proteins when gene knockout is not feasible. In recent years many researchers have started to search for small chemical compounds which can control the activity of the SUMO pathway. Two small chemical SUMOylation inhibitors, ginkgolic acid and kerriamycin B, have been identified in 2009 from natural products using a low-throughput microscope-based method (42, 43). These two compounds can inhibit SUMOylation *in vitro* and in cell cultures in micromolar range, yet they have other side effects such as antibacterial activities and inhibition of histone acetylation. In order to find compounds targeting the SUMO pathway with higher potency and specificity, there

is an urgent need in the development of high-throughput screening assays to test compounds from synthetic libraries, which contain a much larger number of compounds than natural products.

Förster Resonance Energy Transfer (FRET): principles and applications

One of the primary goals of my research is to set up high-throughput screening assay to look for small chemical inhibitors of the SUMO pathway. To achieve this goal, I would like to develop methods to detect the non-covalent and covalent interactions between proteins involved in SUMOylation in a real-time manner, and FRET is selected as the major technology to set up these methods. Originally predicted by German scientist Theodor Förster, FRET is a physical phenomenon in which dipole-dipole resonance interaction results in energy transfer between excited donor and acceptor chromophores (44). The interaction occurs between oscillating dipoles with similar resonance frequencies, and is dependent on the spectroscopic and geometric properties of the donor-acceptor pair. In the theory proposed by Förster, the rate constant (k_T) of energy transfer is given by:

$$k_T = r^{-6}\kappa^2 J n^{-4} k_F \times 8.71 \times 10^{23}\,\mathrm{sec}^{-1},$$

and the efficiency (E) of energy transfer can be represented by:

$$E = \frac{R_0^6}{R_0^6 + r^6}.$$

The variables used in the expressions are: r, the distance between the center of donor and acceptor chromophores; κ^2, the orientation factor of the dipole-dipole interaction; J, the overlap integral of donor emission spectrum and acceptor excitation spectrum; n, the refractive index of the medium between donor and acceptor chromophores; k_F, the rate constant of fluorescent emission from the donor chromophore; R_0, the distance between donor and acceptor chromophores when the efficiency of energy transfer is 50%. The theory of FRET has been validated by many subsequent studies, and the effects of different parameters to the efficiency of FRET have been carefully examined (45-47).

The theory of FRET has been validated by many subsequent studies, and the effects of different parameters to the efficiency of FRET have been carefully examined. Stryer and Haugland (46) synthesized poly-L-proline containing up to 12 residues as the linker to separate a pair of fluorophores, and correlated the observed efficiencies of energy transfer with the reverse sixth power of the donor-acceptor distances. An r^{-6} dependence was also confirmed by Bücher et al. (45) using fatty acid layers with known dimensions to separate donor and acceptor chromophores. The dependence of FRET efficiency on the spectrum overlap integral (J) was later verified by the work of Haugland et al. (47), in which J was varied over 40-fold by changing the solvent and shown to have a linear relationship to the energy transfer rate constant. Orientation factor (κ^2) is dependent on the relative orientation of the donor and acceptor dipoles, and is given by:

$$\kappa^2 = (\cos\alpha - 3\cos\beta\cos\gamma)^2 \ ,$$

in which α is the angle between the donor and acceptor transition moments, β is the angle between the donor moment and the line joining the centers of the donor and acceptor, and γ is the angle between the acceptor moment and the line joining the centers of the donor and acceptor. Compared with molecular distance (r) and spectrum overlap integral (J), the value of κ^2 is often hard to be obtained experimentally due to the uncertainty of molecular motions. Stryer (48) analyzed the probability distribution of donor-acceptor relative angles and showed that while the theoretical value of κ^2 can vary from 0 to 4, its range is narrower in practice and will introduce no more than 20% variation to the determination of donor-acceptor distance. In most FRET studies the value of κ^2 is assumed to be 2/3, which corresponds to the ideal case that both donor and acceptor chromophores undergo unrestrictive motion (48, 49).

The inverse sixth power relationship between energy transfer rate and donor-acceptor distance makes FRET very sensitive to changes in molecular distance. When the distance of the donor and acceptor narrows from R_0 to $0.5R_0$, the efficiency of FRET increases from 50% to near maximum.

On the other hand, when the donor-acceptor distance increases by 100% of R_0, FRET efficiency decreases to an almost undetectable level of 1.5%. This high sensitivity serves as the basis of two types of FRET-based applications. First, FRET can be used as a spectroscopic ruler to precisely measure molecular distance when the donor and acceptor distance is not far from their R_0; second, when the exact molecular distance is not concerned, the "on" and "off" status of FRET can be monitored to determine the status of molecular interaction. FRET has been widely used in many biological applications including study of protein folding, monitoring biomolecular interactions and sensory of signaling pathways (50-52). FRET is also extensively used in high-throughput screening. Some examples include a membrane-potential assay for K_{ir} channel inhibitors and an assay for phosphatase inhibitors (53, 54). In the first assay, activation of the potassium ion channel changes the membrane potential, which leads to translocation of two organic fluorophores on the plasma membrane and increased FRET efficiency. Inhibition of the channel can therefore be determined by monitoring the ratio of emission intensities from the FRET donor and acceptor. In the second assay, a pair of fluorophores is tagged to the N- and C-terminus of a peptide. Processing of the peptide by active phophatase leads to cleavage of the peptide and separates the FRET pair apart. Inhibition of the phophatase by compounds can then be detected by persistent FRET signals. In most FRET-based high-throughput screening assays, alteration in molecular interaction or enzymatic activities changes the distance between the FRET pair and results in decreased or increased FRET efficiency, which can detected via various parameters such as individual fluorophore emission, the emission ratio of donor and acceptor, and the lifetime of the donor fluorophore. In this dissertation, I will use FRET to detect the protein-protein interactions in the SUMO pathway and set up high-throughput screening to look for small chemical compounds to control the activity of this pathway. The identified compounds I got from the assay will not only become powerful tools to study the biological function of SUMO, but may

also serve as potential drugs for the treatment of diseases related to misregulation of the SUMO pathway.

CHAPTER 1: Development of FRET-based assay to determine the dissociation constant of protein-protein interactions

Abstract

Dissociation constant (K_d) is an important parameter for quantitative measurement of molecular interactions. As an important protein post-translational modification, SUMOylation is a multi-step enzymatic cascade and involves multiple covalent and non-covalent protein-protein interactions. Understanding the binding affinity between different proteins will greatly contribute to the understanding of this modification machinery. FRET has been widely used in biological studies and is very powerful in the study of protein-protein interactions. In this chapter I will describe the development of a FRET-based assay to determine the K_d of the non-covalent interaction between SUMO1 and Ubc9, and further test of its consistency and accuracy. Consistent results were derived at different experimental conditions, and the K_d values are compatible with those determined with other traditional approaches, such as surface plasmon resonance (SPR) and isothermal titration calorimetry (ITC). These results indicate this FRET-based assay can be useful in general for quantitative measurement of protein-protein interaction disassociation constant.

Introduction

Post-translational modification by ubiquitin (Ub) and ubiquitin-like proteins (Ubls), such as SUMO, is an important mechanism that regulates protein activities and stability in eukaryotes. The conjugation of ubiquitin, SUMO and other Ubls to target substrates shares an evolutionary conserved, but distinct enzyme cascade that involves the sequential actions of E1, E2 and E3 ligases (6). E1s activate Ub/Ubls in two major steps: The adenylation of the Ub/Ubls at its C-terminus using ATP, and a covalent thioester bond formation between catalytic cysteine of E1 and the C-terminus of Ub/Ubls by replacing the adenylate group (16). The activated Ubls will then be transferred to E2 by a transthiolation reaction of E2, resulting in the formation of thioester bond between E2 catalytic cysteine and Ub/Ubls. With helps of a variety of E3s, which are generally considered to determine substrate specificity *in vivo*, Ub/Ubls are finally conjugated to lysine residues of substrates (6). As multiple protein-protein interactions are involved in the sequential protein-transferring reactions, studies of these interactions will gain much insights into the mechanism of the cascades.

Dissociation constant (K_d) is one of the most important parameters to characterize protein-protein interactions (55). K_d is related to binding affinity, and the measurement of K_d is generally conducted by techniques including surface plasma resonance (SPR) (56, 57), isothermal titration calorimetry (ITC) (58, 59), and radioactive ligand binding assay (60). While these techniques serve as the standard methods to measure the K_d of protein-protein interactions, they either require special instrumentation or radioactive labeling of proteins. FRET has been widely used in biological assay *in vitro* and *in vivo* for both static and real-time measurements (50-52). In recent years FRET has been used in the development of quantitative assays to determine the K_d of protein-protein interactions. In a study published in 2008 (61), a FRET donor and acceptor pair (classic ECFP/VenusYFP) was conjugated to SUMO1 and the SUMO E2 enzyme, Ubc9,

respectively. When CFP-SUMO1 and YFP-Ubc9 recombinant proteins were mixed, the interaction of SUMO1 and Ubc9 leads to FRET between ECFP and YFP (Figure 3A). The concentration of CFP-SUMO1 was fixed in the assay and different amount of YFP-Ubc9 was added to the system. The fluorescent spectrum of the mixture of CFP-SUMO1 and YFP-Ubc9 was compared with that from the control pair of CFP and YFP-Ubc9 to derive the FRET emission from YFP-Ubc9 (Figure 3B). The FRET emission intensity was then fitted with YFP-Ubc9 concentration by an exponential equation to get the maximum FRET emission intensity (Figure 3C) and the bound YFP-Ubc9 concentration was calculated from the FRET emission in a linear relationship. The bound and free YFP-Ubc9 concentrations were then fitted with a hyperbolic equation to derive the K_d (Figure 3D). There are several drawbacks associated with this FRET-based K_d measurement assay. The fluorescence intensity at the emission peak wavelength of YFP-Ubc9 is consisted of the FRET emission of YFP-Ubc9 as well as the direct emission of CFP-SUMO1 and YFP-Ubc9. This FRET assay used a pair of control proteins, CFP and YFP-Ubc9, to calculate the direct emission of CFP and YFP. This control not only requires purification of extra proteins but also did not consider the fact that quenching of CFP-SUMO1 by FRET decreases its direct emission. Furthermore, while the FRET emission intensity and total YFP-Ubc9 concentration fit well into the exponential equation, the mathematical background of this equation was not provided. In order to stand as a solid method for K_d measurement, major improvement is needed to solve these issues.

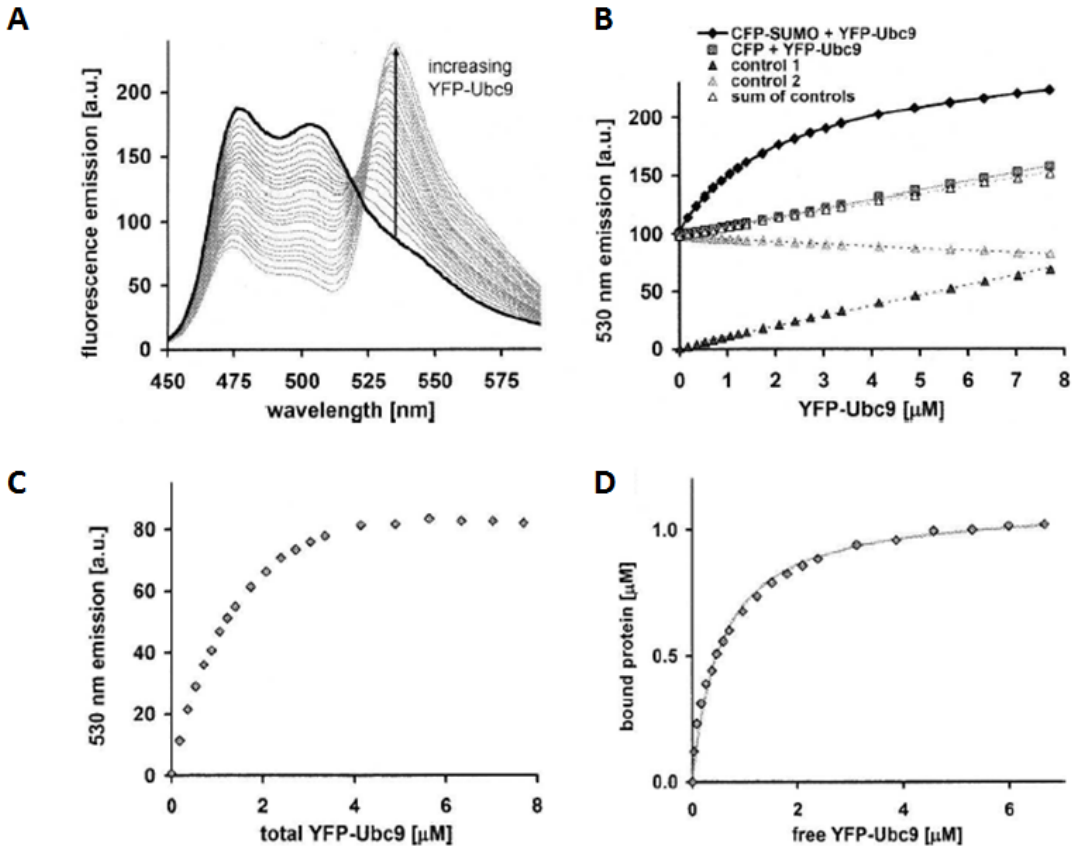

Figure 3. Summary of a previously published FRET-based K_d measurement assay (61). (A) YFP-Ubc9 was titrated into 1.1 μM CFP-SUMO1 in increments up to 8 μM. The fluorescent spectra were collected at the excitation wavelength of 400nm. (B) The fluorescent intensity at 530nm was corrected by that from the control pair CFP and YFP-Ubc9 to get the FRET emission from YFP. (C) The FRET emission at 530nm was plotted vs. total concentration of YFP-Ubc9 by an exponential curve to get the theoretical maximal FRET emission. (D) Concentration of bound YFP-Ubc9 was then calculated and plotted against free YFP-Ubc9 to get the value of K_d.

In this chapter I will describe the development of a FRET-based K_d measurement assay. The proteins used in the assay are SUMO1 and the E2 enzyme, Ubc9. SUMO1 non-covalently binds to Ubc9 in 1:1 ratio. The non-covalent interaction between SUMO and Ubc9 promotes the formation of poly-SUMO chain in SUMOylation reactions and has been well characterized by a variety of methods (61-63). SUMO1 and Ubc9 also have smaller sizes than most of proteins in the SUMO pathway, which makes them easy to express and purify. These characteristics make SUMO1 and Ubc9 good candidates for the development of FRET-based K_d measurement assay. In order to improve the FRET signal, instead of traditional CFP and YFP, CyPet and YPet are conjugated to the N-terminus of SUMO1 and Ubc9, respectively. CyPet and YPet is a pair of fluorescent proteins developed from CFP and YFP in 2005 with optimized FRET efficiency (64). Using CyPet and YPet as the FRET pair could provide substantially improved sensitivity and dynamic range in the detection of protein interactions. The development of this assay will have several significances. First, this will establish a method to detect the non-covalent protein-protein interactions involved in the SUMO pathway. Due to the ease of fluorescence measurement, it would be possible to convert this assay into a high-throughput platform to screen small chemical compounds that can disrupt protein-protein interactions. Second, this assay should be an improvement over previous published FRET-based methods. Instead of using control protein pairs, the FRET emission intensity should be derived directly from the whole spectrum. The relationship between FRET emission and protein concentration should also be carefully examined.

Material and Methods

Molecular cloning of DNA constructs

The open reading frames of CyPet, YPet, SUMO1 and Ubc9 were amplified by PCR using primers containing NheI/SalI sites (CyPet/YPet) or SalI/NotI sites (SUMO1/Ubc9) and the PCR products were cloned into pCRII-TOPO vector (Invitrogen). The fragments encoding SUMO1 and Ubc9 were extracted by SalI/NotI digestion and inserted into pCRII-CyPet or pCRII-YPet plasmids which were linearized by SalI and NotI. After the sequences were confirmed, the cDNA encoding CyPet-SUMO1 and YPet-Ubc9 were cloned into the NheI/NotI sites of pET28(b) vector (Novagen) (Figure 4).

In order to get non-fluorescent tagged SUMO1 and Ubc9 as control proteins, the open reading frames of SUMO1 and Ubc9 were amplified by PCR and cloned into the SalI/NotI sites or pET28(b) vector.

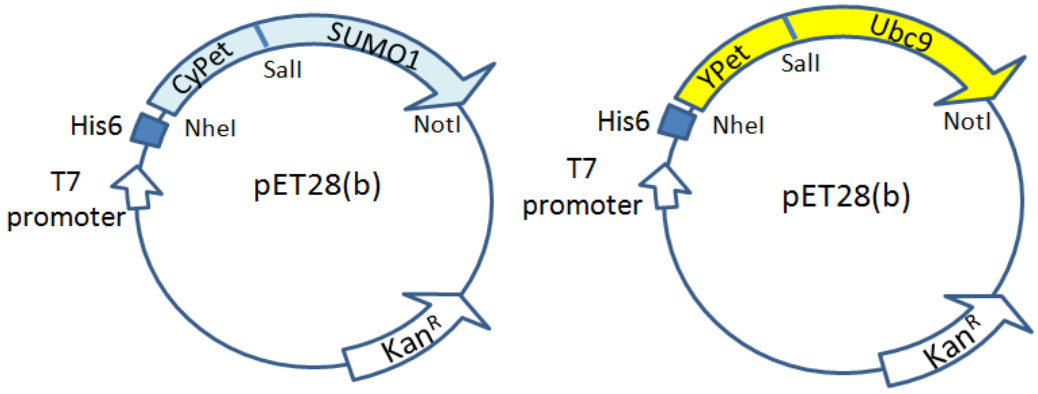

Figure 4. Map of the bacterial expression plasmids encoding CyPet-SUMO1 and YPet-Ubc9. The open reading frames of CyPet-SUMO1 and YPet-Ubc9 were fused with a poly-histidine tag so that the recombinant proteins can be purified with Ni-NTA affinity chromatography. The expression of proteins is driven by T7 promoter and induced by addition of IPTG to the culture medium.

Recombinant protein expression and purification

BL21(*DE3*) *Escherichia coli* (*E. coli*) cells were transformed with pET28 vectors encoding CyPet-SUMO1 or YPet-Ubc9. The transformed bacteria were plated on LB agar plates containing 50 μg/mL kanamycin, and single colony was picked up and inoculated in 2xYT medium. The expression of polyhistidine-tagged recombinant proteins was induced with 0.1 mM IPTG at 25˚C overnight. Bacteria cells were spinned down at 6000 rpm 15 min, resuspended in buffer containing 20 mM Tris-HCl (pH=7.5), 0.5 M NaCl and 5 mM imidazole, and sonicated with an ultrasonic liquid processor (Misonix). Cell lysate containing recombinant proteins was cleared by centrifugation at 25000 g 30 min. The recombinant proteins were then bound to Ni^{2+}-NTA agarose beads (QIAGEN) and eluted by buffer containing 20 mM Tris-HCl (pH=7.5), 0.2 M NaCl and 150 mM imidazole. After the proteins were dialyzed overnight in buffer containing 20 mM Tris-HCl (pH=7.5), 50 mM NaCl and 1 mM DTT, they were concentrated and purified by gel filtration HPLC using Superdex75 10/300 GL column on a HPLC purification system. The purity of the proteins was confirmed by SDS-PAGE and Coomassie blue staining, and their concentrations were determined by Coomassie Plus Protein Assay (Thermo) with known quantities of bovine serum albumin as standards. Aliquots of final products were stored in -80˚C.

FRET measurement

Recombinant CyPet-SUMO1 and YPet-Ubc9 proteins were diluted with buffer containing 20 mM Tris-HCl (pH=7.5) and 50 mM NaCl, and mixed in a 384-well plate to 100 μL in each well. Four groups of mixture were prepared. The final concentrations of CyPet-SUMO1 in these four groups were 0.1 μM, 0.5 μM, 1.0 μM and 1.5 μM, respectively. In each group YPet-Ubc9 was added in increment up to 4 μM. The fluorescence emission spectrum of each well was determined by a fluorescence multi-well plate reader FlexstationII^{384} (Molecular Devices, Sunnyvale, CA). The emission intensities at 475 nm and 530 nm were measured at the excitation wavelength of 414 nm

with a cutoff filter of 455 nm, and the emission intensity at 530 nm was measured at the excitation wavelength of 475 nm with a cutoff filter of 495 nm. The experiments were repeated three times and the average value of fluorescence intensity was calculated for each specific condition.

Surface plasma resonance (SPR) assay

All analyses of interaction between CyPet-SUMO1 and YPet-Ubc9 or SUMO1 and Ubc9 were performed on BIACORE X100 system equipped with NTA sensor chips (BIACORE AB, Uppsala, Sweden) at a flow rate of 30 μL/min. For immobilization of proteins, the chip was treated with 500 μM NiCl2 for 1 min before 10 μg/mL purified CyPet-SUMO1 or 4 μg/mL purified SUMO1 protein was injected for 180 s and stabilized for 60 s. Then 20~150 μg/mL thrombin-digested YPet-Ubc9 or 5~50 μg/mL thrombin-digested Ubc9 protein was injected for 90 or 120 sec and disassociated for 10 min. In order to continuously monitor the non-specific background binding of samples to the NTA surface, YPet-Ubc9 and Ubc9 proteins were injected into a control flow cell without treatment of $NiCl_2$ and CyPet-SUMO1/SUMO1 proteins. All measurements were performed at 25°C in a buffer containing 50mM sodium phosphate (pH=7.4), 150 mM NaCl and 50 μM EDTA. The value of K_d was derived by BIACORE X100 evaluation software ver.1.0 (BIACORE).

Data processing

The fluorescence intensities determined by FlexstationII^{384} were converted by Softmax 5 (Molecular Devices) into text file and processed by Excel. Data fitting was performed by Prism 5 (GraphPad). The results were reported as mean ± SD.

Results

Detection of the non-covalent interaction between SUMO1 and Ubc9 by FRET

Once the recombinant proteins of CyPet-SUMO1 and YPet-Ubc9 were expressed and purified, their fluorescent spectra were determined. The excitation/emission peak wavelengths of CyPet and YPet are 414/475 nm and 515/530 nm, respectively (64). When CyPet-SUMO1 protein is excited at 414 nm, an emission peak at 475 nm is observed (Figure 5A, blue line). When YPet-Ubc9 protein was added, the emission at 475 nm decreased (Figure 5A, green line), and the increase of emission at 530 nm was greater than the emission from YPet-Ubc9 when it was excited alone (Figure 5A, yellow line), which proved the FRET between CyPet-SUMO1 and YPet-Ubc9. I further determined if the disruption of SUMO1-Ubc9 interaction led to decreased FRET. To estimate the relative level of FRET, I calculated the ratio of the emission intensity at 530 nm to 475 nm when the proteins were excited at 414 nm. The emission ratio of the mixture of CyPet-SUMO1 and YPet-Ubc9 proteins decreased upon dilution (Figure 5B) or addition of SUMO1 proteins without fluorescent tag (Figure 5C). Overall, these experiment results confirmed that the non-covalent interaction of SUMO1 and Ubc9 can be detected by FRET and the disruption of interaction results in decreased FRET.

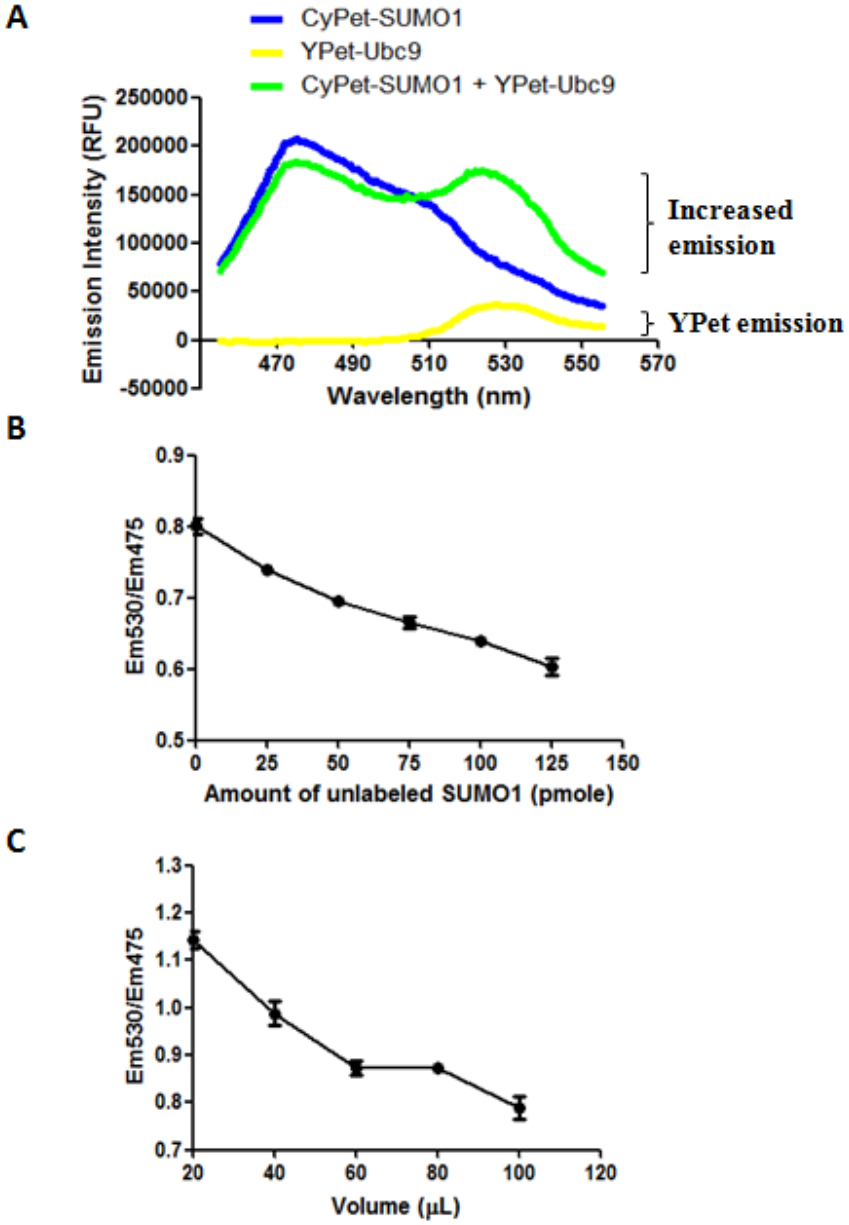

Figure 5. Detection of non-covalent interaction of SUMO1 and Ubc9 by FRET. (A) Protein interaction results in quenching of CyPet-SUMO1 emission and increased emission from YPet-Ubc9. 20 pmole CyPet-SUMO1 and 40 pmole YPet-Ubc9 proteins were mixed in a total of 20 µL. The fluorescence emission spectrum was determined at the excitation wavelength of 414 nm and compared with those of CyPet-SUMO1 or YPet-Ubc9 alone. (B) Disruption of protein interaction by dilution decreases Em_{530}/Em_{475} ratio. 10 pmole CyPet-SUMO1 and 10 pmole YPet-Ubc9 were mixed in different total volumes from 20 µL to 100 µL. Em_{530}/Em_{475} ratio at each condition was determined in triplicate. (C) Competitive inhibition of protein interaction decreases Em_{530}/Em_{475} ratio. 10 pmole CyPet-SUMO1 and 10 pmole YPet-Ubc9 were mixed in a total volume of 20 µL in the presence of 0 to 125 pmole non-labeled SUMO1. Em_{530}/Em_{475} ratio at each condition was determined in triplicate.

FRET assay of CyPet-SUMO1 and YPet-Ubc9

When YPet-Ubc9 protein is added to CyPet-SUMO1 protein, some of the protein molecules will bind to each other and form protein complex. When the mixture is excited at 414 nm, a portion of CyPet-SUMO1 which is bound to YPet-Ubc9 will transfer energy to their binding partners. Raising the concentration of YPet-Ubc9 will increase the concentration of protein complex and result in increased emission from YPet-Ubc9 at 530 nm and decreased emission from CyPet-SUMO1 at 475 nm. In the FRET assay, a series of protein mixtures were prepared with the same total volume and CyPet-SUMO1 concentration. The concentration of YPet-Ubc9 will gradually increase. Figure 6A shows the fluorescent spectra of a series of protein mixtures at the excitation wavelength of 414nm, in which CyPet-SUMO1 concentration was fixed to 1.5 μM. As the concentration of YPet-Ubc9 was gradually increased from 0 to 4 μM, binding of YPet-Ubc9 to CyPet-SUMO1 results in energy transfer from CyPet to YPet and reduces the direct emission from CyPet-SUMO1 from $1.3x10^6$ RFU to $0.76x10^6$ RFU. At the same time the emission at 530nm was increased from $0.45x10^6$ RFU to $2.7x10^6$ RFU. A total of four sets of experiments were carried out, with the concentrations of CyPet-SUMO1 fixed to 0.1 μM, 0.5 μM, 1.0 μM or 1.5 μM, respectively, and the concentration of YPet-Ubc9 increased from 0 to 4 μM. The fluorescence emission spectra of all mixtures were then determined under the excitation wavelengths of 414 nm and 475 nm. As shown in Figure 6B and 6C, increase of YPet-Ubc9 concentration results in decreased emission at 475 nm and increased emission at 530 nm at the excitation wavelength of 414 nm. However, the emission at 530nm is not only consisted of FRET emission from YPet-Ubc9, but also emission from both YPet-Ubc9 and unquenched CyPet-SUMO1 due to direct excitation, as shown in Figure 5A.

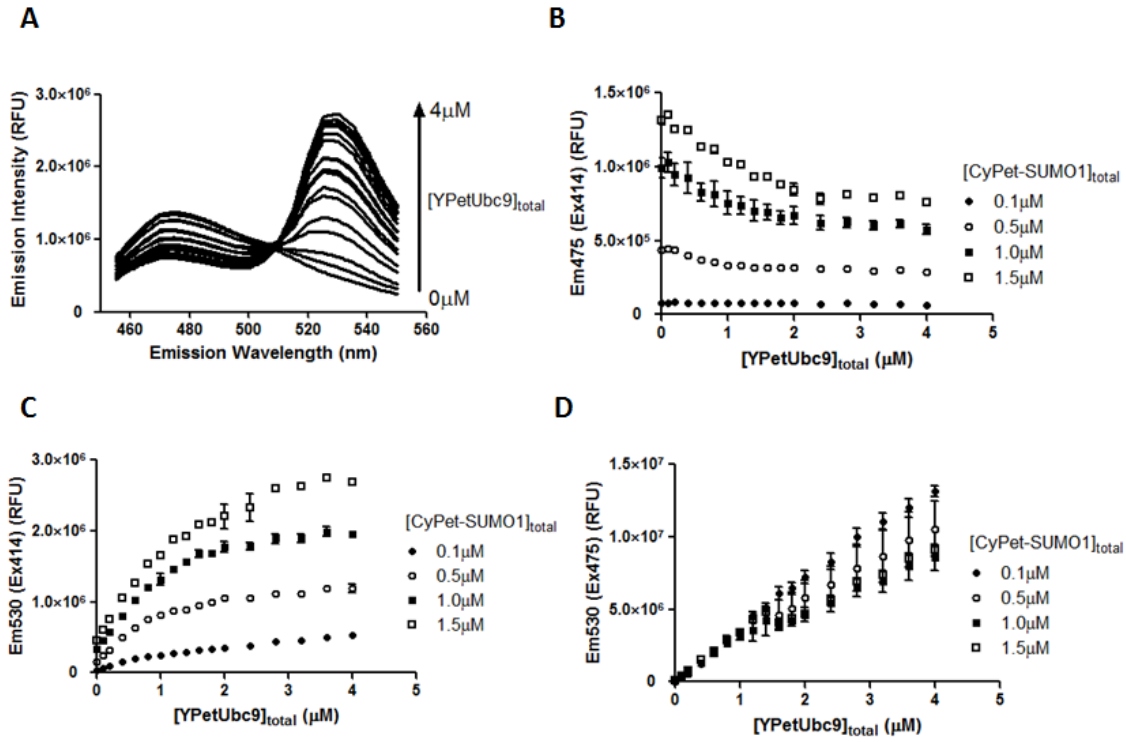

Figure 6. FRET assay to determine the K_d of SUMO1 and Ubc9. (A) An example of fluorescence spectrum under excitation wavelength of 414nm from one set of experiment in Kd measurement; [CyPetSUMO1] =1.5 μM, [YPetUbc9]=0-4 μM; (B) The plot for total emissions of various concentrations of mixed CyPet-SUMO1 and YPet-Ubc9 at 530 nm when excited at 414 nm. (C) The emission plot of CyPet-SUMO1 in the mixed solutions at 475 nm when excited at 414 nm. (D) The emission plot of Ypet-Ubc9 in the mixed solution at 530 nm when excited at 475 nm. In (B), (C), and (D), four concentrations of CyPet-SUMO1, 0.1 μM, 0.5 μM, 1 μM and 1.5 μM were used in the assay. The concentration of YPet-Ubc9 was increased from 0 to 4 μM in each assay.

Analysis of fluorescent spectrum to calculate FRET emission from YPet-Ubc9

In order to obtain the intensity of FRET emission for K_d measurement, the direct emissions at 530 nm of CyPet-SUMO1 and YPet-Ubc9 need to be determined and excluded from the total emission at 530 nm. When the mixture of CyPet-SUMO1 and YPet-Ubc9 is excited at 414 nm, two emission peaks can be observed at 475 nm and 530 nm (Figure 7A), respectively. Emission at 475nm is from the emission of unquenched CyPet-SUMO1 (FL_{DD}). The emission intensity at 530 nm (FL_{DA}, Figure 7A orange) is consisted of three components: the direct emission of unquenched CyPet-SUMO1 (Figure 7A blue), the direct emission of YPet-Ubc9 (Figure 7A light green) and the emission of YPet-Ubc9 excited by energy transferred from CyPet-SUMO1 (Em_{FRET}, Figure 7A light yellow). Excited at 475 nm, an emission peak at 530 nm (FL_{AA}) can be observed which resulted from the direct excitation of YPet-Ubc9 but not CyPet-SUMO1 (Figure 7B). Because the direct emission of CyPet-SUMO1 at 530 nm (Ex=414nm) is proportional to FL_{DD} with a ratio factor of α (Figure 7C), and the direct emission of YPet-Ubc9 at 530 nm (Ex=414nm) is proportional to FL_{AA} with a ratio factor of β (Figure 7D), Em_{FRET} can be determined by:

$$\mathrm{Em_{FRET}} = (\mathrm{FL_{DA}}) - \alpha \times (\mathrm{FL_{DD}}) - \beta \times (\mathrm{FL_{AA}}) , \qquad \text{Equation 1}$$

in which $\mathrm{FL_{DA}}$ refers to the total fluorescence emission at the acceptor wavelength when excited at the donor excitation wavelength, $\mathrm{FL_{DD}}$ is the fluorescence emission at the donor wavelength when excited at the donor excitation wavelength, and $\mathrm{FL_{AA}}$ is the fluorescence emission at the acceptor wavelength when excited at the acceptor excitation wavelength.

In order to determine the ratio constants α and β, two series of experiments were conducted. First in order to determine the factor α, CyPet-SUMO1 solutions with different concentrations were prepared. The emission intensities of CyPet-SUMO1 at 475 nm and 530 nm (Ex=414nm) were determined and divided to determine the value of α. In the second series of experiment, YPet-

Ubc9 solutions with different concentrations were prepared. The emission intensity of YPet-Ubc9 at 530 nm (Ex=414 or 475nm) was determined. The value of β was derived by dividing the emission at 530 nm (Ex=414nm) by the emission at 530 nm (Ex=475nm). From these experiments, I got the value of α to be 0.35 ± 0.01 (Figure 7C) and β to be 0.029 ± 0.002 (Figure 7D). The fluorescent spectrum data in figure 6 was then analyzed with equation 1 to derive Em_{FRET} at each specific CyPet-SUMO1 and YPet-Ubc9 concentrations (Figure 8A). Therefore the FRET emission intensity of YPet-Ubc9 can be directly calculated using Equation 1 in contrast to previous studies which requires at least three series of control proteins (61). Using this spectrum analysis method, I also tested if modification of SUMO1 and Ubc9 by CyPet and YPet may introduce any non-specific interactions. After the recombinant proteins of CyPet and YPet were purified, CyPet or CyPet-SUMO1 was mixed with YPet or YPet-Ubc9 at different concentrations. Significant FRET emission was only seen in the mixture of CyPet-SUMO1 and YPet-Ubc9 (Figure 8B), which indicates that this FRET-based assay is not affected by potential non-specific interactions between fluorescent tags and the binding proteins.

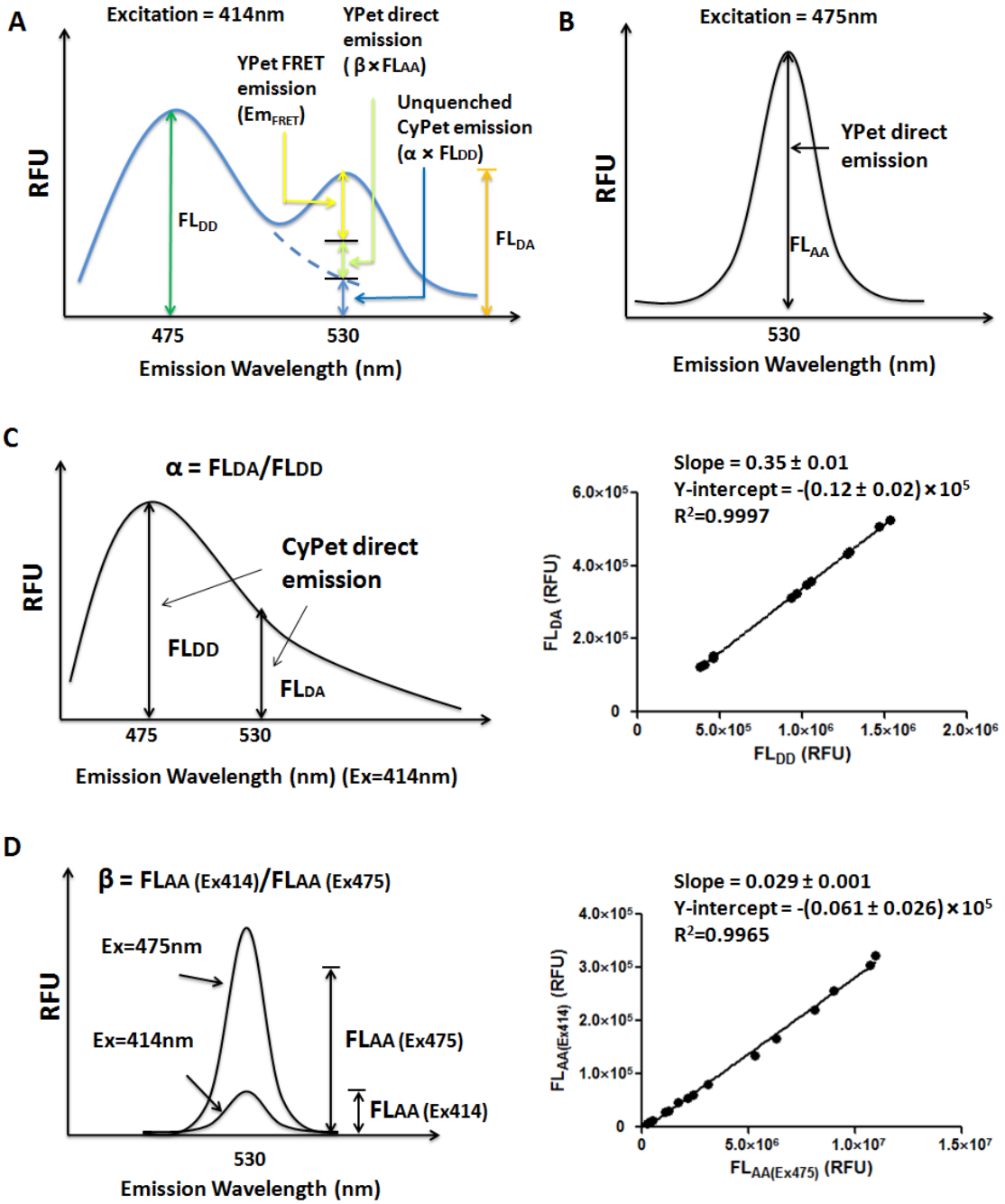

Figure 7. Quantitative analysis of fluorescence signals of FRET emission. (A) Fluorescent emission at 530 nm at the excitation wavelength of 414 nm (FL_{DA}) can be divided into three components: FRET emission from YPet-Ubc9, direct emission of unquenched CyPet-SUMO1, and direct emission of YPet-Ubc9. (B) Fluorescent emission at 530 nm at the excitation wavelength of 475 nm (FL_{AA}) is consisted of direct emission of YPet-Ubc9. (C) Calculation of α factor using CyPet-SUMO1. (D) Calculation of β factor using YPet-Ubc9.

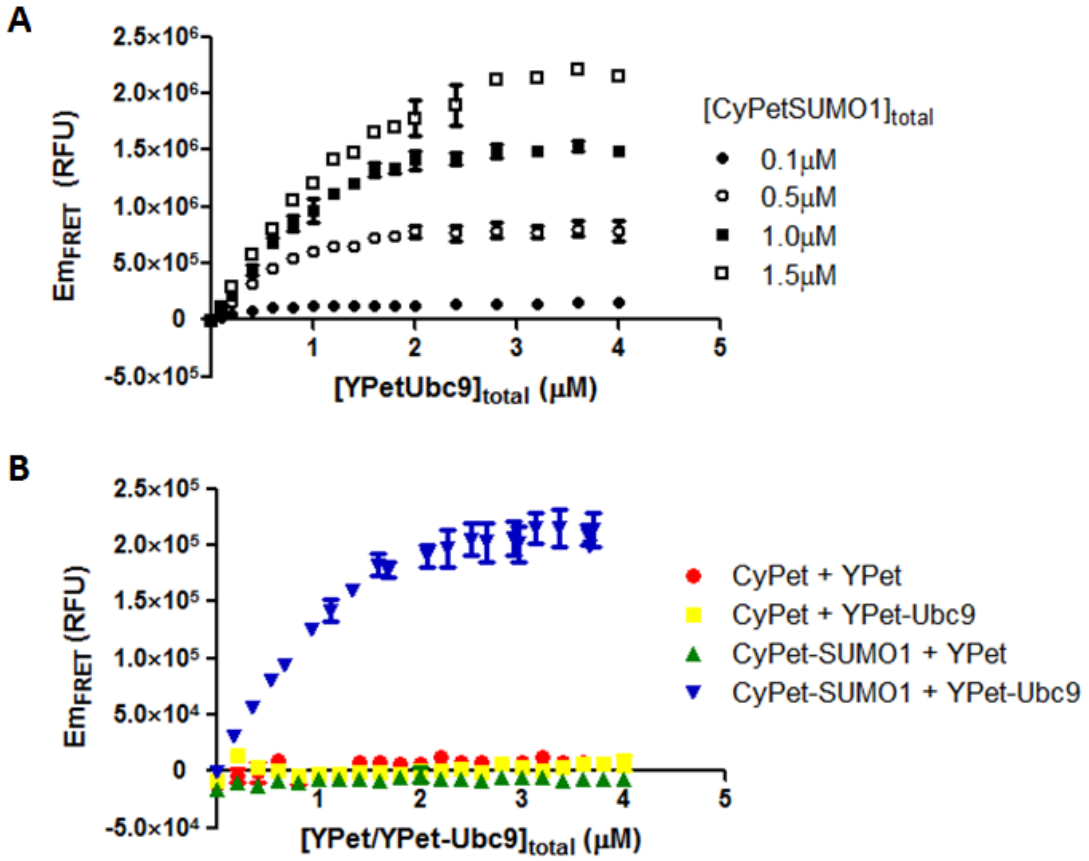

Figure 8. Determination of FRET emission. (A) Calculation of the FRET emission intensity from YPet-Ubc9. YPet-Ubc9 protein was added into 0.1, 0.5, 1.0 or 1.5 μM CyPet-SUMO1 in increment up to 4 μM. (B) Test of non-specific interaction between CyPet/YPet and SUMO1/Ubc9. YPet or YPet-Ubc9 proteins were added into 1.0 μM CyPet or CyPet-SUMO1 in increment up to 4 μM. The FRET emission intensity from YPet or YPet-Ubc9 was calculated at each specific condition.

Derivation of the relationship between FRET emission and protein concentration

From the general law of mass action for CyPet-SUMO1 and YPet-Ubc9 interaction,

$$\mathrm{CyPetSUMO1} + \mathrm{YPetUbc9} \leftrightarrow \mathrm{CyPetSUMO1 \cdot YPetUbc9}$$

K_d can be determined by following expression,

$$K_d = \frac{[\mathrm{CyPetSUMO1}]_{\mathrm{free}}[\mathrm{YPetUbc9}]_{\mathrm{free}}}{[\mathrm{CyPetSUMO1 \cdot YPetUbc9}]} \qquad \text{Equation 2}$$

The concentration of bound proteins, $[\mathrm{CyPetSUMO1 \cdot YPetUbc9}]$ or $[\mathrm{YPetUbc9}]_{\mathrm{bound}}$ should be proportional to the FRET emission intensity as following,

$$\frac{[\mathrm{YPetUbc9}]_{\mathrm{bound}}}{[\mathrm{YPetUbc9}]_{\mathrm{bound\ max}}} = \frac{\mathrm{Em}_{\mathrm{FRET}}}{\mathrm{Em}_{\mathrm{FRET\ max}}} \qquad \text{Equation 3}$$

In this equation $[\mathrm{YPetUbc9}]_{\mathrm{bound\ max}}$ refers to the theoretical maximal value of $[\mathrm{YPetUbc9}]_{\mathrm{bound}}$, and $\mathrm{Em}_{\mathrm{FRET\ max}}$ refers to the theoretical maximal value of $\mathrm{Em}_{\mathrm{FRET}}$ when $[\mathrm{YPetUbc9}]_{\mathrm{bound}}$ reaches its maximum. Because SUMO1 binds to Ubc9 in 1:1 ratio, $[\mathrm{YPetUbc9}]_{\mathrm{bound\ max}}$ equals to the concentration of CyPetSUMO1 in the system. Therefore, in a series of experiments with fixed CyPet-SUMO1 concentration, the values of $\mathrm{Em}_{\mathrm{FRET\ max}}$ and $[\mathrm{YPetUbc9}]_{\mathrm{bound\ max}}$ will be constant. Using this principle, $\mathrm{Em}_{\mathrm{FRET}}$ derived in the assay can be easily correlated to the concentration of bound protein, and further to K_d.

In a given set of conditions with fixed total concentration of CyPet-SUMO1 ($[\mathrm{CyPetSUMO1}]_{\mathrm{total}}$), the K_d can be calculated as following:

$$K_d = \frac{[\mathrm{CyPetSUMO1}]_{\mathrm{free}}[\mathrm{YPetUbc9}]_{\mathrm{free}}}{[\mathrm{CyPetSUMO1} \cdot \mathrm{YPetUbc9}]}$$

$$= \frac{([\mathrm{CyPetSUMO1}]_{\mathrm{total}} - [\mathrm{CyPetSUMO1}]_{\mathrm{bound}})[\mathrm{YPetUbc9}]_{\mathrm{free}}}{[\mathrm{YPetUbc9}]_{\mathrm{bound}}}$$

$$= \frac{([\mathrm{YPetUbc9}]_{\mathrm{bound\ max}} - [\mathrm{CyPetSUMO1}]_{\mathrm{bound}})[\mathrm{YPetUbc9}]_{\mathrm{free}}}{[\mathrm{YPetUbc9}]_{\mathrm{bound}}} \quad \text{Equation 4}$$

The above equation can be converted to:

$$[\mathrm{YPetUbc9}]_{\mathrm{bound}} = \frac{[\mathrm{YPetUbc9}]_{\mathrm{bound\ max}}[\mathrm{YPetUbc9}]_{\mathrm{free}}}{\mathrm{K_d} + [\mathrm{YPetUbc9}]_{\mathrm{free}}} \quad \text{Equation 5}$$

Combining Equation 3 and 5 yields:

$$\mathrm{Em_{FRET}} = \mathrm{Em_{FRET\ max}} \times \frac{[\mathrm{YPetUbc9}]_{\mathrm{free}}}{\mathrm{K_d} + [\mathrm{YPetUbc9}]_{\mathrm{free}}} \quad \text{Equation 6}$$

If I set the total concentration of CyPet-SUMO1 ($[\mathrm{CyPetSUMO1}]_{\mathrm{total}}$) to constant A, the concentration of total YPet-Ubc9 ($[\mathrm{YPetUbc9}]_{\mathrm{total}}$) to variable X and the concentration of free YPet-Ubc9 ($[\mathrm{YPetUbc9}]_{\mathrm{free}}$) to variable Y, respectively, the concentration of $[\mathrm{YPetUbc9}]_{\mathrm{bound}}$ and $[\mathrm{CyPet\text{-}SUMO1}]_{\mathrm{free}}$ can be converted to:

$$[\mathrm{YPetUbc9}]_{\mathrm{bound}} = \mathrm{X} - \mathrm{Y} \quad \text{Equation 7}$$

$$[\mathrm{CyPetSUMO1}]_{\mathrm{free}} = \mathrm{A} - [\mathrm{YPetUbc9}]_{\mathrm{bound}} = \mathrm{A} - \mathrm{X} + \mathrm{Y} \quad \text{Equation 8}$$

Based on the definition of K_d and Equations 7 and 8,

$$K_d = \frac{[\mathrm{CyPetSUMO1}]_{\mathrm{free}}[\mathrm{YPetUbc9}]_{\mathrm{free}}}{[\mathrm{YPetUbc9}]_{\mathrm{bound}}} = \frac{(\mathrm{A} - \mathrm{X} + \mathrm{Y}) \times \mathrm{Y}}{\mathrm{X} - \mathrm{Y}} \quad \text{Equation 9}$$

The above equation can be converted to following,

$$\mathrm{Y}^2 - \mathrm{XY} + \mathrm{AY} = K_d\mathrm{X} - K_d\mathrm{Y}$$

$$Y^2 - (X - A - K_d)Y - K_d X = 0$$

$$Y = \frac{1}{2}(X - A - K_d + \sqrt{(X - A - K_d)^2 + 4K_d X}) \quad \text{Equation 10}$$

Combining Equation 6 and 10 yields:

$$Em_{FRET} = Em_{FRET\,max}(1 - \frac{2K_d}{X - A + K_d + \sqrt{(X - A - K_d)^2 + 4K_d X}}) \quad \text{Equation 11}$$

Therefore fitting the dataset of Em_{FRET} and $[YPetUbc9]_{total}$ (X) with Equation 11 will derive the values of $Em_{FRET\,max}$ and K_d simultaneously.

Determination of K_d

The datasets of Em_{FRET} and $[YPetUbc9]_{total}$ in figure 8A were fitted by equation 11 using the software Prism 5 and the four regression plots corresponding to the four concentrations of CyPet-SUMO1 used in our experiments (0.1, 0.5, 1.0 and 1.5 μM) were generated (Figure 9A). The non-linear regression fitted the data well (R^2 from 0.96 to 0.99). From the non-linear regression, the values of predicted $Em_{FRET\ max}$ are $1.56x10^5$, $8.92x10^5$, $1.67x10^6$, and $2.45x10^6$ RFU, respectively (Table 2). $Em_{FRET\ max}$ has a very good linear relationship with the corresponding amount of CyPet-SUMO1 (R^2= 0.998) (Figure 9B). The values of K_d from these four independent experiments are 0.32 ± 0.03 μM, 0.33 ± 0.04 μM, 0.27 ± 0.03 μM, and 0.29 ± 0.04 μM, respectively (Figure 9C and Table 2). As K_d is an intrinsic property of molecular interaction and is independent of the concentration of binding partners, the consistency of these K_d values confirmed the reliability of this FRET-based assay. These values are also very close to the results of K_d, 0.35μM using Surface Plasma Resonance assay (see below), and 0.25uM using Isothermal titration calorimetry (63). In summary these results suggest that this FRET-based assay can quantitatively measure the value of K_d with high consistency and accuracy.

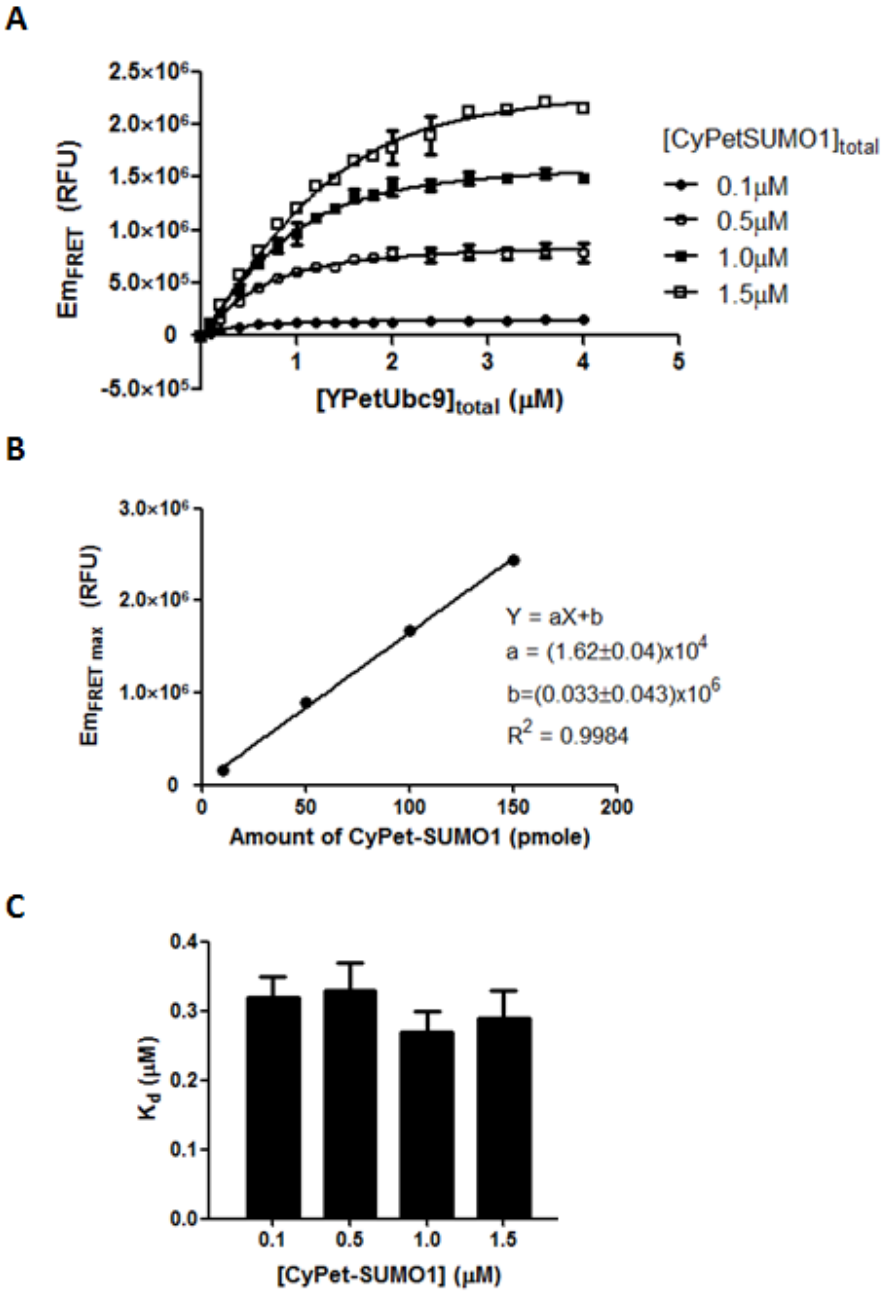

Figure 9. Determination of K_d by FRET. (A) Fitting Em_{FRET} and $[YPetUbc9]_{total}$ with our algorithm derives maximal FRET emission intensity and K_d value at the same time. (B) The maximal FRET emission is proportional to the amount of CyPet-SUMO1 in the system. (C) The FRET-based assay gives a consistent result of K_d regardless of different CyPet-SUMO1 concentrations used in the experiments.

[CyPetSUMO1] (μM)	0.1	0.5	1	1.5
$Em_{FRET\ max}$ (RFU)	$(1.56 \pm 0.03) \times 10^5$	$(8.92 \pm 0.21) \times 10^5$	$(1.67 \pm 0.03) \times 10^6$	$(2.45 \pm 0.06) \times 10^6$
K_d (μM)	0.32 ± 0.03	0.33 ± 0.04	0.27 ± 0.03	0.29 ± 0.04

Table 2. Summary of $Em_{FRET\ max}$ and K_d derived in the assay.

Validation by surface plasmon resonance (SPR) assay

To validate the results of K_d from the FRET-based assay, the interaction affinity of CyPet-SUMO1 and YPet-Ubc9 was measured by SPR assay. As one of the standard methods to measure the binding affinity of protein-protein interactions, SPR assay takes advantage of the fact that accumulation of molecular mass on the metal surface changes the surface electromagnetic wave and results in changes of the minimal reflection angle (65, 66). His-tagged CyPet-SUMO1 protein was expressed in bacterial cells and purified using Ni-NTA agarose beads. After dialysis, His-tagged CyPet-SUMO1 was immobilized onto a NTA sensor chip. YPet-Ubc9 without His tag was obtained by digesting His-tagged YPet-Ubc9 protein on Ni-NTA agarose beads by thrombin. The cleaved YPet-Ubc9 was then further purified by HPLC. Non-specific binding of YPet-Ubc9 to the NTA chip was subtracted as described in Materials and Methods. The binding kinetics analysis showed the binding response of the bound CyPet-SUMO1 to injections of a series of different concentrations of YPet-Ubc9 (Figure 10A). CyPet-SUMO1 bound to YPet-Ubc9 with moderate kinetics. The K_d was calculated to be 0.35 μM, which is consistent with the K_d determined by the FRET-based assay described above.

To further analyze the possible interference of fluorescence tag to the interaction, a control experiment was performed using SUMO1 and Ubc9 proteins without fluorescent tags. Similar to the experiment above, His-tagged SUMO1 was immobilized onto NTA sensor chip. Cleaved Ubc9 was purified by HPLC. SUMO1 shows binding response to a series of injected different Ubc9 concentrations in similar kinetics as fluorescent protein-tagged proteins (Figure 10B). The K_d of SUMO1 and Ubc9 interaction was determined to be 0.1 μM, which is in the same range with that of CyPet-SUMO1 and YPet-Ubc9.

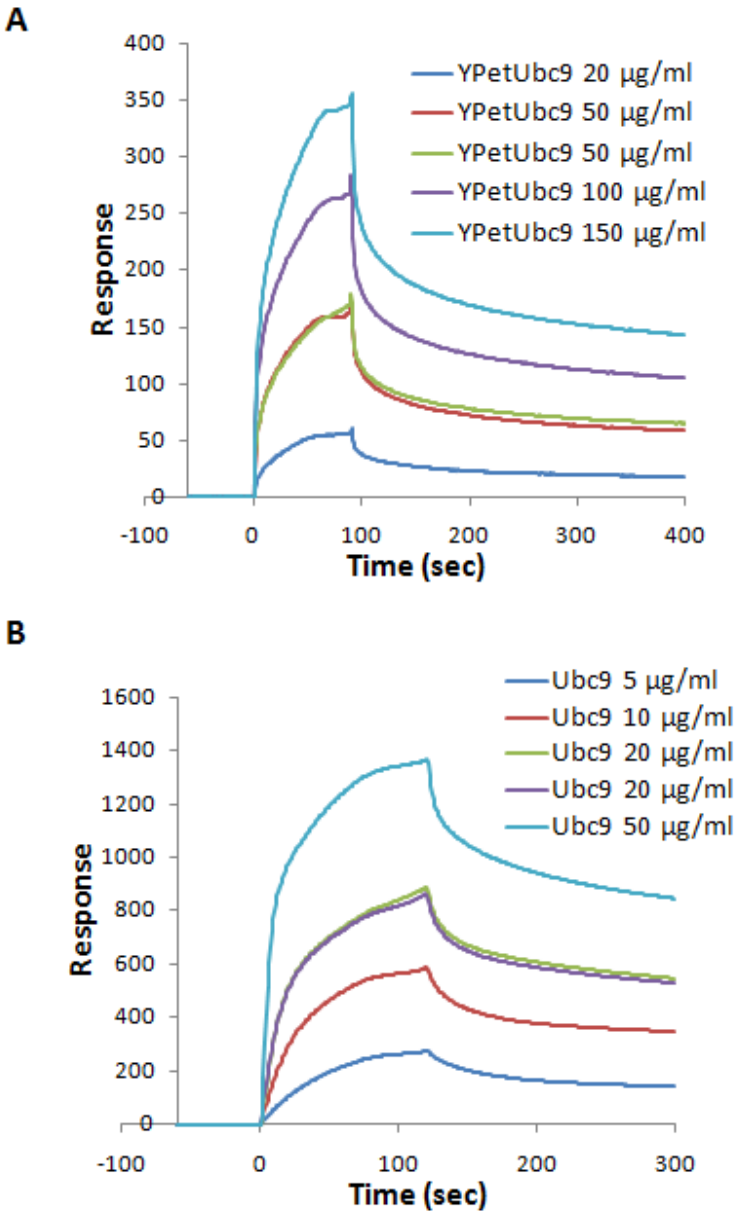

Figure 10. Determination of K_d by surface plasmon resonance assay. (A) CyPet-SUMO1 + YPet-Ubc9; (B) SUMO1 + Ubc9.

Comparison with algorithms from previously published FRET-based K_d assay

In the method published by Martin et al. (61), the datasets of Em_{FRET} and $[YPetUbc9]_{total}$ were fitted by an exponential equation to derive the theoretical maximal FRET emission from YPet-Ubc9:

$$Em_{FRET} = Em_{FRET\,max} \times (1 - e^{-k[YPetUbc9]_{total}}) \qquad \text{Equation 12}$$

The value of $[YPetUbc9]_{bound}$ in each specific condition was then determined by Equation 3 assuming $[YPetUbc9]_{bound\,max}$ equals to $[CyPetSUMO1]_{total}$. After $[YPetUbc9]_{free}$ is calculated by subtracting $[YPetUbc9]_{bound}$ from $[YPetUbc9]_{total}$, the dataset of $[YPetUbc9]_{free}$ and $[YPetUbc9]_{bound}$ was fitted by a hyperbola curve (Equation 5) with $[YPetUbc9]_{bound\,max}$ equaling to $[CyPetSUMO1]_{total}$ to derive the value of K_d. In order to test which algorithm gives more consistent and accurate result at different experimental conditions, the datasets of Em_{FRET} and $[YPetUbc9]_{total}$ in Figure 8A were analyzed by the method of Martin et al. and compared with the results described above. Both non-linear regression fitted the data well (Figure 11A), and the values of $Em_{FRET\,max}$ are not significantly different from each other (Figure 11B). When it comes to K_d, the method of Martin et al. could also generate consistent results regardless of different concentrations of CyPet-SUMO1 used in the assay, although the average value of K_d slightly decreased from 0.30 μM to 0.20 μM when the analytic method is switched to the exponential fitting method (Figure 11C). Overall this exponential fitting algorithm can still be considered as a good empirical solution, which generates results comparable to those from my assay.

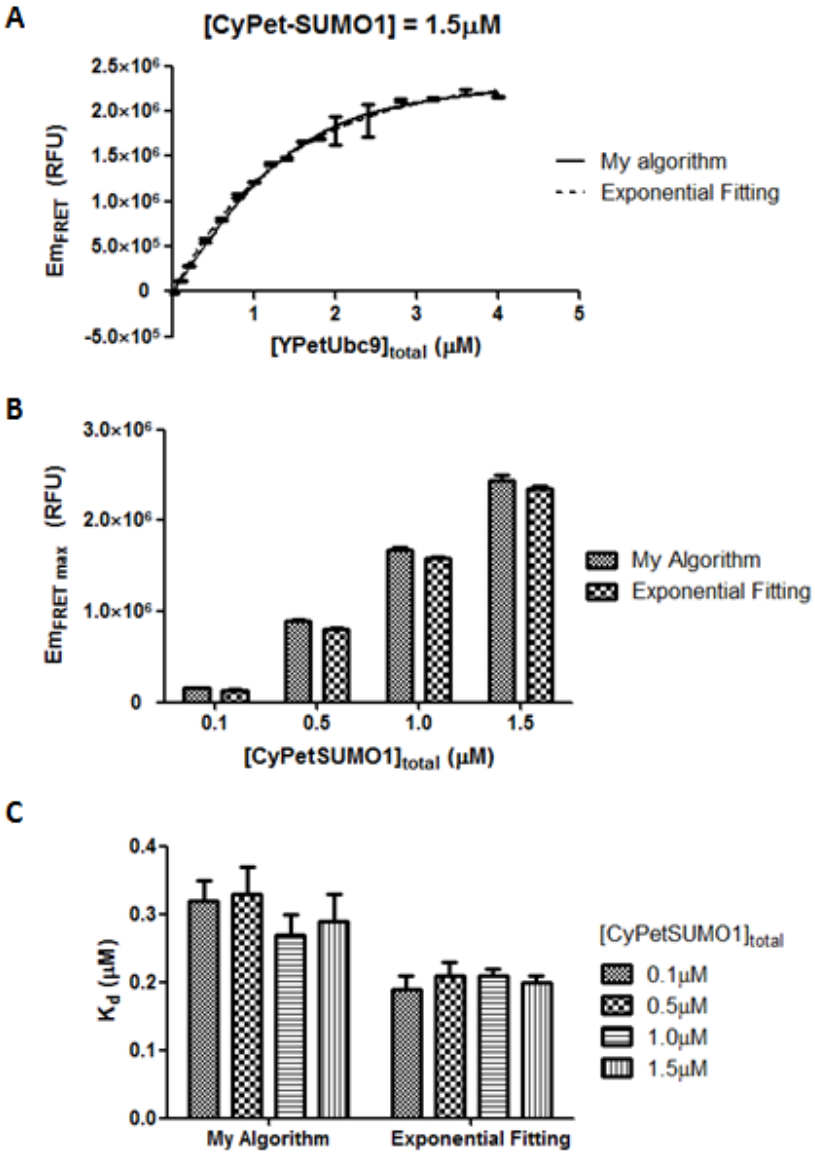

Figure 11. Comparison of the algorithm developed in my assay and previously published one using exponential fitting. (A) Fitting Em_{FRET} and $[YPetUbc9]_{total}$ using the algorithm I developed and previously published exponential fitting method at the CyPet-SUMO1 concentration of 1.5 μM. (B) The exponential fitting method tends to give smaller values of theoretical maximal FRET emission. (C) The algorithm I developed gives similar results to those from exponential fitting method.

Discussion

In summary, I have developed a FRET-based assay to quantitatively measure the K_d of SUMO1 and Ubc9. Compared with previous published FRET-based methods, the fact that donor emission is quenched by FRET is taken into account. With the new method of spectrum analysis, the FRET emission from the binding partners, CyPet-SUMO1 and YPet-Ubc9, can be calculated directly from their fluorescent spectrum without the need of control protein pairs. The new mathematic algorithm also allows the K_d to be derived directly from the FRET emission intensity. While these improvements simplify the experimental and data analysis procedures, this FRET-based assay can also generate accurate and reliable results. The K_d determined at different concentrations of donor, CyPet-SUMO1, ranging from 0.1 μM to 1.5 μM, are very close to each other and that obtained by other biochemical methods. It is noteworthy that at the CyPet-SUMO1 concentration of 1.5 μM, the maximal YPet-Ubc9 concentration in the assay (4 μM) is less than three folds of the CyPet-SUMO1 concentration, yet the result of K_d is still consistent with those from smaller CyPet-SUMO1 concentrations. This is contrast to traditional biochemical approaches for K_d determination such as radioisotope-labeled protein binding assay, which requires at least a range of 100 folds of labeled ligand in order to predict maximum binding (67).

The FRET-based K_d measurement assay can provide several advantages over other current standard K_d measurement methods. First, except the fluorescent tags which in most cases would not interfere with protein interactions, the FRET-based approach does not require specific conjugation or orientation on a solid surface which could interfere with free interactions of proteins, such as the case with surface plasmon resonance which requires conjugation of a partner on chip surface. Second, this method only requires general fluorescence readers or fluorescence microscopes, which are widely available. Other approaches for K_d determination, such as surface plasma resonance or isothermal titration calorimetry, require multiple steps and special

instrumentation (59, 68). Finally, the FRET-based assay can be applied in general to study protein-protein, protein-small molecule or small molecule-small molecule interactions. There are indeed several drawbacks associated with the general application of this assay. Because the FRET efficiency is highly dependent on the distance between the donor and acceptor, it is possible that the size or the conformation of the complex makes FRET hard to detect even when the FRET pair is conjugated to the binding partners. Another potential problem is that the bulk size of fluorescent proteins used in the assay may affect the interaction. Possible solutions to solve these issues include conjugation of fluorescent proteins to the N- or C-terminus of target proteins, modification by small organic fluorophores, and incorporation of fluorescent unnatural amino acids to specifically residues.

This FRET-based K_d measurement assay was performed in 384-well plates, which makes it suitable for high-throughput assays. After the genomic era, large-scale and genome-wide mapping of protein-protein interactions can provide comprehensive understanding of protein interaction networks in cells and potential new drug targets (69-71). While FRET assay has become very popular in biological and biomedical research, quantitative estimations of protein interactions could provide another level of information and a powerful tool for drug discovery targeting protein-protein interactions.

CHAPTER 2: Development of FRET-based high-throughput screening for small chemical compounds disrupting SUMO1-Ubc9 interaction

Abstract

While enzyme-ligand is the major target of compounds used in biological research and clinical applications, small chemical compounds that target protein-protein interactions have emerged as promising tools to control biological processes. SUMOylation is important machinery for post-translational protein modification, which involves multiple enzymes and protein-protein interactions in a cascade of reactions. In this chapter I will describe the development of high-throughput screening assays to look for small chemical inhibitors of SUMO1-Ubc9 interaction. Based on the high efficiency of FRET between CyPet-SUMO1 and YPet-Ubc9, the high-throughput screening assays were set up either *in vitro* with recombinant proteins or in mammalian stable cell lines. The protocol of screening was optimized and small-scale pilot screenings were performed to validate the platform. Carried out in 384-well plates, these FRET-based high-throughput screening assays provide a powerful tool for large-scale and high-throughput applications.

Introduction

Numerous small chemical compounds have been used in biological research and disease treatment. The majority of bioactive compounds target enzymes and function by either activating or inhibiting enzymatic activities. Although protein–protein interactions are essential components of virtually all cellular processes, it is hard to target these interactions with chemical compounds because of the large and often featureless interaction interfaces (72). Over the last two decades, there has been significant interest in the search of small chemical compounds that inhibit specific protein–protein interactions and increasing numbers of small molecules that function in this manner with reasonable potency have been identified. Several examples are nutlin-3, an antagonist of Mdm2 by inhibiting p53-Mdm2 interaction (73), Memoquin, an anti-Alzheimer drug which inhibits the aggregation of Amyloid-β (74), and chelerythrine, an apoptosis-inducing compound which disrupts Bak/Bcl interaction (75). The development of these protein-protein interaction inhibitors provides a new strategy to control biological processes.

Protein-protein interactions are crucial for the SUMOylation cascade. X-ray crystallography and biochemical methods, such as yeast two-hybrid assay, have been used to examine the interactions (16, 76-79), and the interaction of SUMO and its E2 enzyme, Ubc9, is one of the best-studied interactions in the SUMO pathway. Studies of the crystal structure of SUMO1-Ubc9 protein complex identified the key residues of the interacting interface and showed they are conserved among SUMO and Ubc9 family members (80). Biochemical studies showed that the non-covalent SUMO-Ubc9 interaction is not essential to the SUMOylation of substrate proteins but is required for the formation of polySUMO chains (62). While SUMO forms a polymeric chain *in vitro* and *in vivo* (81, 82), the biological significance of polySUMO chain is still unknown. Chemical tools that disrupt the SUMO-Ubc9 interaction will be useful to understand its biological function. However, while considerable effort has been invested in the search of small chemical inhibitors

of the SUMO pathway (42, 43, 83), little has been done to identify compounds that disrupt the SUMO-Ubc9 interaction.

In chapter 1 I developed a FRET-based assay to detect the non-covalent interaction between SUMO1 and Ubc9 and determine the dissociation constant of their interaction. In the assay, a pair of fluorescent protein, CyPet and YPet, was conjugated to the N-terminus of SUMO1 and Ubc9, respectively. Interaction of SUMO1 and Ubc9 pulls CyPet and YPet close to each other and results in FRET from CyPet to YPet. Disruption of SUMO1-Ubc9 interaction can be observed by monitoring the ratio of emission at 530 nm to emission at 475 nm at the excitation wavelength of 414 nm, as shown in figure 5B. In this chapter I will describe the work to convert this FRET assay into high-throughput screening, in which disruption of interaction between CyPet-SUMO1 and YPet-Ubc9 by small chemical inhibitors will be captured by a fluorescence reader in multi-well plate manner (Figure 12). Depending on the environment of protein-protein interactions, the high-throughput screening assay will be established either *in vitro* with purified recombinant proteins or in cells using mammalian cell lines which stably express the binding pair. These high-throughput screening assays will hopefully provide new tools to study the mechanism and function of the SUMO pathway.

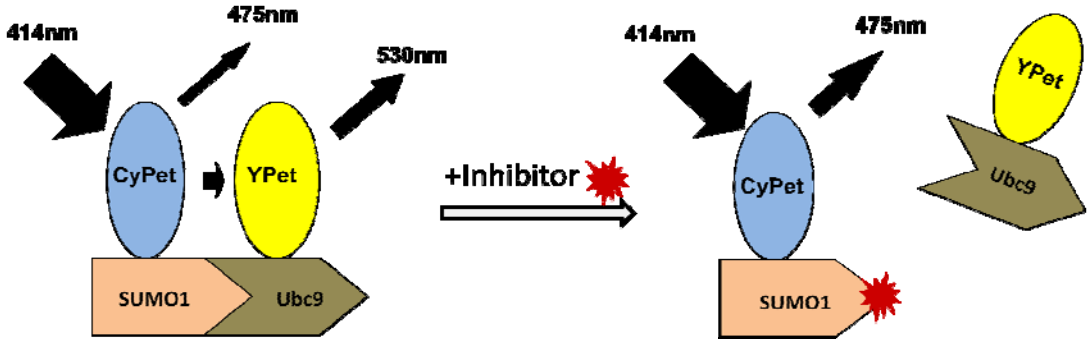

Figure 12. Principle of high-throughput screening of small chemical compound disrupting SUMO1-Ubc9 interaction. Disruption of the interaction between CyPet-SUMO1 and YPet-Ubc9 by small chemical inhibitors results in a decrease of Em_{530}/Em_{475} emission ratio at the excitation wavelength of 414 nm.

Materials and methods

Molecular cloning of DNA constructs

The open-reading frames of CyPet and YPet were amplified by PCR with primers containing NheI/SalI sites (CyPet/YPet) or SalI/NotI sites (SUMO1/Ubc9), and the PCR products were cloned into pCRII-TOPO vector (Invitrogen). The fragments encoding SUMO1 and Ubc9 were extracted by SalI/NotI digestion and inserted into the SalI/NotI sites of pCRII-CyPet or pCRII-YPet, respectively. For expression of recombinant proteins in bacteria, the cDNAs encoding CyPet-SUMO1 and YPet-Ubc9 were cloned into the NheI/NotI sites of pET28(b) vector (Novagen). For expression of recombinant proteins in mammalian cell culture, the cDNAs encoding CyPet-SUMO1 and YPet-Ubc9 were cloned into the NheI/NotI sites of pcDNA3.1-hygro and pcDNA3.1-V5His (Invitrogen), respectively (Figure 13A).

Generation of stable cell lines expressing CyPet-SUMO1 and YPet-Ubc9

All cell culture supplies including media, serum, and antibiotics were purchased from Invitrogen (Carlsbad, CA). To generate cell lines which can stably express CyPet-SUMO1 and YPet-Ubc9 proteins, HEK293 cells were transfected with pcDNA3.1hygro-CyPet-SUMO1 using FuGene6 (Roche) in a 6-well plate, diluted to several 10cm dishes, and selected in DMEM medium supplemented with 150 μg/mL hygromycin. After two weeks, cell colonies were transferred and cultured on 96-well plates. In order to determine the expression of CyPet-SUMO1, the fluorescence emission intensities of individual colonies at 475 nm (Excited at 414 nm) were scanned using FlexstationII^{384} (Molecular Devices). The colony having the highest emission intensity was picked up and expanded. This CyPet-SUMO1-expressing HEK293 stable cell line was then transfected with pcDNA3.1V5His-YPet-Ubc9 and selected with 750 μg/mL geneticin for two weeks (Figure 13B). The fluorescence intensities of cell colonies at 475 nm and 530 nm (Excited at 414 nm) were measured using FlexstationII^{384} (Molecular Devices), and the

Em_{530}/Em_{475} emission ratio of each well was then calculated by dividing the emission intensity at 530 nm by that at 475 nm. The colony having the highest Em_{530}/Em_{475} emission ratio was picked up and used for subsequent screening assays.

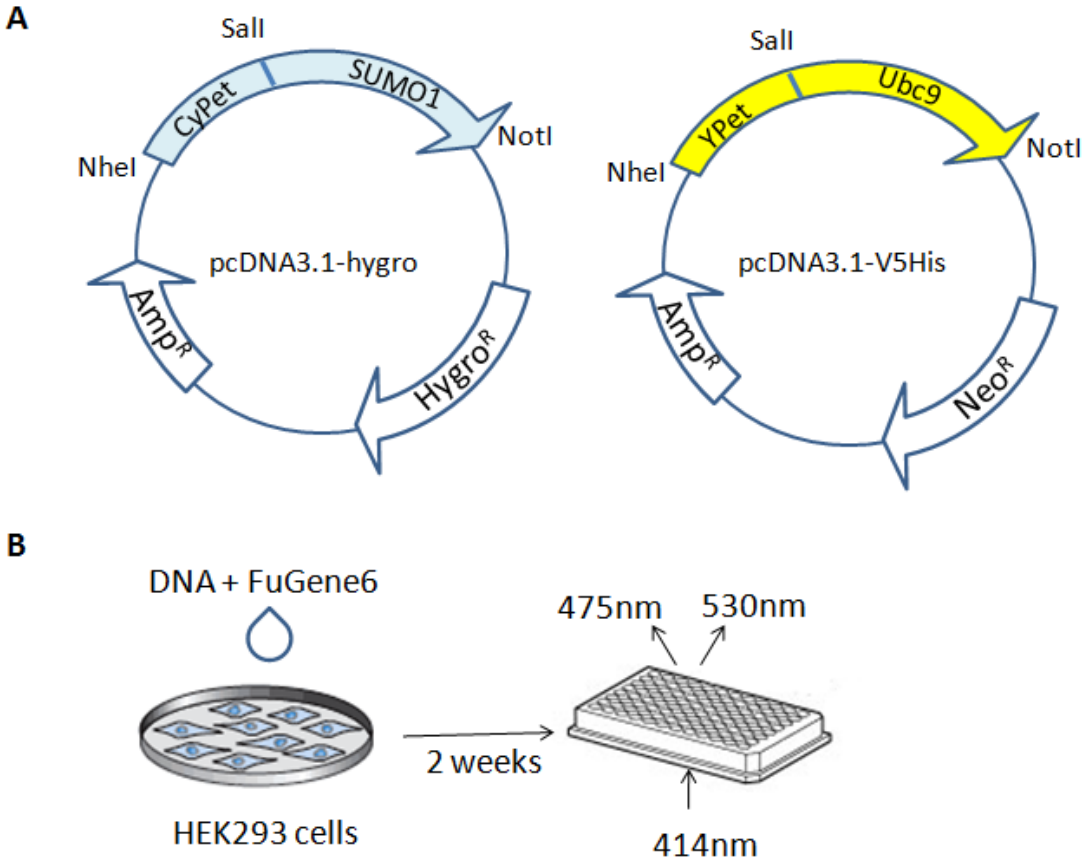

Figure 13. Generation of mammalian stable cells expressing CyPet-SUMO1 and YPet-Ubc9. (A) Map of the mammalian expression plasmids encoding CyPet-SUMO1 and YPet-Ubc9. pcDNA3.1-hygro encodes the gene Hygro^R which confers resistance to hygromycin. pcDNA3.1-V5His encodes the gene Neo^R which confers resistance to geneticin. (B) Stable transfection of HEK293 cells and screening of single colonies by fluorescence.

Cell-based screening of small-chemical compounds that disrupt the SUMO1-Ubc9 interaction

HEK293 cells stably expressing CyPet-SUMO1 and YPet-Ubc9 were diluted to 500 cells per μL with PBS. 60 μL resuspended cells were then aliquoted into each well of 384-well plates (Falcon) using a liquid handler (Molecular Devices, AquaMax DW4). To screen the compound library for inhibitors of SUMO1-Ubc9 interactions, 1 μL 500 μM chemical compound was added to each well using the liquid handling module of FlexstationII^{384} (Molecular Devices). After incubation at 37°C for 2 hours, they were excited at 414 nm and the fluorescence emission intensities of each well at 475 and 530 nm were measured using FlexstationII^{384}. The Em_{530}/Em_{475} emission ratio was then calculated for all the wells.

Expression, purification and fluorescence measurement of recombinant proteins

Recombinant CyPet-SUMO1 and YPet-Ubc9 proteins were expressed and purified as described in chapter 1. The fluorescent emissions of CyPet-SUMO1 and YPet-Ubc9 were determined by the fluorescent plate reader Flexstation II^{384} (Molecular Devices) in 384-well plates at the excitation wavelength of 414 nm with a cutoff filter of 455 nm. The readings were later corrected by the background fluorescence of the plate to get the emission intensities of the fluorescent proteins. The Em_{530}/Em_{475} emission ratio of each well was then calculated.

Optimization of *in vitro* high-throughput screening

To determine the urea concentration that completely disrupts the interaction of CyPet-SUMO1 and YPet-Ubc9, 15 pmole of YPet-Ubc9 protein was mixed with 15 pmole of CyPet-SUMO1 or CyPet in a total volume of 60 μL of buffer containing 20 mM Tris-HCl (pH=7.5), and 500 mM NaCl in the presence of 0, 0.7, 1.3, 2.7, 4, or 5.3 M urea. At each urea concentration, the emission ratio of the mixture of CyPet-SUMO1 and YPet-Ubc9 was measured and compared with the emission ratio of CyPet and YPet-Ubc9.

To determine the best molar ratio of CyPet-SUMO1 and YPet-Ubc9 in the screening assay, two proteins were mixed in a total of 60 μL buffer containing 20 mM Tris-HCl (pH=7.5), and 500 mM NaCl in the presence or absence of 2.7 M urea. The amount of CyPet-SUMO1 was fixed to 15 pmole and the molar ratio of CyPet-SUMO1 to YPet-Ubc9 changed from 1:0.6 to 1:2.6. After the emission ratio of each condition was determined, Z factor was calculated as described previously (84).

To determine the best molar concentration of CyPet-SUMO1 and YPet-Ubc9 in the screening assay, two proteins were mixed in a total of 60 μL of buffer containing 20 mM Tris-HCl (pH=7.5), and 500 mM NaCl in the presence or absence of 2.7 M urea. The molar ratio of CyPet-SUMO1 to YPet-Uba9 was fixed to 1:1.8, and the amount of CyPet-SUMO1 changed from 9 to 30 pmole. After the emission ratio of each condition was determined, the Z factor was calculated using the equation described above.

***In vitro* screening of small-chemical compounds that disrupt the SUMO1-Ubc9 interaction**

Compounds were acquired from Maybridge (Cornwall, UK) and dissolved in DMSO to 500 μM. CyPet-SUMO1 and YPet-Ubc9 proteins were mixed and aliquoted into 384-well plate by Aquamax4 (Molecular Devices). Each well contained 12 pmole of CyPet-SUMO1 and 21.6 pmole of YPet-Ubc9 in a total of 60 μL buffer. The compound (1.2 μL) was transferred to each well and mixed with the proteins by gently shaking the plates. After the fluorescent emission intensities at 475 and 530 nm and the excitation wavelength of 414 nm were determined by FlexstationII^{384} (Molecular Devices), the emission ratios of all the wells were calculated and compared to look for compounds that decrease the emission ratio.

Data analysis

All data were processed by Prism 5 (GraphPad) and reported in the format of mean ± SD.

Results

Generation of cell lines stably expressing CyPet-SUMO1 and YPet-Ubc9 for cell-based screening

When I began to investigate the feasibility of a high-throughput screening platform for compounds disrupting SUMO1-Ubc9 interaction, I decided to set up the screening in a cell-based environment. Compared with *in vitro* assays based on recombinant proteins, the major advantage of cell-based screening assays is that they resemble physiological conditions and provide extra levels of selection. Compounds which are converted into non-active form in cells or cannot penetrate the cell membranes will be unlikely to function in living organisms and can be excluded from the positive hits in cell-based screening assays. However, development of cell-based high-throughput screening has its unique challenge due to the non-uniform nature of cells. In order to achieve high signal-to-noise ratio and low variation, stable mammalian cell lines expressing CyPet-SUMO1 and YPet-Ubc9 were generated in a sequential manner. At the beginning, HEK293 cells were first transfected with plasmid encoding CyPet-SUMO1, selected by addition of hygromycin and screened for the highest expression level of CyPet-SUMO1 by checking the CyPet fluorescence emission. At the second round, the colony was then transfected with plasmid encoding YPet-Ubc9, selected by addition of geneticin and screened for the highest YPet expression by checking the emission ratio of YPet (530 nm) to CyPet (475 nm) at the CyPet excitation wavelength (414 nm) (Figure 14A). When the cells were excited at 414 nm, the Em_{530}/Em_{475} emission ratios of double-transfected stable cell lines were around 0.8 to 1.2, while those of the control cell lines expressing only CyPet-SUMO1 were 0.4 to 0.6. Compared with CyPet-SUMO1 expressing cell lines, cells expressing CyPet-SUMO1 and YPet-Ubc9 showed significant decreased emission at 475 nm and increased emission at 530 nm when excited at 414 nm (Figure 14B).

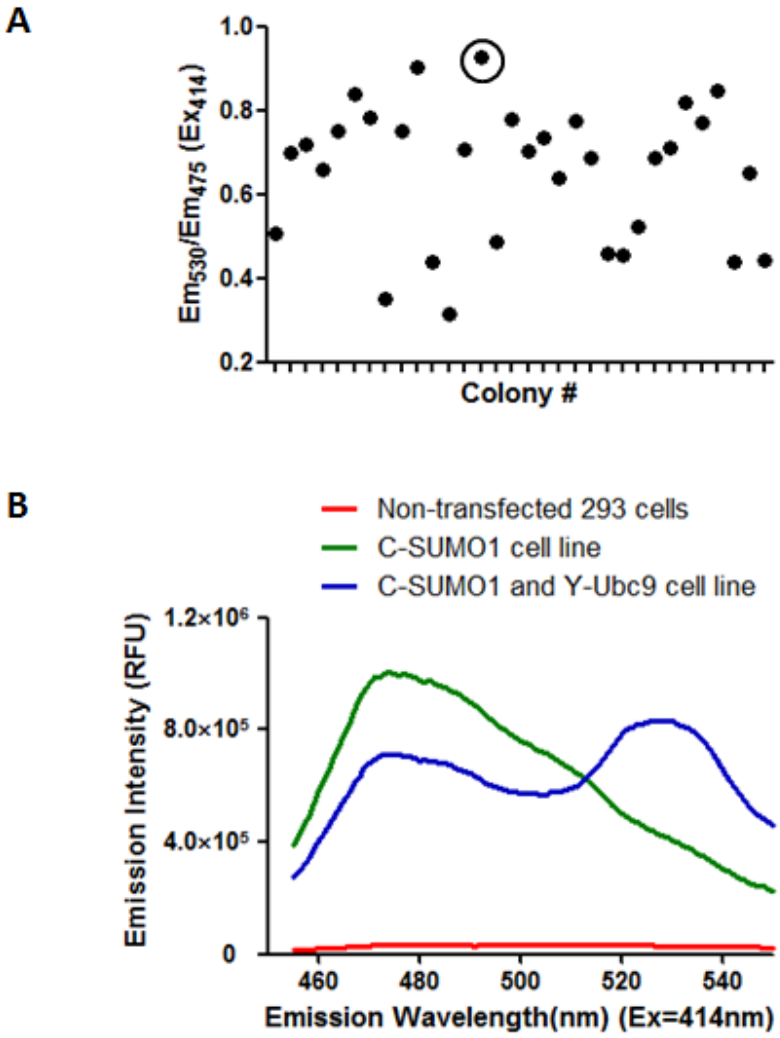

Figure 14. Selection and characterization of stable cell lines. (A) FRET characterization of stable cell lines expressing CyPet-SUMO1 and YPet-Ubc9. The colony marked by black circle was picked up for subsequent experiments. (B) Fluorescence spectrum of non-transfected 293 cells, single transfected stable cell line (green line), and double transfected stable cell line (blue line) when excited at 414 nm. The number of cells is 1×10^6.

Non-covalent interaction of CyPet-SUMO1 and YPet-Ubc9 in the stable cell line

In order to prove that the FRET between CyPet-SUMO1 and YPet-Ubc9 in the stably transfected cells is due to their non-covalent interaction and also to estimate the dynamic range of FRET signal changes of the stable cell line in order to estimate the screening criteria, I examined the effect of detergent on the FRET signal. The FRET spectrum (Ex=414nm) of stably transfected cells in phosphate-buffered saline (PBS) or lysis buffer containing 200 mM NaCl, 10 mM Tris-HCl (pH=7.4) and 1.0% Triton X-100 is shown in figure 15A. Lysis of cells significantly decreased the fluorescent emission at 530 nm and recovered the emission at 475 nm when excited at 414 nm. The Em_{530}/Em_{475} emission ratio decreased from 1.2 to 0.6 upon cell lysis (Figure 15B), which indicated that the interaction of CyPet-SUMO1 and YPet-Ubc9 in the cells is non-covalent and can be disrupted.

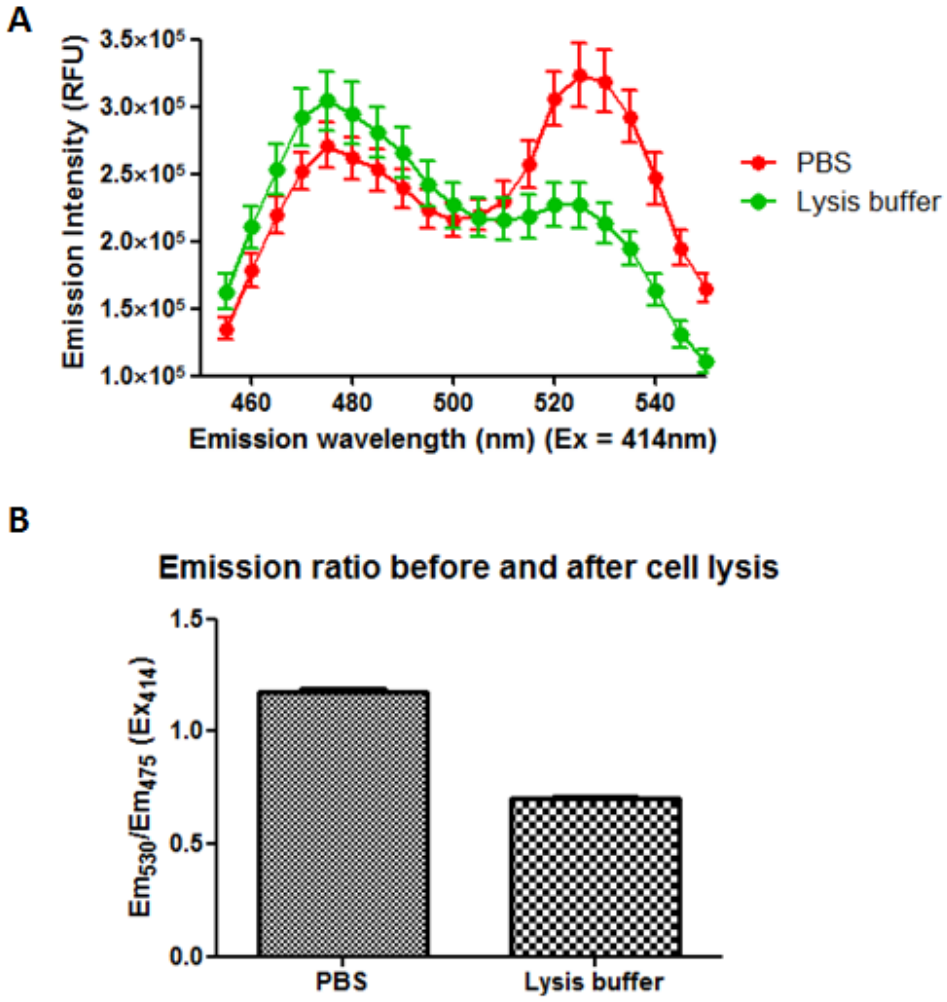

Figure 15. Reversible interaction of CyPet-SUMO1 and YPet-Ubc9 in living cells. (A) The emission spectra of 3×10^5 HEK293 cells stably expressing CyPet-SUMO1 and YPet-Ubc9 in phosphate-buffered saline (PBS) or buffer containing detergent. The experiment was performed in triplicate. (B) Plot of Em_{530}/Em_{475} emission ratio of cells treated with or without lysis buffer as in A.

Development of cell-based high-throughput screening assay for inhibitors of SUMO1-Ubc9 interaction

A highly predictable and reproducible assay is required for high-throughput screening and miniaturization is a critical step in the high-throughput screening development. In principle, a hit should have a signal in an assay with 95-99% confidence depending on the screenings, which suggests that a hit should be picked at least two to three times the standard deviation (SD) beyond the mean value of the control hits. In this FRET-based high-throughput screening assay, the Em_{530}/Em_{475} emission ratio was used as screening signal and the coefficient of variation (CV) of signals in 384-well plate format was used as the variation assessment. In order to optimize the assay, different numbers of HEK293 stable cells were resuspended in PBS and aliquoted into 384-well plates. The CV at each condition was then determined to figure out the best number of cells in each well. As shown in figure 16A, increasing number of cells per well lowers the CV. 30000 cell per well was used as the condition of subsequent screening, as it has a CV just less than 10%. To validate this FRET-based high-throughput screening platform, a small-scale pilot screening was then performed for 12000 compounds. 30000 cells were dispensed into each well and compounds were added to a final concentration of 10 μM. The Em_{530}/Em_{475} emission ratios were then determined for all wells. As shown in figure 16B, the emission ratios have a mean value of 0.95 and standard deviation of 0.15, and the FRET signals of most compounds were centered at mean. The cut-off of primary hits was set at 0.5, which is the value of Mean-3×SD. However, when the 136 compounds picked up from this screening were tested by *in vitro* binding assay, all of them were proven to be false positive mainly due to their high fluorescence background.

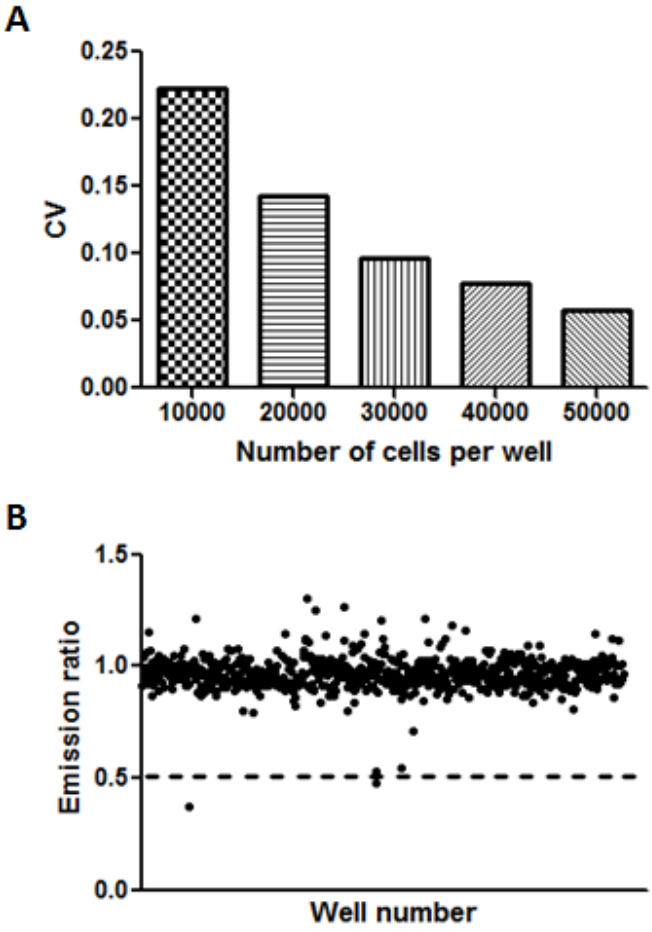

Figure 16. Optimization and small-scale performance of the cell-based screening. (A) Different number of cells per well were resuspended in PBS and aliquoted in 384-well plates. The Em_{530}/Em_{475} emission ratios (Ex=414nm) of all wells were determined and CV was calculated by dividing the standard deviation by the mean value. (B) Example screening results. The dash line indicates the value of mean-3SD.

Development of *in vitro* screening for inhibitors of SUMO1-Ubc9 interaction

While cell-based high-throughput screenings resemble the physiological conditions and provide extra selection of compounds, it is not easy to adjust the expression level of proteins in the cells. There are also certain challenges with the specific instrumentation in our lab, such as the liquid dispenser whose metal needles is easily clogged by cell clusters. In order to more precisely control the amount and ratio of proteins used in the screening and get an improved signal-to-noise ratio, I then used purified recombinant proteins to set up an *in vitro* screening platform. Instead of expressed in mammalian cells, CyPet-SUMO1 and YPet-Ubc9 proteins will be expressed and purified from *E. coli* and mixed *in vitro*. The fluorescence of the compounds will be determined and subtracted from the spectrum of protein-compound mixture. This way the interference of compound fluorescence can be eliminated to hopefully decrease the number of false positive hits.

Because of the absence of any known compounds disrupting SUMO1-Ubc9 interaction, the reagent urea, which disrupts protein interactions at high concentrations, is used as the positive control in this FRET-based screening assay. When urea was added to the mixture of CyPet-SUMO1 and YPet-Ubc9 proteins, the SUMO1-Ubc9 interaction was disrupted and resulted in increase of the emission at 475 nm and decrease of emission at 530 nm at the excitation wavelength of 414 nm (Figure 17A). Because very high concentration of urea might disrupt the tertiary structure of fluorescent proteins, I would like to find the minimal concentration of urea that completely disrupted the SUMO1-Ubc9 interactions. As a control protein, recombinant CyPet protein was expressed and purified as described in Materials and Methods session. YPet-Ubc9 protein was then mixed with CyPet-SUMO1 or CyPet, and the Em_{530}/Em_{475} emission ratios of the mixtures were measured at different concentrations of urea to determine the condition in which the emission ratio of the interacting protein pair (CyPet-SUMO1 + YPet-Ubc9) equals to that of the non-interacting control pair (CyPet + YPet-Ubc9). When urea concentration was

increased from 0 to 5.3 M, the emission ratio of CyPet-SUMO1 and YPet-Ubc9 decreased from 0.78 to 0.45, while the emission ratio of CyPet and YPet-Ubc9 stayed in the range of 0.46 to 0.5 (Figure 17B). The two lines converged at the concentration of 2.7 M urea, which is used in later experiments to determine the quality of the screening assay.

The Z factor was introduced in 1999 to estimate the quality of high-throughput screening assays (84). As a function of the mean values and standard deviations of the positive and negative populations in a screening, Z factor in my assay is calculated by:

$$\text{Z factor} = 1 - \frac{3(\sigma_p + \sigma_n)}{|\mu_p - \mu_n|},$$

in which μ_p, μ_n, σ_p, σ_n refer to the mean values and standard deviations of the emission ratio of CyPet-SUMO1 and YPet-Ubc9 mixture in the presence and absence of urea, respectively. With a theoretical upper limit of 1, a higher Z factor indicates a greater signal difference between positive and negative populations and less signal variation within each population. In general practice, a Z factor of 0.5 to 1 indicates the excellent quality of a screening assay.

Using urea as the positive control, I determined the minimal amount of CyPet-SUMO1 and YPet-Ubc9 required for a satisfactory Z factor in the assay. After the proteins were mixed and added to 384-well plates, urea was added by the liquid transfer module of the fluorescent plate reader, and the emission ratios of each well were determined. First, I fixed the amount of CyPet-SUMO1 to 15 pmole per well and varied the amount of YPet-Ubc9 from 9 to 39 pmole. At each condition, proteins were mixed with either H_2O or urea to a final concentration of 2.7 M and added to 16 wells with the same volume of 60 µL in each well. Emission ratios of all mixtures were determined, mean values and standard deviations of each group were calculated, and a Z factor was calculated for each [CyPet-SUMO1]:[YPet-Ubc9] ratio (Figure 17C). At ratios of 1:0.6 and 1:1, the Z factors were only 0.13 and 0.17, respectively. At a ratio of 1:1.4, the Z factor was barely above 0.50. When the ratio was 1:1.8 or higher, the Z factors were all above 0.7, mainly

due to larger change of emission ratio upon addition of urea. Next I fixed the molar ratio of CyPet-SUMO1 to YPet-Ubc9 at 1:1.8 and repeated the assay with different amounts of proteins added to each well. Changing the amount of CyPet-SUMO1 from 9 to 30 pmole with a fixed [CyPet-SUMO1]:[YPet-Ubc9] ratio of 1:1.8 increased the Z factor from 0.39 to 0.90 (Figure 17D), and it went beyond 0.5 from 12 pmole CyPet-SUMO1. Based on these experiments, the final recipe of this *in vitro* screening assay is determined to be 12 pmole of CyPet-SUMO1 and 21.6 pmole of YPet-Ubc9 in a total volume of 60 μL of buffer in each well of 384-well plates.

To validate the *in vitro* FRET-based high-throughput screening platform, a small-scale pilot screening was performed with a collection of 300 compounds purchased from Maybridge. To eliminate the interference of the fluorescent emission from compounds during the screening, compound fluorescence was determined before the addition of proteins and subtracted from the spectrum of the final mixtures to calculate the emission ratios of the fluorescent proteins (Figure 18A). The emission ratio has a mean value of 0.86 and a standard deviation of 0.06. The FRET signals of most compounds were in the range of mean±3SD (Figure 18B). Only one compound showed a significantly decreased emission ratio of 0.18, which was due to the high fluorescence background from the compound. While I did not find any inhibitors that disrupted the SUMO1-Ubc9 interaction in this small collection, these results showed that this *in vitro* FRET-based assay has a high signal-to-noise ratio and good reproducibility and is suitable for screening of a broader range of compounds.

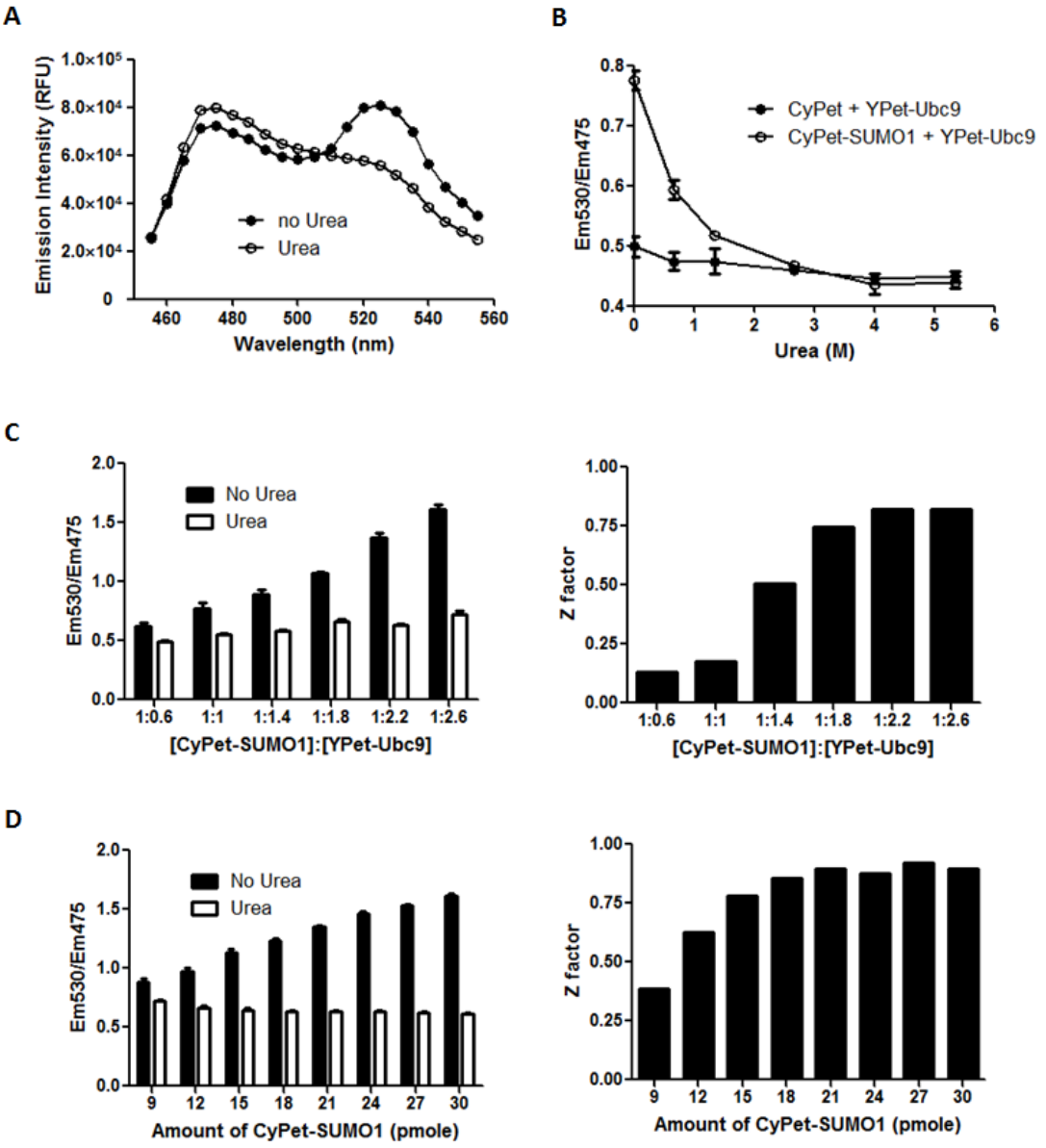

Figure 17. Optimization of the *in vitro* high-throughput screening assay using urea which mimics the effect of positive control. (A) Effect of 2.7M Urea on the FRET between CyPet-SUMO1 and YPet-Ubc9. Excitation wavelength is 414 nm. (B) Titration of urea into mixtures of CyPet-SUMO1 + YPet-Ubc9 or CyPet + YPet-Ubc9. (C) Effect of different [CyPet-SUMO1]:[YPet-Ubc9] ratio on the quality of the screening assay. The amount of CyPet-SUMO1 is fixed to 15 pmole per well. (D) Effect of different amount of proteins on the quality of the screening assay. The [CyPet-SUMO1]:[YPet-Ubc9] ratio is fixed to 1:1.8.

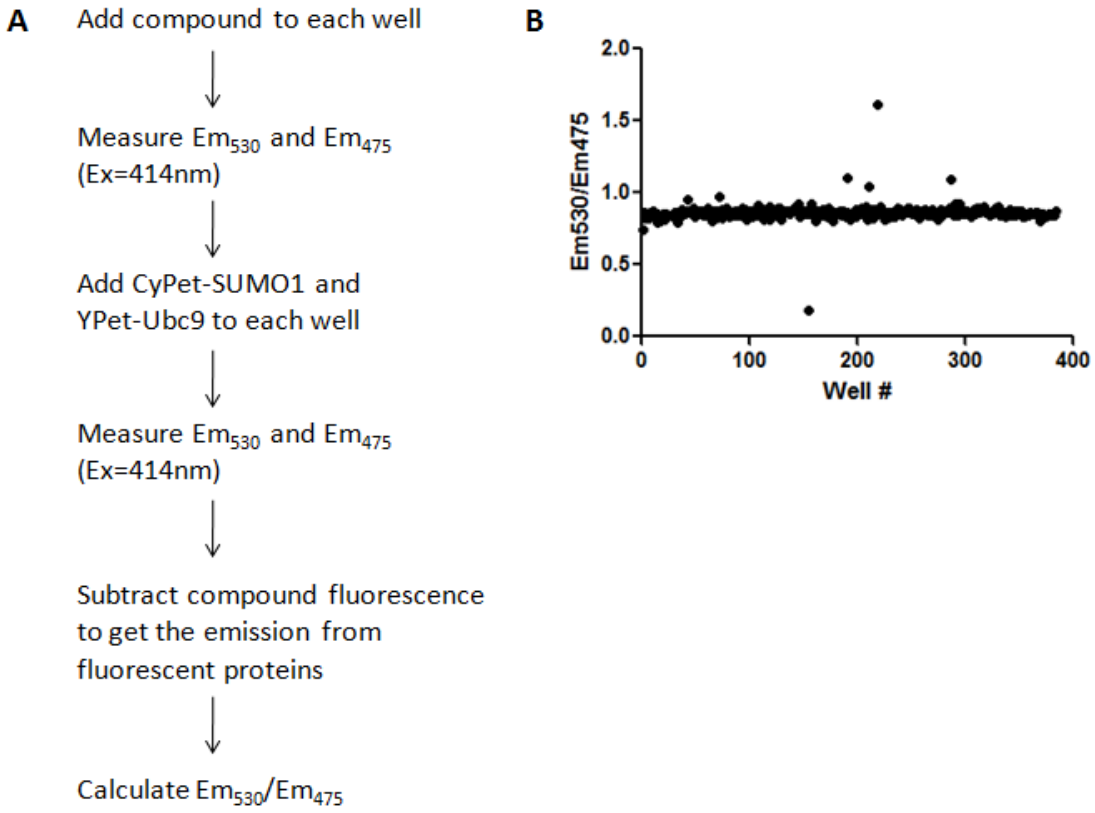

Figure 18. Procedure and small-scale performance of the *in vitro* high-throughput screening assay. (A) Procedure of *in vitro* high-throughput screening. Compound library was first transferred to 384-well plates and the emission intensities of each compound were determined. 12 pmole CyPet-SUMO1 and 21.6 pmole YPet-Ubc9 were then aliquoted to each well to a final volume of 60 µL. The final concentration of compound is 10 µM. The emission intensities of fluorescent proteins in each well were determined by subtracting the compound fluorescence from the total fluorescence. Em_{530}/Em_{475} emission ratios were then calculated. (B) Representative data from a 384-well plate. Each closed circle represents the Em_{530}/Em_{475} emission ratio of an individual well.

Discussions

In this chapter, I have described the development of two FRET-based high-throughput screening assay for small chemical inhibitors of SUMO1-Ubc9 interaction. One of these assays was based on mammalian cell lines which stably express fluorescent-tagged SUMO1 and Ubc9, and the other assay was based on the *in vitro* interaction of purified recombinant proteins. Both assays were optimized so that the disruption of SUMO1-Ubc9 interaction can results in significant changes of FRET signal from CyPet and YPet. Their qualities are also validated by small-scale compound screening. Although no inhibitor was confirmed from the small collection of compounds, these results showed the usability of FRET-based screening assays and the potential to apply this high-throughput technology in the search of compounds targeting other protein-protein interactions in the SUMO pathway.

The strategy using fluorescent proteins as fluorescent marker for bound and free partner measurements can be a general method for high-throughput screening technology (85-87). There are several advantages with this method. First, this approach is environmentally friendly and easy to handle because it does not require radioisotope labeling or chemical modification of proteins. Second, the fluorescent-tagged proteins are in aqueous phase, which is mostly close to their natural environment in cells. Third, the fluorescence intensity can be determined by general fluorescence plate reader, which is widely available. These characteristics make fluorescent protein-based FRET screening appealing for protein-protein interaction.

When the *in vitro* and cell-based high-throughput screening assays are compared, each assay has its own advantages and drawback. Cell-based assay better resembles physiological conditions and evaluate the stability and membrane permeability of chemical compounds in the cells. Yet controlling the expression level of FRET donor and acceptor in cells is difficult, and the FRET signal from different cell batches can vary due to the nature of stable transfection. *In vitro* assay

in turn allows precise control of the amount of proteins used in the screening but does not allow the test of compounds on their ability to function in the cells. Furthermore, compounds which are metabolized to active form in the cells will be missed in the *in vitro* screening assay. The nature of the target and the specific requirement of screening will determine the type of platform to be used.

Several factors might have prevented the finding of inhibitors that disrupt the SUMO1-Ubc9 interaction in the pilot study. The small size of the library is the most obvious factor. Examining a larger library would improve the chance of finding an inhibitor. Second, protein-protein interactions generally have interfaces larger than typical enzyme-ligand reaction interfaces, therefore making them more difficult to disrupt by small chemicals. *In silica* screening using the crystal structures of binding proteins could possibly be used to predict the molecular scaffold of compounds that might bind to their interaction interface. Furthermore, I tried to eliminate the interference of compound fluorescence by subtracting their emission from the total emission. This "correction" might nonetheless have inadvertently hidden effect as highly fluorescent compound may absorb the emission from fluorescent proteins and result in aberrant values of the emission ratio. To solve this issue, fluorophores with longer half-life such as terbium-based dyes may be used to set up time-resolved FRET assays, in which compound emission is outside the window of measurement.

CHAPTER 3: An *in vitro* high-throughput screening assay for small chemical inhibitors of the SUMO pathway

Abstract

SUMO as an important protein post-translational modifier has been discovered for over 15 years. While more than 1000 proteins are identified as the targets of SUMO, in many cases the biological function of SUMO modification remains unclear. In recent years significant effort has been made in the search of small chemical compounds targeting the SUMO pathway, which may be used in the study of SUMO functions and its potential role in pathogenesis. However, no synthetic chemical inhibitor of the SUMO pathway has been identified, and there is an urgent need of high-throughput methods to screen the large pool of synthetic compounds. In this chapter I will describe the development and optimization of an *in vitro* FRET-based high-throughput screening to look for compounds that can inhibit SUMOylation of target proteins. Over 200,000 compounds have been screened using this platform and the first synthetic SUMOylation inhibitor has been identified. This screening platform provides a new strategy to identify small chemical inhibitors of the SUMO pathway, and may also expand to the area of other protein modifications.

Introduction

First identified in 1996, SUMO has emerged as an important modifier to regulate the function and localization of target proteins. More than 1000 proteins have been identified as SUMO targets including transcriptional factors, signaling transducers and cell-surface receptors (14). Because the effect of SUMO modification is highly target-specific, in many cases its biological significances remain to be uncovered (6). Misregulation of the SUMO pathway has been discovered in various diseases (29). These facts indicate that small chemical compounds regulating this pathway will be very useful in both research and therapeutic applications. In recent years increasing effort has been taken in the search of inhibitors of the SUMO pathway. In 2009 a Japanese research group identified the first two chemical inhibitors of SUMOylation, ginkgolic acid and kerriamycin B, from natural products (42, 43)(Figure 19A). The IC_{50} (half maximal inhibitory concentration) of ginkgolic acid and kerriamycin B is 3.0 μM and 11.6 μM, respectively, and they both target the formation of thioester bond between SUMO and E1. Both compounds were identified in an *in situ* cell-based assay (Figure 19B), in which Hela cells were permeabilized with detergent and incubated with GFP-tagged SUMO1, E1, E2 and ATP. After free GFP-SUMO1 is washed off, the level of conjugation by GFP-SUMO1 in cells was determined by fluorescent microscope (88). Due to the restriction of microscopy, this method is quite low-throughput and requires enormous amount of work to screen just hundreds of natural extracts. In order to expand the search of compounds targeting the SUMO pathway to the large pool of synthetic chemical compounds, which often has a scale in millions, there is an urgent need to develop high-throughput screening methods for the SUMO pathway.

High-throughput screening has been commonly used to find small chemical compounds which can regulate specific biological pathways. When it comes to the SUMO pathway, methods are needed to monitor SUMO conjugation of its substrates in a high-throughput manner. FRET will

be ideal for this application because of its high sensitivity to molecular distance. A FRET-based high-throughput screening assay for SUMOylation inhibitors has been reported in 2009 (83). In this assay, chemical fluorophore-tagged SUMO1 was conjugated to a substrate protein, which was then recognized by a fluorescent antibody. The FRET between SUMO1 and the antibody was then detected by a plate reader and inhibition of SUMOylation will result in the decrease of FRET. The major issues of this assay are that both SUMO and the antibody used in the assay need to be chemically modified, and antibody-antigen binding does not always maintain a 1:1 ratio. To solve these issues, I would like to substitute small chemical fluorophores with fluorescent proteins, which can be easily conjugated to target proteins by molecular cloning methods. Furthermore, instead of using antibody to target SUMO substrate proteins, I will directly conjugate fluorescent protein to the N- or C-terminus of target proteins. CyPet and YPet, which were used in previous chapters, should also serve well in this FRET-based screening due to their high FRET efficiency. The development of this FRET-based high-throughput screening assay will provide new strategy to look for compounds targeting the SUMO pathway, and greatly facilitate the research of this important cell machinery.

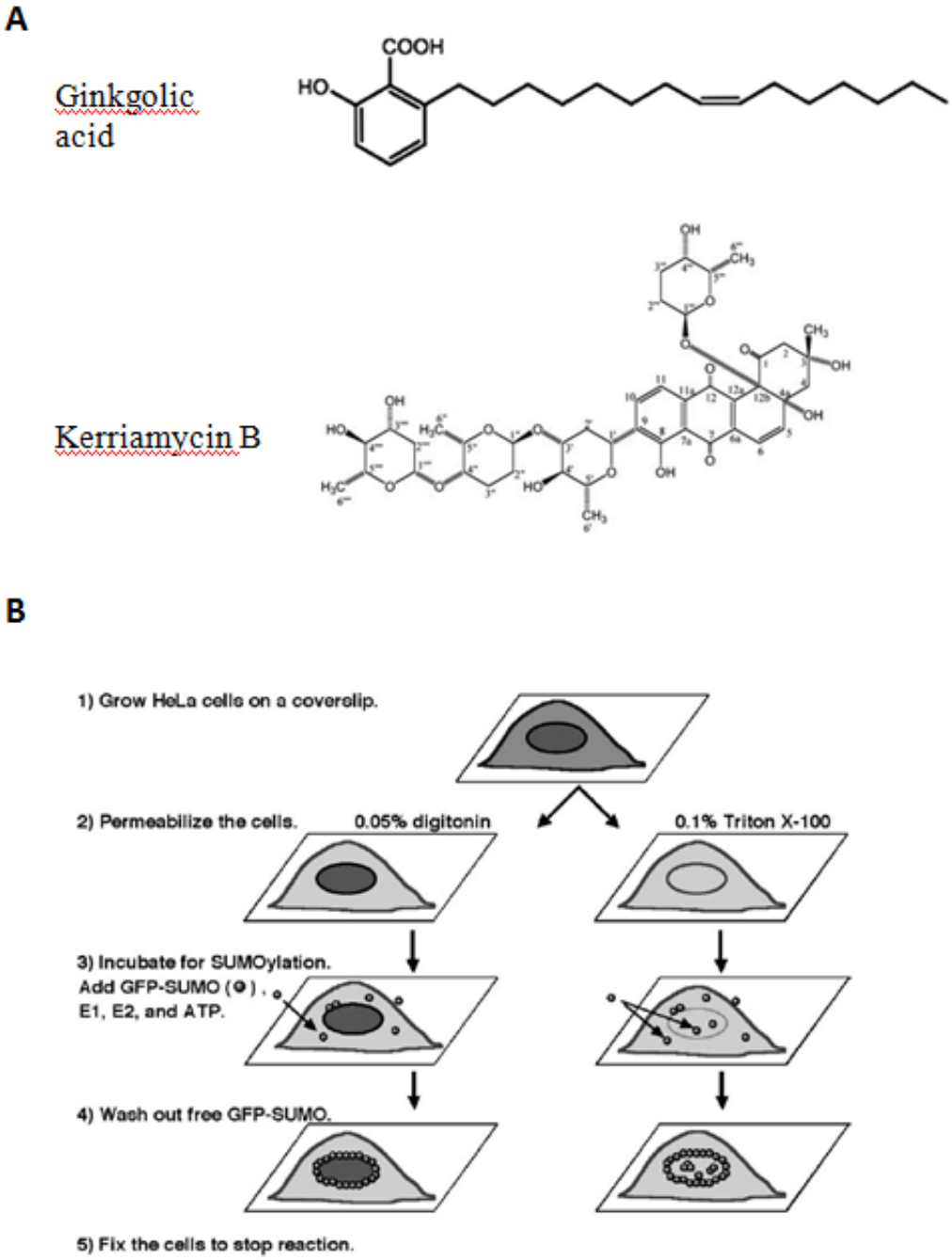

Figure 19. *In situ* cell-based assay used to identify two SUMOylation inhibitors from natural extracts (88). (A) Structures of two SUMOylation inhibitors reported in 2009. (B) Procedure of in situ cell-based assay to identify these two compounds. Fluorescent microscope was used at the last step to quantify the GFP signal from fixed and permeabilized cells.

Material and Methods

Molecular cloning of DNA constructs

The open reading frames of CyPet, YPet, SUMO1, C-terminal domain (420-587) of RanGAP1 (RanGAP1C) were amplified by PCR using primers containing NheI/SalI sites (CyPet/YPet) or SalI/NotI sites (SUMO1/RanGAP1C) and the PCR products were cloned into pCRII-TOPO vector (Invitrogen). The fragments encoding SUMO1 and RanGAP1C were extracted by SalI/NotI digestion and inserted into the SalI/NotI sites of pCRII-CyPet or pCRII-YPet, respectively. After the sequences were confirmed, the cDNA encoding CyPet-SUMO1 and YPet-RanGAP1C were cloned into the NheI/NotI sites of pET28(b) vector (Novagen). A short c-myc tag was added to the N-terminus of YPet to facilitate protein analysis by Western Blotting. The open reading frames of FLAG-tagged RanGAP1C, SUMO1, Aos1, Uba2, Ubc9 and the catalytic domain of SENP1 and SENP2 were also amplified by PCR using primers containing SalI/NotI sites and inserted into pET28(b) vector following similar protocols.

Protein expression and purification

BL21(DE3) *Escherichia coli* (*E. coli*) cells were transformed with pET28 vectors encoding CyPet-SUMO1, YPet-RanGAP1C, FLAG-RanGAP1C, SUMO1, Aos1, Uba2 or Ubc9. After the transformed bacteria were plated on LB agar plates containing 50 μg/mL kanamycin, single colony was picked up and inoculated in 2xYT medium. The expression of polyhistidine-tagged recombinant proteins was induced with 0.1 mM IPTG at 25˚C overnight. Bacterium cells were centrifuged at 6000 rpm 15 min, resuspended in buffer containing 20 mM Tris-HCl (pH=7.5), 0.5 M NaCl and 5 mM imidazole, and sonicated with an ultrasonic liquid processor (Misonix). Cell lysate containing recombinant proteins was cleared by centrifugation at 25000g 30min. The recombinant proteins were then bound to Ni^{2+}-NTA agarose beads (QIAGEN) and eluted in buffer containing 20 mM Tris-HCl (pH=7.5), 0.2 M NaCl and 150 mM imidazole. The proteins

were later dialyzed in buffer containing 20 mM Tris-HCl (pH=7.5), 50 mM NaCl and 1 mM DTT. The purity of the proteins was confirmed by SDS-PAGE followed by Coomassie blue staining, and their concentrations were determined by Coomassie Plus Protein Assay (Thermo) using known quantities of bovine serum albumin as standards. Aliquots of final products were stored in -80˚C.

Final procedures of the high-throughput screenings

For the screening performed in University of California, Riverside, 54000 compounds were dissolved in DMSO to 10 mM and stored in 384-well plates. The compounds of every four stock plates were combined into the corresponding wells in a single screening 384-well plate. Briefly, 25 μL H_2O was dispensed into each well of the screening plates and four compounds of 0.5 μL each were added using Biomek FX workstation (Beckman Coulter). Overall 44 screening plates were prepared from 172 stock plates. 25 μL protein solution containing 10 pmole CyPet-SUMO1, 10 pmole YPet-RanGAP1C, 25 pmole Ubc9, 1.25 pmole Aos1, 1.25 pmole Uba2, 0.6 μL 0.4 M $MgCl_2$, 0.06 μL 1 M DTT and 6 μL 0.5 M Tris-HCl (pH=7.4) was then dispensed into each well using Aquamax 4 (Molecular Devices). After the fluorescence emission intensity at 530 nm at the excitation wavelength of 414 nm (Em_{530}) was determined using FlexstationII^{384} (Molecular Devices), 10 μL 1 mM ATP was added into each well using Aquamax 4. After the plates were incubated at 37ºC for 2 hours the fluorescence intensity of Em_{530} was determined again. 10 μL protein solution containing 0.4 μg catalytic SENP2, 0.4 μL 0.5 M EDTA, 1 μL 0.5 M Tris-HCl (pH=7.4) was then dispensed into each well using Aquamax 4. After the plates were incubated at 37ºC for 2 hours the fluorescence intensity of Em_{530} was determined.

For the screening performed in University of Illinois, Urbana-Champaign, 175000 compounds were dissolved in DMSO to 1mM and stored in 384-well plates. Briefly, 3 μL compound was transferred to the screening 384-well plates using Matrix Platemate Plus (Thermo Scientific), and

47 µL protein solution containing 18 pmole CyPet-SUMO1, 18 pmole YPet-RanGAP1C, 25 pmole Ubc9, 1.25 pmole Aos1, 1.25 pmole Uba2, 0.6 µL 0.4 M $MgCl_2$, 0.06 µL 1 M DTT and 6 µL 0.5 M Tris-HCl (pH=7.6) was then dispensed into each well using Matrix Platemate Plus. The fluorescence emission intensity at 530±10nm at the excitation wavelength of 425±17.5nm (Em_{530}) was determined using Analyst HT (Molecular Devices). 10 µL 1 mM ATP was then added into each well using Matrix Platemate Plus. After the plates were incubated at 37ºC for 2 hours the fluorescence intensity of Em_{530} was determined again. 10 µL protein solution containing 5ng catalytic SENP1 and 1 µL 0.5 M Tris-HCl (pH=7.6) was then dispensed into each well using Matrix Platemate Plus. After the plates were incubated at 37ºC for 2 hours the fluorescence intensity of Em_{530} was determined.

As the positive control in the screening of SUMOylation inhibitors, one column of each screening plate was not supplemented with ATP. Another column of each screening plate was supplemented with ATP but has DMSO instead of compounds in the library to serve as the negative control. Half of this column was supplemented with SENP proteins and serve as the positive control of the deSUMOylation inhibitor screening, and the other half without SENP proteins was the negative control of the deSUMOylation inhibitor screening.

Analysis of screening results

In the screening of SUMOylation inhibitors, the increase of Em_{530} of each well was calculated by subtracting the Em_{530} before ATP addition from the Em_{530} 2 hours after ATP addition. The mean value and the standard deviation of the positive control and negative control columns were then calculated. In UCR screening, we picked up and tested all compounds whose Em_{530} increase was beyond the range of Mean ± 3×SD of the negative control. In UIUC screening, we picked up and tested all compounds whose Em_{530} increase was in the range of Mean ± 3×SD of the positive control.

In the screening of deSUMOylation inhibitors, the decrease of Em_{530} of each well was calculated by subtracting the Em_{530} 2 hours after SENP addition from the Em_{530} before SENP addition. The mean value and the standard deviation of the positive control and negative control columns were then calculated. In UCR screening, we picked up and tested all compounds whose Em_{530} increase was beyond the range of Mean ± 3×SD of the negative control. In UIUC screening, we picked up and tested all compounds whose Em_{530} increase was in the range of Mean ± 3×SD of the positive control.

***In vitro* SUMOylation and deSUMOylation assay**

0.08 μg SUMO1, 0.1 μg FLAG-RanGAP1C, 0.2 μg Ubc9, 0.02 μg Aos1 and 0.04 μg Uba2 proteins were mixed in 20 μL aqueous buffer containing 4 mM $MgCl_2$, 1 mM DTT, 0.2 mM ATP and 50 mM Tris-HCl (pH=7.6). The mixture was incubated at 37ºC for 1 hour, supplemented with loading buffer containing SDS and DTT, and denatured at 95ºC for 5 min. After 10 μL mixture was separated by 10% SDS-PAGE, the amount of unSUMOylated and SUMOylated RanGAP1C was determined by Western blotting using anti-FLAG antibody.

In the deSUMOylation assay, after the SUMOylation reaction was performed following the method described above, 0.16 μg catalytic SENP2 or 0.2 ng catalytic SENP1 was added to the mixture and incubated at 37ºC for 1 hour. The amount of unSUMOylated and SUMOylated RanGAP1C was determined following the method described above.

Whole cell SUMOylation assay

HEK293 cells were plated in 60 mm culture dishes in DMEM medium supplemented with 10% FBS and grown at 37ºC until 80% confluency. The medium was changed fresh and compounds were added to various concentrations. After 4h treatment, the medium was aspirated. The cells were scraped off in 500 μL PBS and transferred to 1.5 mL microtubes. Cell pellets were spinned down at 3000 rpm for 2 min, washed with PBS, and resuspended in 120 μL whole cell lysis

buffer containing 50 mM N-ethylmaleimide and protease inhibitor. Cells were then shaked at 4ºC for 30 min and spinned down at 13200 rpm 3 min to clear the lysate. After the concentration of cell lysate was determined and normalized, loading buffer with SDS and DTT was added and cell lysate was denatured at 95ºC for 5 min. 30 μL sample was separated by 6% SDS-PAGE, and the amount of high molecular weight SUMOylated protein was determined by Western blotting using anti-SUMO1 antibody.

Results

Detection of SUMOylation of RanGAP1C by FRET

Using molecular cloning methods, I tagged CyPet and YPet, a pair of engineered fluorescent proteins with improved FRET efficiency, to the N-terminus of SUMO1 and the C-terminal domain of RanGAP1 (RanGAP1C), respectively. RanGAP1 was the first identified SUMO substrate. The formation of an isopeptide bond between SUMO and Lys526 of RanGAP1 *in vitro* occurs in the presence of E1, E2 and ATP, and this reaction does not require E3 ligase (9). I would like to use FRET between CyPet and YPet to monitor the conjugation and deconjugation of SUMO1 to RanGAP1C and further set up assays to look for compounds that can inhibit the SUMO pathway. The excitation and emission peak wavelengths of CyPet and YPet are 414nm/475nm and 515nm/530nm, respectively. When the system is excited at 414nm and energy transfers from excited CyPet to YPet in close proximity, increased emission at 530 nm (Em_{530}) can be observed. In the presence of Aos1/Uba2 (E1), Ubc9 (E2), ATP and necessary cofactors, CyPet-SUMO1 will be covalently linked to YPet-RanGAP1C and results in increase of Em_{530}. On the other hand, deconjugation of CyPet-SUMO1 from YPet-RanGAP1C catalyzed by SENP will result in decrease of Em_{530} (Figure 20A). We further set up a FRET assay to test this model. CyPet-SUMO1 and YPet-RanGAP1C proteins were mixed with Aos1, Uba2 and Ubc9 proteins in a buffered system without ATP. ATP was added at time point 0 and the Em_{530} of the protein mixture was monitored every 5 min. Compared with the negative control sample which did not have ATP, the sample with ATP showed significant increase of Em_{530} and reached the plateau in 20 min (Figure 20B). Addition of SENP protease quickly cleaved off SUMO1 from RanGAP1C and reduced Em_{530} to baseline. This proves that the conjugation of CyPet-SUMO1 to YPet-RanGAP1C is fully reversible and the status of conjugation can be monitored by FRET in a real-time manner.

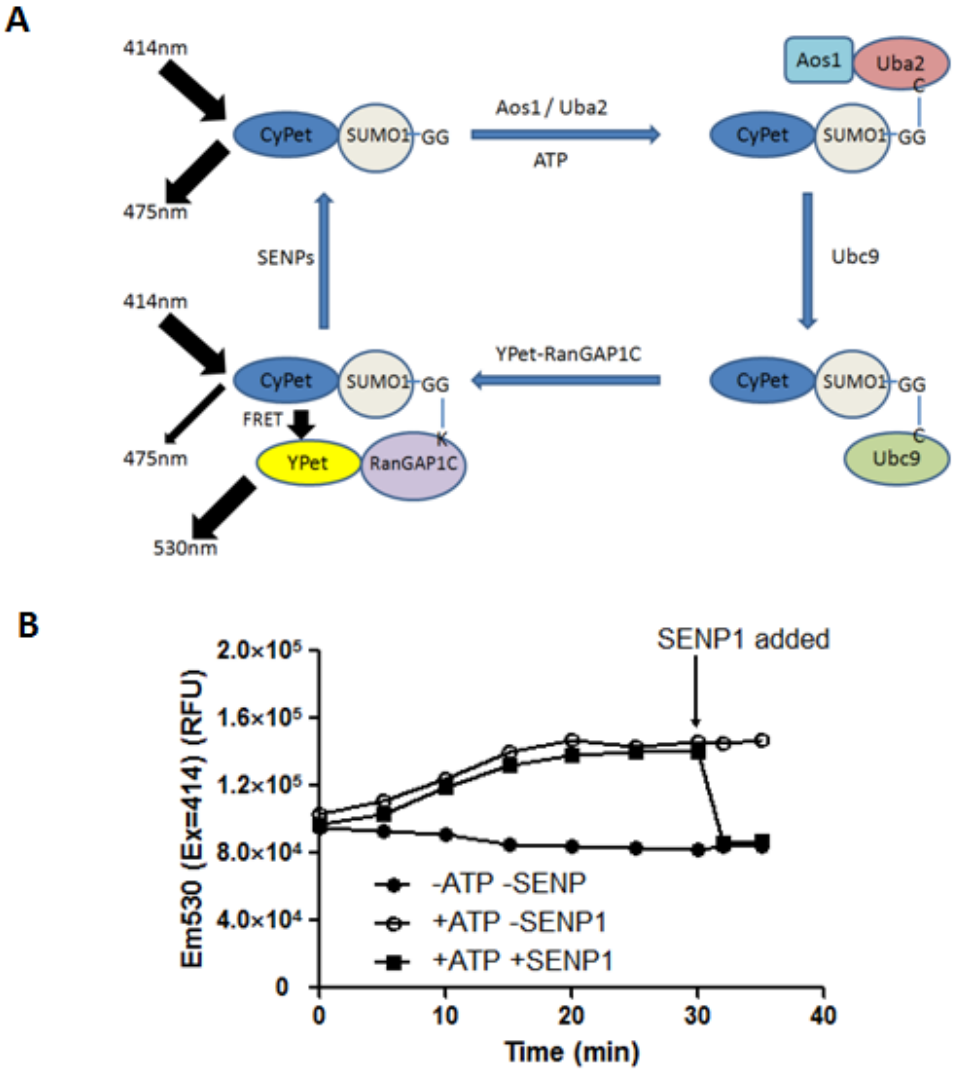

Figure 20. FRET can be used to monitor the SUMOylation of RanGAP1C *in vitro*. (A) Principle of high-throughput screening assay of small chemical inhibitors of SUMOylation/deSUMOylation. Modification of YPet-RanGAP1C by CyPet-SUMO1 in the presence of E1 (Aos1/Uba2), E2 (Ubc9) and ATP results in FRET between CyPet and YPet and can be detected as increase of emission at 530 nm at the excitation of 414 nm. (B) FRET can be used to monitor SUMO conjugation in real-time manner.

Optimization of *in vitro* high-throughput screening of SUMOylation inhibitors

While SUMO1 forms monoconjugate on the Lys526 residue of RanGAP1 (9), it still has to be determined if the best molar ratio of CyPet-SUMO1 to YPet-RanGAP1C is 1:1 in this assay. 10 pmole CyPet-SUMO1 was mixed with different amount of YPet-RanGAP1C in the presence of E1/E2 enzymes and cofactors. The mixtures were incubated for an excess period of time so that the conjugation reaction could be complete. The amount of Em_{530} increase reached the plateau at a molar ratio of 1:1 and did not have significant increase if more YPet-RanGAP1C was added into the system (Figure 21A). Similar results were obtained when the amount of YPet-RanGAP1C was fixed to 10pmole and various amount of CyPet-SUMO1 was added (Figure 21B). These results indicate that a 1:1 molar ratio of CyPet-SUMO1 and YPet-RanGAP1C would be enoughI further tested the amount of each protein used in the screening. The concentration of either Aos1/Uba2 or Ubc9 was fixed and the other enzyme was tuned to find the optimal concentration that can complete the reaction in a period of 2 hours (Figure 22A and 22B). The final recipe of the SUMOylation inhibitor screening is 10 pmole CyPet-SUMO1, 10 pmole YPet-RanGAP1C, 25 pmole Ubc9, 1.25 pmole Aos1 and 1.25 pmole Uba2 in 60 μL buffer. In the deSUMOylation screening, 0.4 μg catalytic SENP2 was added to deconjugate SUMO1 from RanGAP1C. I determined the Z factor of both screening assay and got 0.56 and 0.61 for the SUMOylation and deSUMOylation inhibitor screening, respectively (Figure 23A and 23B), which indicates this screening assay has an excellent quality and is suitable for large-scale screening.

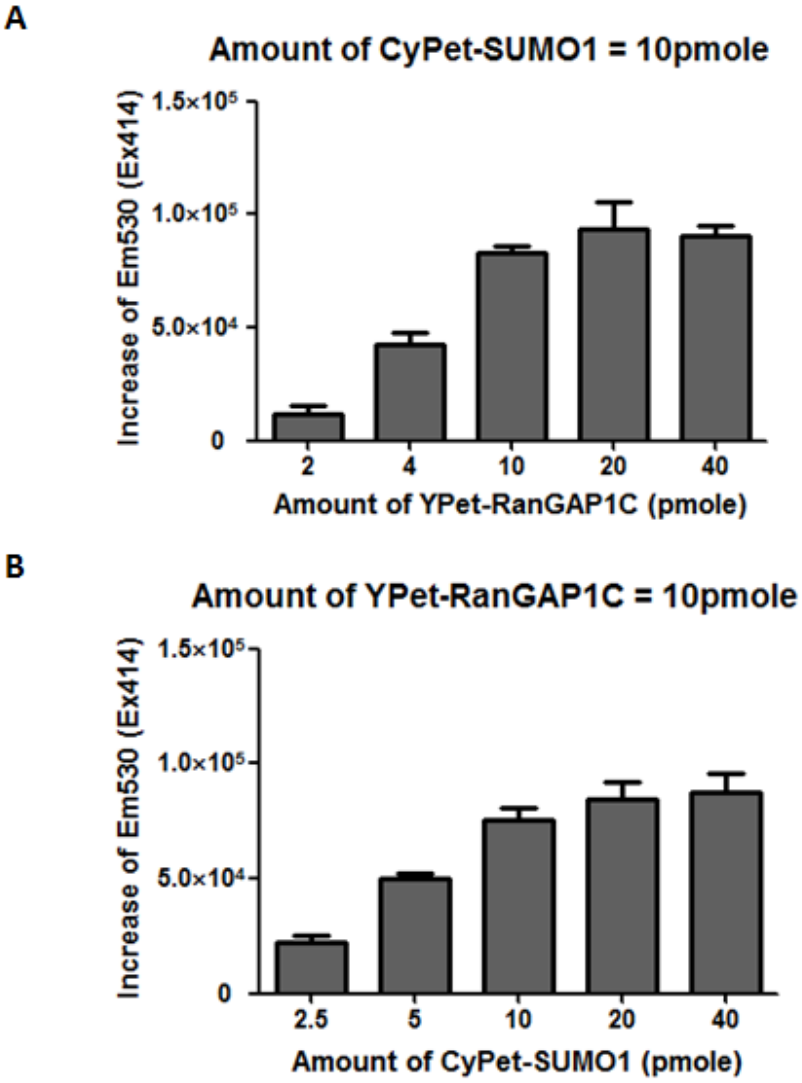

Figure 21. Determination of the best ratio of CyPet-SUMO1 and YPet-RanGAP1C proteins used in the screening assay. (A) CyPet-SUMO1 was fixed to 10 pmole in 60 µL buffer and different amount of YPet-RanGAP1C was added. E1, E2 and ATP were added and the reaction mixture was incubated long enough for the completion of reaction. The increase of emission at 530 nm (Ex=414nm) before and after the reaction was determined. (B) Similar as (A) except YPet-RanGAP1C was fixed to 10 pmole in 60 µL buffer and different amount of CyPet-SUMO1 was added.

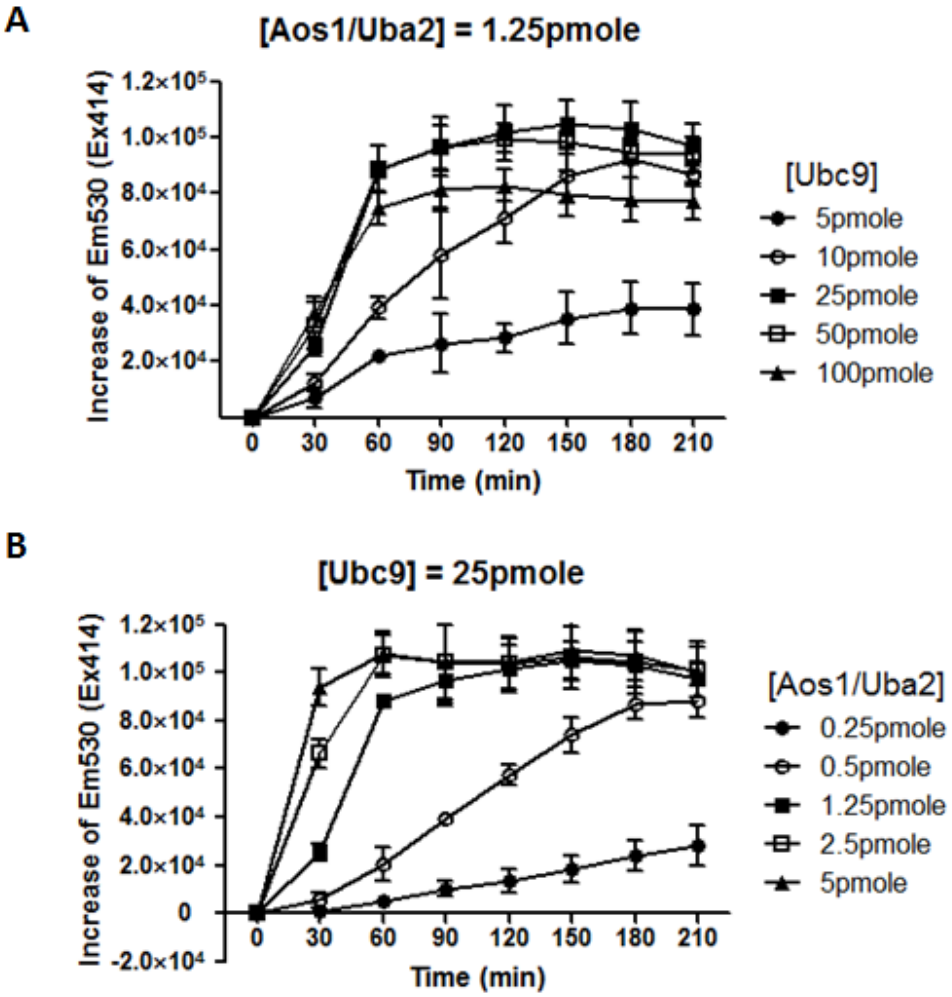

Figure 22. Determination of amount of E1 and E2 used in the assay. CyPet-SUMO1 and YPet-RanGAP1C were fixed to 10 pmole in 60 µL buffer. (A) Aos1 and Uba2 were fixed to 1.25 pmole and Ubc9 was varied. (B) Ubc9 was fixed to 25 pmole and Aos1/Uba2 was varied.

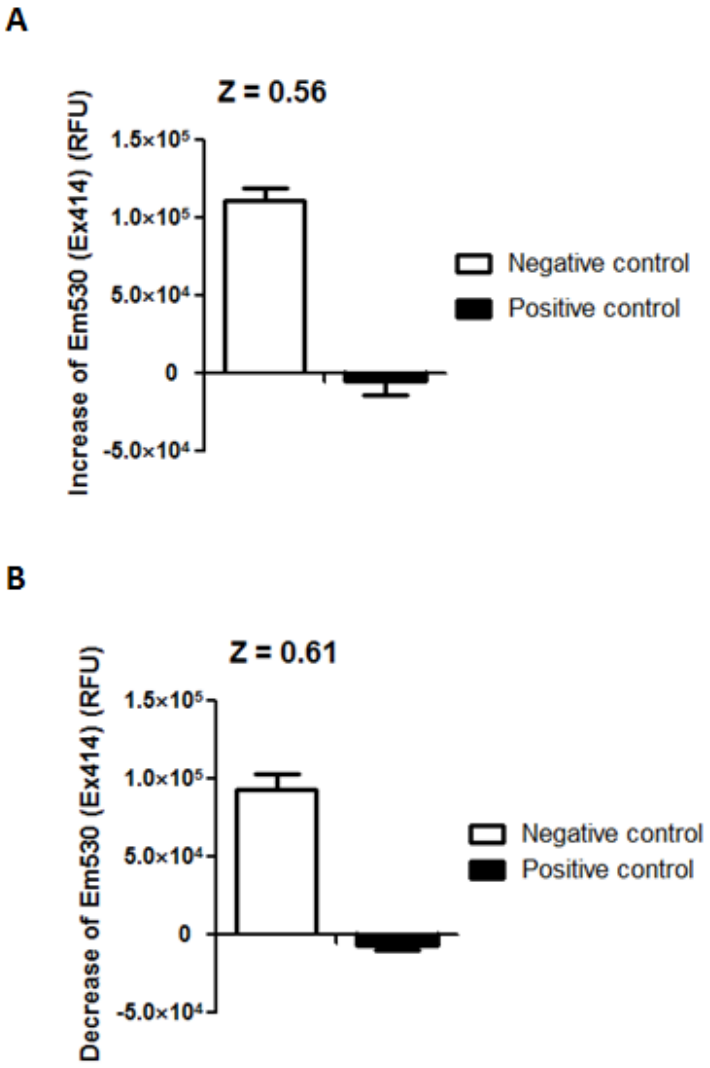

Figure 23. Determination of Z factors. (A) In SUMOylation inhibitor screening, ginkgolic acid was used as the positive control and DMSO is the negative control. (B) In deSUMOylation inhibitor screening, DMSO served as the negative control. SENP protein was not added in the positive control.

Screening of small chemical compounds

In the screening performed in UC Riverside, I used the FRET-based assay to screen 54,000 compounds for SUMOylation or deSUMOylation inhibitors. In order to save proteins and plates, I combined every four stock 384-well plates into one screening plate, screened the compound mixtures at a concentration of 80 μM, and picked up corresponding compounds for further characterization. Out of 14000 wells we screened, significant inhibition of Em_{530} increase upon ATP addition were shown in 91 wells (Figure 24A), and significant inhibition of Em_{530} decrease upon SENP2 addition were shown in 4 wells. The compound mixtures in these wells were then validated by *in vitro* SUMOylation assay. In this assay, non-fluorescent tagged SUMO1 and FLAG-tagged RanGAP1C were mixed with E1, E2 and ATP and incubate at 37ºC. The reaction mixture was separated by SDS-PAGE and blotted by anti-FLAG antibody. SUMOylation of RanGAP1C results in its shift on the gel from ~22kDa to ~37kDa (Figure 24B). 45 mixtures were still able to inhibit the SUMOylation of FLAG-RanGAP1C, but none of the 4 mixtures picked up for SENP inhibitor passed the assay. I then used the FRET-based assay to run a small-scale screening of the 164 compounds which corresponds to the 45 mixtures. 43 compounds were shown positive in a one-compound-one-well basis. These compounds were then tested by *in vitro* SUMOylation assay at a concentration of 50 μM and 25 compounds were finally confirmed as positive. In order to make the quantitative assessment of these compounds more accurate, I purchased 17 compounds from companies and test their potency to inhibit SUMOylation at 200, 50, 10 and 1 μM (Figure 24C). While most of the compounds were active at 200 μM, 10 of them were active at 50 μM, and 6 compounds were active at 10 μM. When the concentration of compounds was reduced to 1 μM, 3 compounds could still partially inhibit the SUMOylation reaction.

Besides the compounds from UC Riverside, I have also used this FRET-based screening platform to screen a total of 175,000 compounds from University of Illinois at a concentration of 50 μM. The final recipe of the SUMOylation inhibitor screening is 18 pmole CyPet-SUMO1, 18 pmole YPet-RanGAP1C, 25 pmole Ubc9, 1.25 pmole Aos1 and 1.25 pmole Uba2 in 60 μL buffer. In the deSUMOylation screening, 5 ng catalytic SENP1 was added to deconjugate SUMO1 from RanGAP1C. 157 compounds and 14 compounds were identified as potential inhibitors of SUMOylation or deSUMOylation, respectively. I took these compounds back to UCR and tested them by *in vitro* SUMOylation assay. A total of 41 SUMOylation inhibitors were confirmed as positive at the concentration of 50 μM but none of the deSUMOylation inhibitors was confirmed.

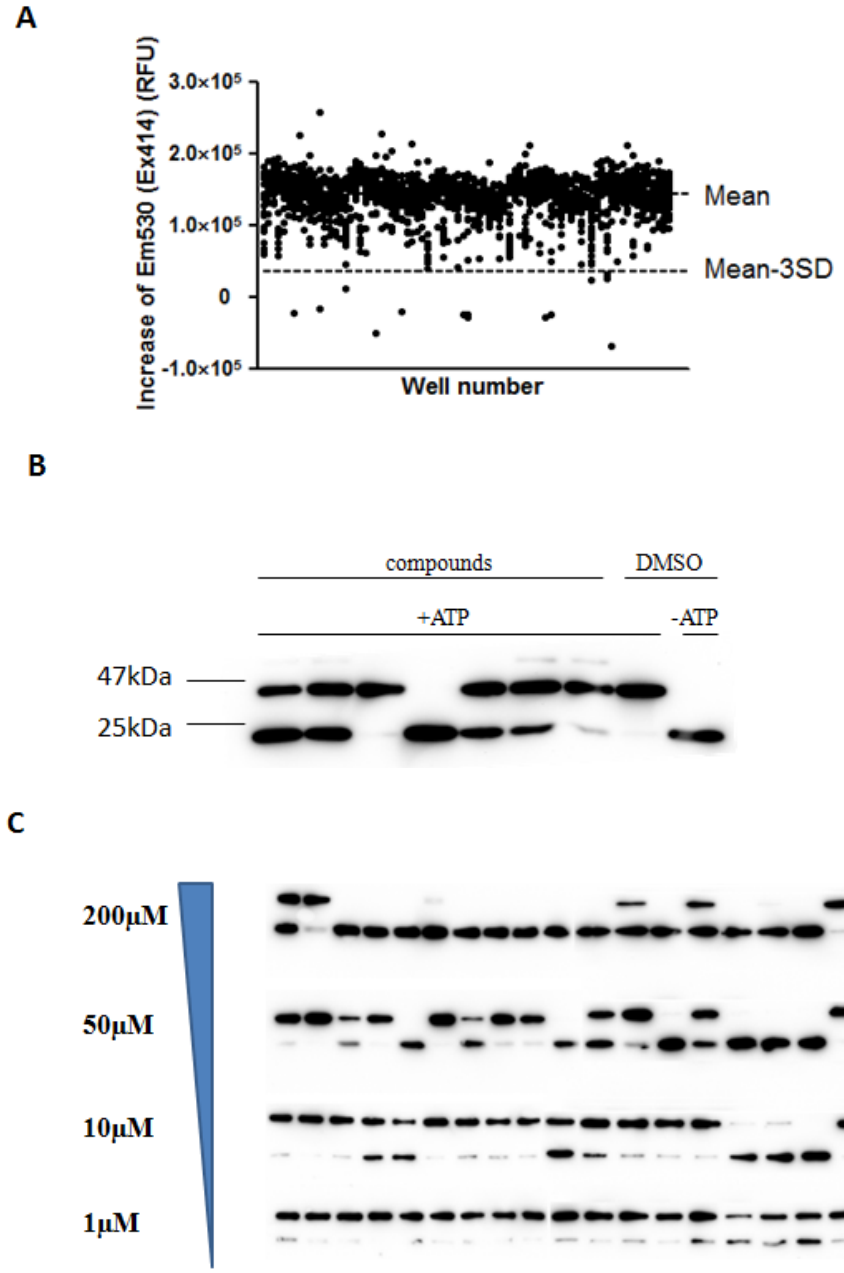

Figure 24. Screening and characterization of SUMOylation inhibitors. (A) Screening data from a sample of five 384-well plates. Compounds with Em_{530} increase less than Mean-3×SD were picked up. (B) *In vitro* SUMOylation assay to validate active SUMOylation inhibitors. (C) The inhibitory activities of compounds were tested at concentrations of 200, 50, 10 and 1 μM.

Characterization of compound activities in mammalian cells

Three most potent compounds were tested for their abilities to inhibit SUMOylation in mammalian cell culture. In the whole cell SUMOylation assay, HEK293 cells were plated in cell culture dishes. Compounds were added to the culture medium to a final concentration of 100 μM. After 4 hours of treatment, cells were collected and lysed. After the protein concentration of cell lysates were normalized, the concentration of high molecular-weight SUMOylation conjugates in the cell lysate was then determined by Western blotting using anti-SUMO1 antibody. Compared with DMSO-treated cells, one compound named ST025091 was able to decrease the in-cell concentration of SUMOylated proteins (Figure 25A). It inhibited SUMOylation in cells at a concentration as low as 10 μM (Figure 25B). As determined by *in vitro* SUMOylation assay, compound A has an IC_{50} (half maximal inhibitory concentration) value of 1.6 ± 0.3μM (Figure 25D), which is more potent than two previously identified SUMOylation inhibitors, ginkgolic acid (3.0 μM) and kerriamycin B (11.7 μM) (42, 43).

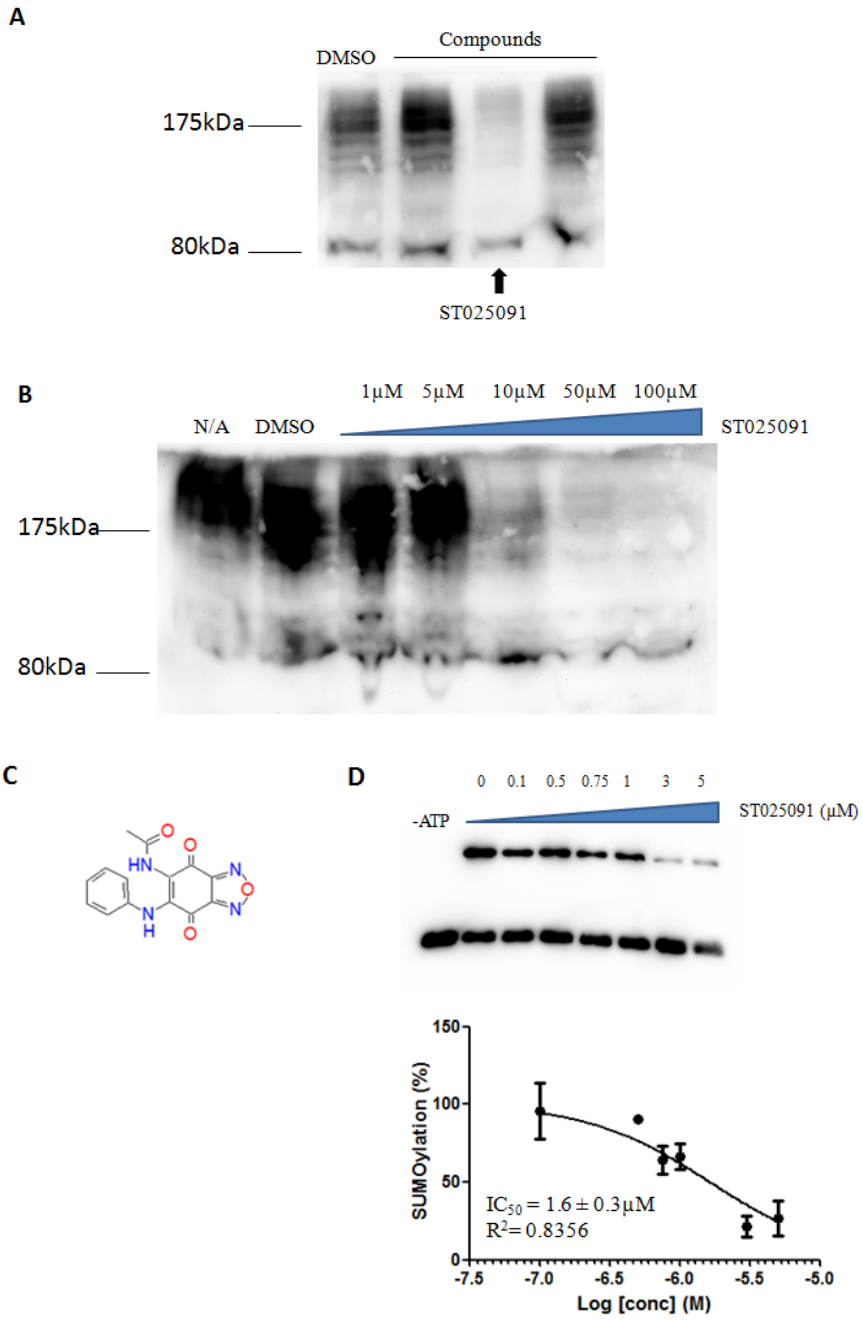

Figure 25. In-cell activity and *in vitro* IC_{50} of ST025091. (A) Test of compounds with whole cell SUMOylation assay. ST025091 was able to decrease the concentration of high molecular weight SUMOylated proteins in cells. (B) Titration of ST025091 to find the minimal functional concentration. (C) Structure of ST025091. (D) Determination of its IC50 by *in vitro* SUMOylation assay.

Discussion

In this chapter, I have developed a robust high-throughput screening platform for inhibitors of the SUMO pathway using the high efficiency energy transfer between SUMO and its substrate. Protein modification with fluorescent proteins is not only easy to achieve by molecular cloning, but also ensures that the optimal 1:1 ratio of FRET donor and acceptor in the assay. Another major advantage is that both SUMOylation and deSUMOylation inhibitors can be screened in the same assay. Furthermore, using changes of fluorescence intensity instead of ratiometric FRET signal as readout also reduces the possible interference of compound fluorescence. While the current assay is specific to SUMO1, it can be expanded to other isoforms including SUMO2 and SUMO3 and hopefully identify isoform-specific small chemical inhibitors of SUMOylation.

This high-throughput screening platform looks for compounds which target any step of the SUMOylation cascade, including activation of SUMO1 by Aos1, formation of thioester bond between SUMO1 and Uba2, transfer of SUMO1 to Ubc9 and to the final substrate RanGAP1C. As inhibitors of these individual steps are not distinguished, the potential hits from this assay may be either general SUMOylation inhibitors or inhibitors specific to RanGAP1C SUMOylation. E3 ligases may be incorporated into this *in vitro* assay in the future to look for compounds specific to the SUMOylation of other target proteins, and RanGAP1C used in current assay may be used as the control.

Screening of compounds from UCR and UIUC has identified the first synthetic SUMOylation inhibitor, ST025091. This compound is a general SUMOylation inhibitor and works both *in vitro* and in cell culture. A number of interesting questions are worthy to be investigated, such as what the mechanism of inhibition is, if changing functional group on the same scaffold can yield compounds with higher potency, and if this compound has a significant effect on biological pathways regulated by SUMOylation. In next chapter I will show some preliminary results on

mapping the target of ST025091. Our lab is also currently working to see its effect on cell death, cell proliferation, and JAK-STAT pathway. These studies will generate a lot of useful information about this inhibitor and help evaluate its potential in SUMO research and therapeutic applications.

CHAPTER 4: A FRET-based assay to detect SUMOylation intermediates

Abstract

SUMOylation is a multi-step reaction, in which SUMO is activated by E1 activating enzyme, transferred to E2 conjugating enzyme, and conjugated to substrates mediated by the E3 ligase *in vivo*. The structural and biochemical basis for the cascade reactions have been elucidated by several studies. However, the study of reaction intermediates has been hindered by their unstable chemical nature and lack of real-time detection method. In this chapter I will describe the development of a FRET-based assay to detect the formation of SUMOylation reaction intermediate *in vitro*. In this assay, fluorescent protein-tagged SUMO1 forms FRET pair with E1 subunits or E2, and the formation of protein complex was revealed by increase of FRET. The dependence on the activity of these enzymes was also confirmed in the assay. I further used this assay to map the target of the SUMOylation inhibitor identified in previous chapter. This FRET-based assay provides a novel strategy to study the activation and transfer cascade of the SUMO pathway, and can be potentially applied to other protein modifiers such as ubiquitin and NEDD8.

Introduction

Post-translational modification by ubiquitin (Ub) and ubiquitin-like proteins (Ubls), such as SUMO and NEDD8, plays critical roles in many physiological and pathological processes in eukaryotes (5, 15). The conjugation of Ubiquitin, SUMO and NEDD8 to target substrates share an evolutionary conserved, but distinct enzyme cascade that involves the sequential actions of E1, E2 and E3 ligases. E1 activates Ub/Ubls in two major steps. First, E1 catalyzes the adenylation of the Ub/Ubls at its C-terminus in the presence of ATP and Mg^{2+}. Second, a catalytic cysteine of E1 forms a covalent thioester bond with the C-terminus of Ub/Ubls by replacing the adenylate group . A transthiolation reaction then takes place between E1 and E2, resulting in the formation of thioester bond between E2 catalytic cysteine and Ub/Ubls. In combination with a variety of E3s, which are generally considered to determine substrate specificity *in vivo*, Ub/Ubls are finally conjugated to lysine residues of their substrates (14, 15).

Several studies have revealed insights into the biochemical and structural basis of Ub/Ubl with E1 and E2 enzyme recognition and successive steps in substrate conjugation (89, 90). First, biochemical studies show that E1 and E2 have different affinities for each other in their free or Ub/Ubl thioester-linked form. Free E1 has low affinity for E2, while as double Ub-loaded E1 binds to E2 with higher affinity (90, 91). These differential affinities between different enzyme forms may contribute to the Ub/Ubl progression along E1-E2-E3 cascade. Another study suggests that there is an intrinsic non-covalent interaction between SUMO and its E2, Ubc9, and this non-covalent interaction is required for poly-SUMOylation of substrates but not for mono-SUMOylation (62). Second, structures of E1 alone or in complexes with substrate, respectively, display similar domain orientations (92-95). Interestingly, the structure of an activation complex of NEDD8 containing heterodimeric E1, double-loaded NEDD8 (one bound non-covalently in the adenylation packet and one linked to E1 catalytic Cys domain via thioester bond), and the

NEDD8 E2 conjugating enzyme Ubc12 bound to the UFD domain revealed two E2 binding sites on E1(95). One binding site comes from conformational change of E1 after binding by NEDD8, and the other binding site comes from E1 and NEDD8 directly. The speculation that a conformational change of E1 upon the binding of Ubl may provide a mechanism to bring E1 and E2 catalytic cysteine domains to a close proximity has been further demonstrated by a recent structure studies of SUMO-E1 adenylate and tetrahedral intermediate analogues (16). A striking conformational change of E1 has been observed after the thioester bond formation between SUMO and E1. This conformational change may potentially bring two catalytic Cys residues of E1 and E2 within 3.5Å which facilitates the transfer of SUMO from E1 to E2 (16).

Although much knowledge for the activation and transfer of Ub/Ubls has been learned from these studies, mechanistic mechanisms of Ubl activation and switches between E1 and E2 ligases have not been completely determined. In addition, the study of reaction intermediates has been hindered by the unstable chemical nature of thioester bonds and lack of real-time detection method. In one example reported in 2010 (16), the reaction intermediates in SUMOylation are detected by using fluorescent-tagged ATP and quickly separating the reaction mixtures on SDS-PAGE followed by immediate imaging. In this chapter I will describe the development of a FRET-based method to detect the conjugation of SUMO to its E1 and E2 enzymes in a real-time manner. In this method, SUMO1 and another protein, either Aos1 or Uba2 or Ubc9, are modified by CyPet and YPet, respectively. Formation of SUMO1-E1 or SUMO1-E2 complex will increase the FRET signal between CyPet and YPet. The development of this method will facilitate the study of enzyme function in the SUMOylation cascade, and also help the characterization of SUMOylation inhibitors I identified from previous high-throughput screening assays.

Materials and methods

Molecular cloning of DNA constructs

The open reading frames of SUMO1, Aos1, Uba2, Ubc9 and the C-terminal domain of RanGAP1 (420-587) were amplified by PCR and the PCR products were cloned into pCRII-TOPO vector (Invitrogen). Point mutations on SUMO1, Uba2 and Ubc9 were created by PCR mutagenesis. After their sequences were confirmed, the cDNAs were ligated into linearized pCRII-CyPet or pCRII-YPet to create fusion genes encoding fluorescence labeled fusion proteins. The cDNAs encoding these proteins were then cloned into pET28(b) vector (Novagen).

Protein expression and purification

BL21 (DE3) *E.coli* cells were transformed with pET28 vectors encoding SUMO1, Aos1, Uba2, Ubc9, RanGAP1C, their mutants, and fluorescent protein-labeled versions. The transformed bacteria were inoculated in 2xYT medium and the expression of polyhistidine-tagged recombinant proteins was induced with 0.1 mM IPTG at 25°C overnight. The recombinant proteins were purified by Ni^{2+}-NTA agarose beads (QIAGEN) followed by gel filtration HPLC using Superdex75 10/300 GL column on a HPLC purification system (GE Healthcare*, ÄKTA™ purifier*). Protein purity was later confirmed by SDS-PAGE followed by Coomassie blue staining and their concentrations were determined by Coomassie Plus Protein Assay (Pierce).

FRET measurement

After the proteins labeled by CyPet or YPet are mixed in the presence or absence of other protein members or cofactors, their fluorescence was determined by the fluorescent plate reader Flexstation II^{384} (Molecular Devices) in a 384-well plate over a period of time. The emission intensities at three wavelengths were collected: 475 nm and 530 nm at excitation wavelength of 414 nm, and 530 nm at excitation wavelength of 475 nm. After the emission intensities were

corrected by subtraction of background fluorescence from the plate, the FRET indexes (see Results) at different time points were calculated and compared.

Protein Interaction and SUMOylation assay

For the interaction of SUMO1 with E1, 20 pmole CyPet-SUMO1 and 20 pmole YPet-Aos1 or YPet-Uba2 were mixed in the presence or absence of 20 pmole Uba2 or Aos1, respectively, in a buffered solution containing 50 mM Tris-HCl (pH=7.4), 1 mM DTT and 4 mM $MgCl_2$ with a total volume of 36 µL. Samples were incubated at 37°C and fluorescence emission was monitored after 4 µL 10 mM ATP or H_2O was added at time zero. For mutant Uba2 interaction assay, 20 pmole CyPet-SUMO1, 20 pmole wild type or mutant YPet-Uba2 and 10 pmole Aos1 were mixed in the buffered above in a total volume of 36 µL. For the interaction of SUMO1 and Uba2 in the presence of Ubc9, 10 pmole CyPet-SUMO1, 10 pmole YPet-Uba2 and 10 pmole Aos1 were mixed in the presence or absence of 100 pmole wild type or mutant Ubc9 in the buffer above. Samples were measured by FRET index after 4 µL of 10 mM ATP was added.

For the interaction assay of SUMO1 and Ubc9, 0.4 µg CyPet-SUMO1 and 0.5 µg YPet-Ubc9 were mixed in 20 µL PBS. 0 to 2 µg nonfluorescence-labeled SUMO1 was added to the mixture and the FRET indexes were determined. In the interaction assay of SUMO1 and Ubc9, 20 pmole CyPet-SUMO1, 20 pmole wild type or mutant YPet-Ubc9, 10 pmole Aos1 and 20 pmole Uba2 were mixed in a buffered solution containing 50 mM Tris-HCl (pH=7.4), 1 mM DTT and 4 mM $MgCl_2$ with a total volume of 36 µL. For mutant Uba2 assay, 10 pmole wild type or mutant Uba2 was added. Samples were incubated at 37°C and fluorescence emission was monitored after 4 µL 10mM ATP or H_2O was added at time zero.

For the interaction assays of wild type or mutant SUMO1 and mutant or wild type Ubc9, respectively, 20 pmole wild type or mutant CyPet-SUMO1 and 20 pmole wild type or mutant

YPet-Ubc9 were mixed in the presence or absence of 10 pmole Aos1 and 10 pmole Uba2 in a buffer above.

For the SUMO1 conjugation assay of mutant SUMO1 peptide, 0.4 µg wild type or mutant CyPet-SUMO1, 0.5 µg YPet-RanGAP1C, 0.05 µg Aos1, 0.1 µg Uba2 and 0.5 µg Ubc9 were mixed in the buffer above, containing 50 mM Tris-HCl (pH7.4), 1 mM DTT, and 4 mM $MgCl_2$ with a total volume of 36 µL. Samples were incubated at 37°C and fluorescence emission was monitored after 4 µL 10 mM ATP or H_2O was added at time zero. Samples were measured by FRET index at different time points.

For the SUMO1 conjugation assay of mutant Ubc9 or Uba2, SUMO1 peptide 0.4 µg CyPet-SUMO1, 0.5 µg YPet-RanGAP1C, 0.05 µg Aos1 were mixed in the presence or absence of 0.1 µg wild type or mutant Uba2 and 0.5 µg wild type or mutant Ubc9 in the buffer above.

The wild type or mutant form of 0.5 µg SUMO1, 0.05 µg FLAG-tagged RanGAP1C, 0.05 µg Aos1, 0.1 µg Uba2 and 0.5 µg Ubc9 were mixed in a buffered solution containing 50 mM Tris-HCl (pH=7.4), 1 mM DTT, 4 mM $MgCl_2$ and 1 mM ATP with a total volume of 40 µL. Samples were incubated at 37°C for 1 hour. After they were separated by 10% SDS-PAGE and transferred to a nitrocellulose membrane, the RanGAP1C proteins were recognized by incubation with mouse anti-FLAG antibody (Sigma Aldrich) followed by HRP-labeled goat anti-mouse IgG antibody (Sigma Aldrich). The chemiluminescence was developed using the Supersignal® West Dura Extended Duration Substrate (Thermo Scientific) and captured by Biospectrum® imaging system (UVP, LLC.).

Results

Design of FRET-based method for monitoring SUMOylation cascade and definition of FRET index.

To determine the formation of the reaction intermediate SUMO-E1 and SUMO-E2 protein complex during the SUMOylation cascade, I used a FRET-based method, which involves the FRET pair CyPet- and YPet-labeled SUMO1, Aos1 (E1 subunit), Uba2 (E1 subunit), Ubc9 (E2), the C-terminal domain (420-587) of RanGAP1 (RanGAP1C, substrate) and their mutants which lose different activities in the SUMOylation cascade (64, 86, 87) (Figure 26A). When CyPet-tagged protein is mixed with YPet-tagged protein *in vitro*, interaction between two proteins can shorten the distance between the FRET pair and result in two emission peaks at 475 nm and 530 nm when the mixture is excited at 414 nm. In order to quantitatively assess the relative extent of FRET in the system, a new spectrum analysis method has been described in chapter 1. In this method, the emission signal at 530 nm emission (Em_{total}) is divided into three components: direct emission from unquenched donor CyPet (CyPet[cont]), direct emission from the acceptor YPet (YPet[cont]), and FRET emission from YPet (Em_{FRET}) (Figure 26B). The direct emission of CyPet and YPet at 530 nm (Ex=414nm) is proportional to their emission at 475 nm (Ex=414nm) (FL_{DD}) and 530 nm (Ex=475nm) (FL_{AA}) by constant ratios α and β, which were determined to be 0.35 and 0.029, respectively. Therefore, I can calculate the CyPet (cont) and YPet (cont), and subtract them from Em_{total} to derive Em_{FRET}. In order to use FRET to monitor the change of protein-protein interaction status, the FRET index r is defined to be the ratio of FRET emission (Em_{FRET}) to the emission at 530 nm (Ex=475nm) (FL_{AA}):

$$r = \frac{Em_{FRET}}{FL_{AA}} = \frac{FL_{DA} - \alpha \times FL_{DD} - \beta \times FL_{AA}}{FL_{AA}}$$

Since FL_{AA} is contributed by direct emission of YPet, the FRET index can indicate the relative percentage of YPet that receives energy from excited CyPet, and therefore the FRET index can be

used as quantitative measurement of FRET signal. When the proteins involved in the SUMOylation process are mixed and the conjugation cascade is initiated, the formation of protein complexes will lead to an increase of the FRET index whereas disruption of protein complexes will result in a decrease of the FRET index.

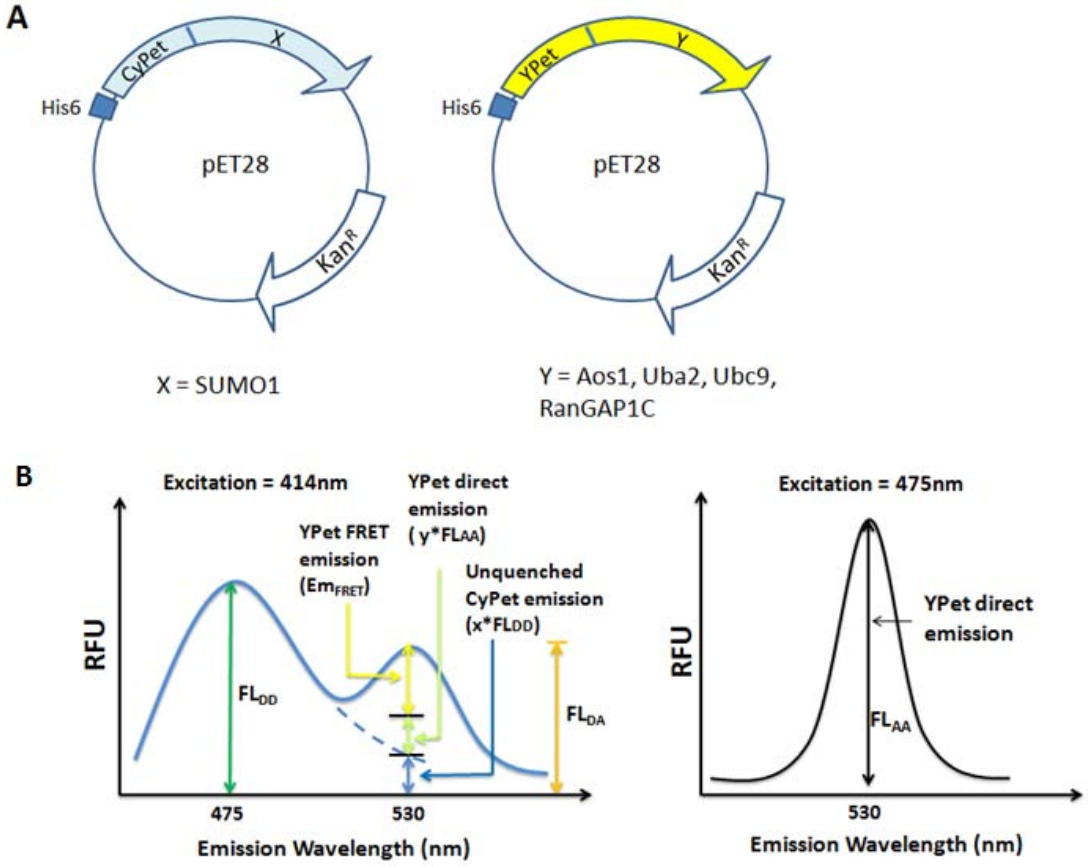

Figure 26. FRET between CyPet- and YPet-tagged proteins. (A) The cloning maps of bacterial expression vectors encoding the fusion proteins. (B) Analysis of fluorescence emission spectra of the mixtures of CyPet and YPet-tagged proteins.

Detection of SUMO-E1 protein complex by FRET

The structures of E1 identified residues from both Aos1 and Uba2 that contact Mg^{2+}/ATP and the Ub/Ubl C-terminal glycine (92-94, 96). I first determined the formation of complex between SUMO1 and heterodimeric E1 (Aos1/Uba2), which initiates the SUMOylation cascade and catalyzes two critical reactions, adenylation with the help of ATP and thioester bond formation with one of E1 subunit, Uba2. When SUMO1 and Aos1 were tagged with CyPet and YPet respectively, no significant FRET was observed between CyPet-SUMO1 and YPet-Aos1 without ATP and Uba2 (Figure 27A). However, in case both Uba2 and ATP were added to the protein mixture, a large increase of FRET index was observed and it reached plateau in about 20 min (Figure 27A, open square). This suggests that interaction between SUMO1 and Aos1 requires the presence of both Uba2 and ATP. Similar results were observed when SUMO1 and Uba2 were labeled with the CyPet and YPet pair, respectively. In consistence with the results above, strong interaction between CyPet-SUMO1 and YPet-Uba2 were observed only after Aos1 and ATP were added (Figure 27B). In case of CyPet-SUMO1 and YPet-Uba2, the FRET index increased to maximum in 5 min and dropped to baseline after about 30 min. Addition of more ATP into the reaction mixture did not rescue the FRET signal (Figure 27B, close square), which suggests the decrease of FRET index is not due to ATP depletion.

The dependence of FRET increase between CyPet-SUMO1 and YPet-Aos1 or YPet-Uba2 on ATP indicates the FRET signal I observed is due to the formation of complex between SUMO1 and E1 upon SUMO1 activation, but whether it is via non-covalent interaction with E1 subunits or covalent conjugation to Uba2 is not clear. To answer this question, I generated a mutant of Uba2 with its catalytic cysteine changed to serine (C173S), which lacks the ability to form thioester bond with activated SUMO1. A strong increase of FRET index was still observed between Uba2 (C173S) mutant and SUMO1, and interestingly the FRET index did not decrease

as fast as its wild type counterpart (Figure 27C). This suggests that the formation of thioester bond between SUMO1 and E1 is not required for their FRET, which is at least partially contributed by the non-covalent interaction between E1 and activated SUMO1.

The activation complex of SUMO-E1-E2 is not stable because SUMO conjugating to Uba2 via thioester bond is readily passed to the catalytic cysteine of E2. It would be interesting to determine how SUMO1-E1 active complex forms in the presence of Ubc9. Consistent with previous result, FRET index between CyPet-SUMO1 and YPet-Uba2 reached the peak in the presence of Aos1 and ATP, and then dropped to the background level of two separated proteins over 30 min (Figure 27D filled circle). In the presence of Ubc9, the FRET signal of SUMO1-Uba2 active complex did not increase as fast as it does in the absence of Ubc9, which suggests a quick transfer of SUMO1 from Uba2 to Ubc9 (Figure 27D open circle). Interestingly, in the presence of catalytic deficient mutant of Ubc9 (C93S), the increase rate of FRET index was comparable to the case where no Ubc9 is present (Figure 27D filled square). These results suggest that the accumulation of SUMO-E1 complex upon SUMO activation can be slowed down by E2, as SUMO forming thioester bond with Uba2 can be quickly transferred to the cysteine catalytic site of Ubc9.

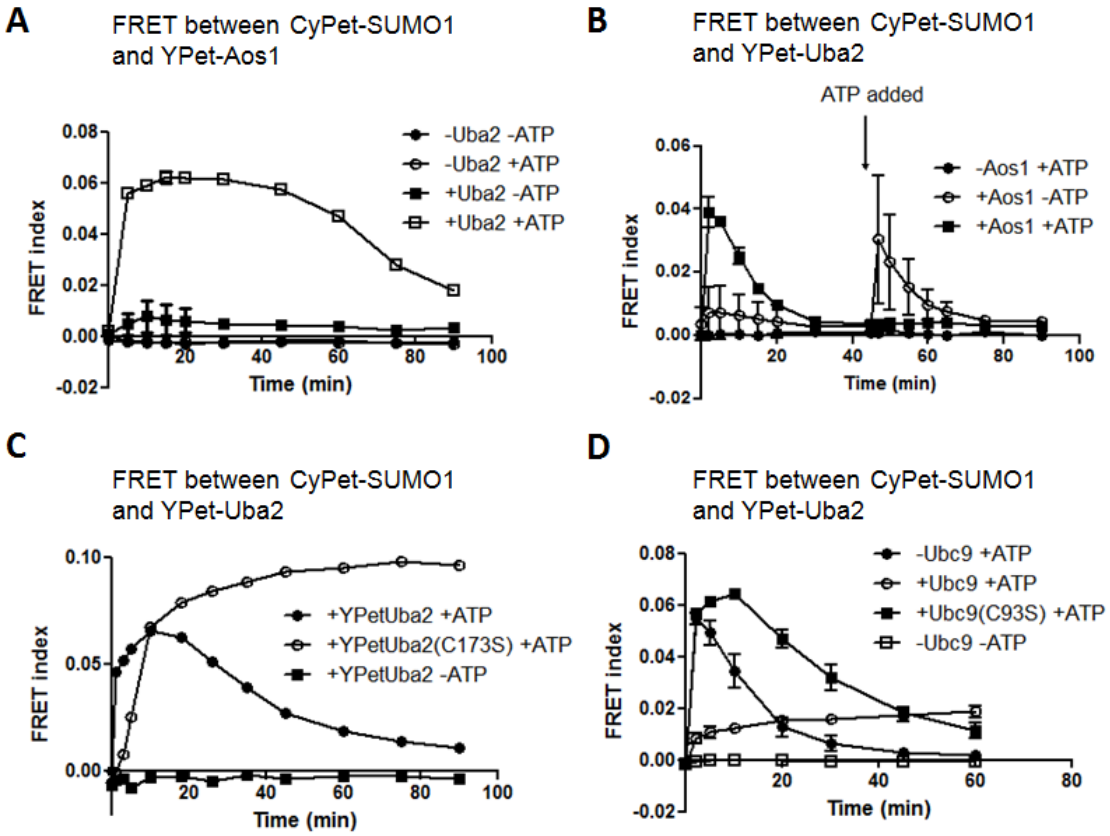

Figure 27. Detection of SUMO-E1 complex by FRET. ATP was added at time zero to initiate the reactions. (A) FRET between CyPet-SUMO1 and YPet-Aos1 in the presence or absence of Uba2 and ATP. (B) FRET between CyPet-SUMO1 and YPet-Uba2 in the presence or absence of Aos1 and ATP. ATP was added to all the samples at 45 min to test if the decrease of FRET index is due to ATP depletion. (C) FRET between CyPet-SUMO1 and YPet-tagged Uba2 (WT) or Uba2 (C173S) in the presence of Aos1. (D) FRET between CyPet-SUMO1 and YPet-Uba2 in the presence of Aos1 and Ubc9 (WT) or Ubc9 (C93S).

Determination of two levels of interaction between SUMO1 and Ubc9.

SUMO1 binds to its E2 enzyme Ubc9 in a non-covalent manner and also form covalent thioester bond with catalytic cysteine of Ubc9 in the SUMOylation cascade (62). To determine whether these two interactions can be distinguished by FRET, I analyzed the interaction between SUMO1 and Ubc9, which were tagged with CyPet and YPet, respectively. In the presence of E1 (Aos1 and Uba2) and ATP, the FRET index between CyPet-SUMO1 and YPet-Ubc9 quickly increased and reached a peak (Figure 28A closed circle), which can be clearly distinguished from the baseline indicating the non-covalent interaction of SUMO1 and Ubc9 (Figure 28A open square). The formation of this SUMO-E2 complex requires the presence of ATP and both active E1 subunits (Figure 28A). In order to investigate if the FRET increase is due to the formation of covalent complex between SUMO1 and Ubc9, I generated a mutant of Ubc9 (C93S) which lacks the ability to form thioester bond with SUMO1. No significant FRET increase was observed between CyPet-SUMO1 and YPet-Ubc9 (C93S) when E1 and ATP were added (Figure 28B). These results suggest that the FRET-based method is able to detect the non-covalent interaction between SUMO1 and Ubc9 as well as the formation of SUMO1-Ubc9 covalent complex in the presence of E1 and ATP.

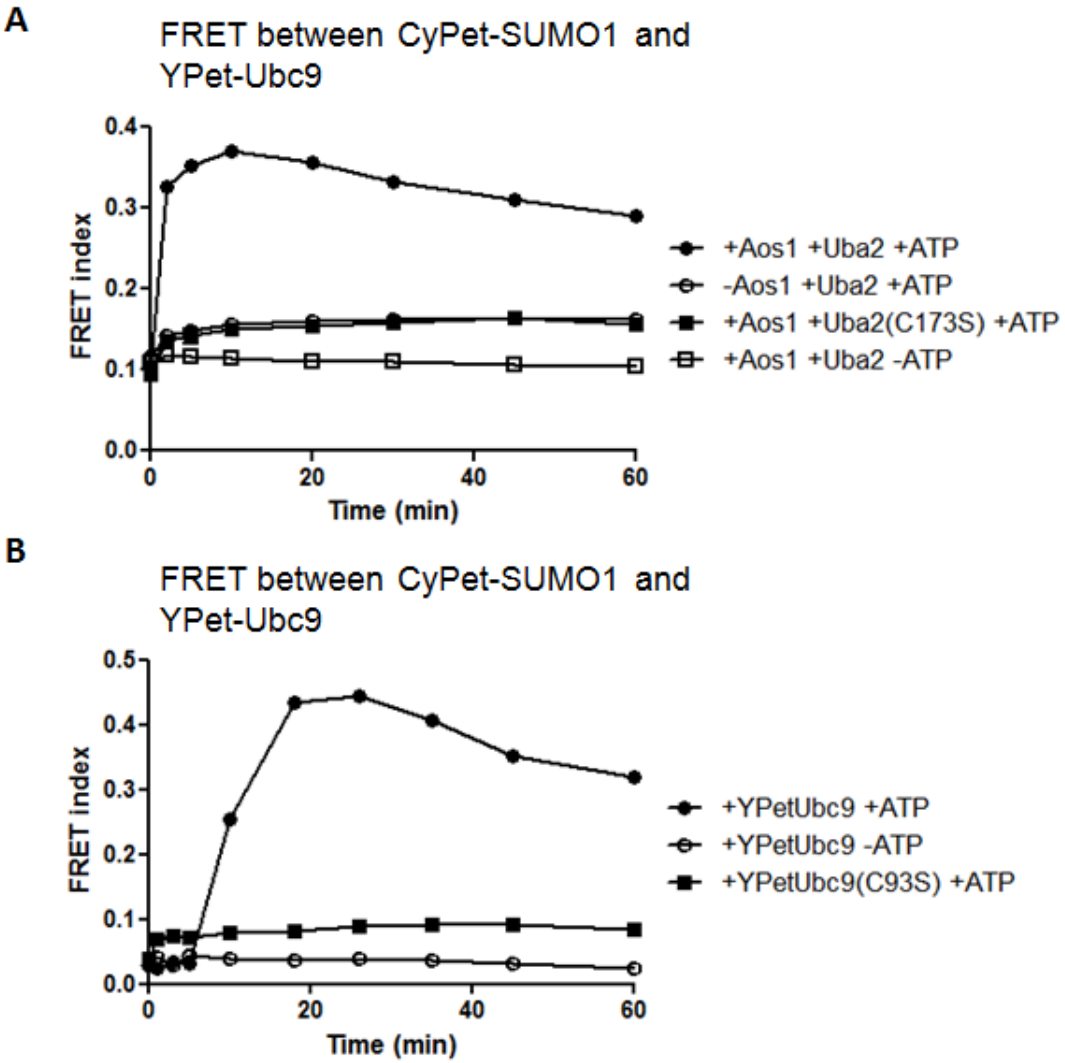

Figure 28. Detection of SUMO-E2 complex by FRET. ATP was added at time zero to initiate the reactions. (A) Increase of FRET between CyPet-SUMO1 and YPet-Ubc9 requires the presence of both ATP and active E1. (B) Mutation of the active cysteine residue of Ubc9 abolished the FRET increase between CyPet-SUMO1 and YPet-Ubc9. Aos1 and Uba2 were added in all samples.

Independence of SUMOylation cascade on the non-covalent SUMO1-Ubc9 interaction

Previous biochemical studies have indicated that the non-covalent interaction of SUMO and Ubc9 is not essential for the SUMOylation cascade but promotes the formation of poly-SUMO chain on substrate proteins (62). In order to validate this FRET assay, I would like to see if this independence can be confirmed by FRET. Mutation of R17E on Ubc9 has been shown to abolish its binding affinity with both E1 and SUMO1 and the mutation of E67R or G68Y on SUMO1 either completely or partially abolished its non-covalent interaction with Ubc9 (62). After a mutant Ubc9 (R17E) and a double mutant of SUMO1 (E67R/G68Y) were generated. The non-covalent interaction between wide type and mutant SUMO1, Uba2 and Ubc9 were then determined using the FRET assay. As shown in figure 29A and 29B, SUMO1 (E67R/G68Y) does not have non-covalent interaction with Ubc9, and Ubc9 (R17E) loses binding affinity with both SUMO1 and Uba2. I further tested if these two mutants can support the formation of covalent SUMO-E2 complex. Wide type and mutant CyPet-SUMO1 and YPet-Ubc9 were supplemented with E1 and ATP and the FRET index was monitored after the reactions were initiated (Figure 30). A significant FRET increase was observed between CyPet-SUMO1 (E67R/G68Y) and YPet-Ubc9 (Figure 30, closed triangle) but not between CyPet-SUMO1 and YPet-Ubc9 (R17E) (Figure 30, open square), which indicates the covalent complex of SUMO1 and Ubc9 is independent of their non-covalent interaction but cannot form when both SUMO1-Ubc9 and Uba2-Ubc9 interactions are disrupted. These mutants were also tested using *in vitro* SUMOylation assay, in which CyPet-SUMO1 is conjugated to YPet-RanGAP1C in the presence of E1, E2 and ATP. Similar results were obtained by FRET (Figure 31A, 31B) or immunoblotting (Figure 31C). These results confirmed that the non-covalent interaction between SUMO1 and Ubc9 is not required for the SUMOylation cascade and showed that this FRET-based assay is a reliable method to study these processes.

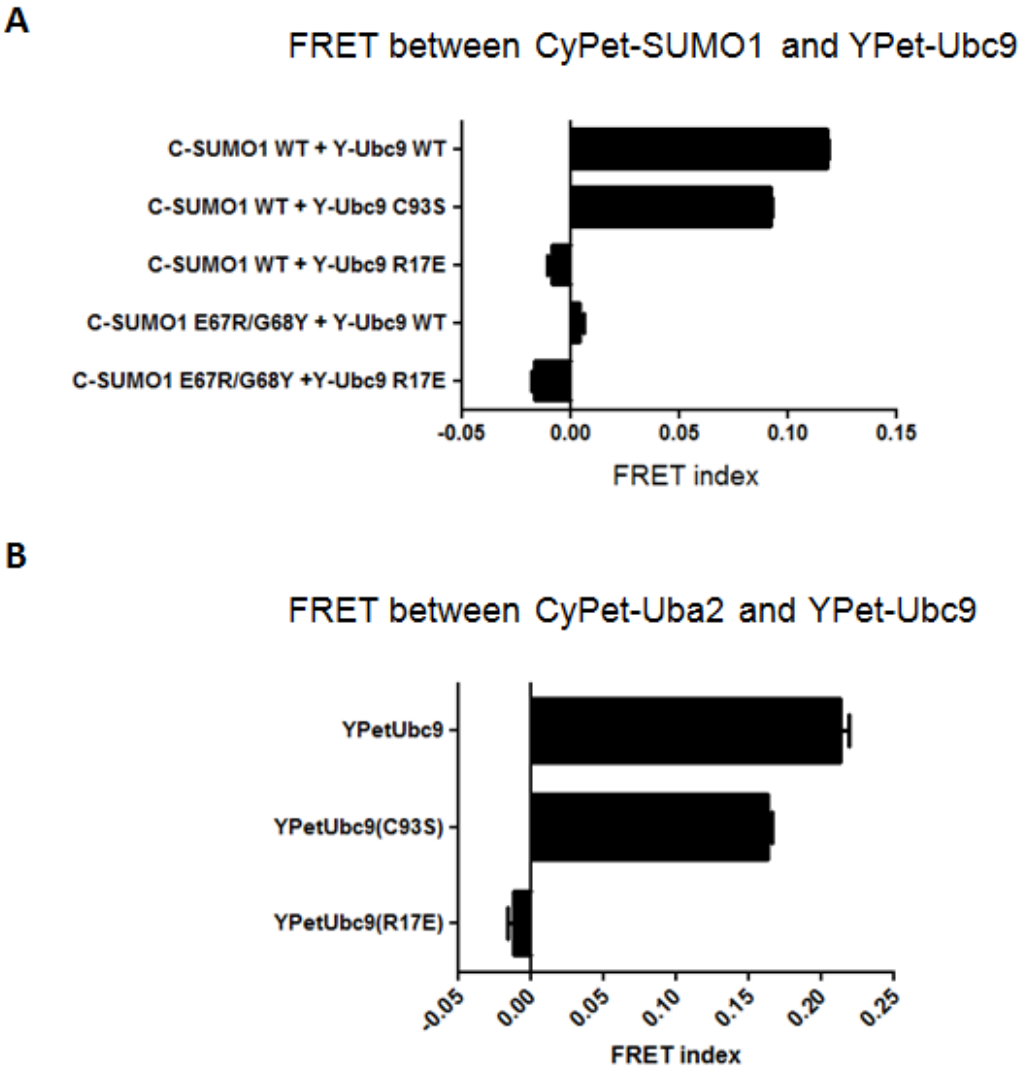

Figure 29. Interaction characteristics of SUMO1 and Ubc9 mutants. (A) 20 pmole CyPet-SUMO1 and 20 pmole YPet-Ubc9 were mixed in 40 µL buffer. FRET index was determined in triplicate. (B) 10 pmole CyPet-Uba2 and 10 pmole YPet-Ubc9 were mixed in 40 µL buffer. FRET index was determined in triplicate.

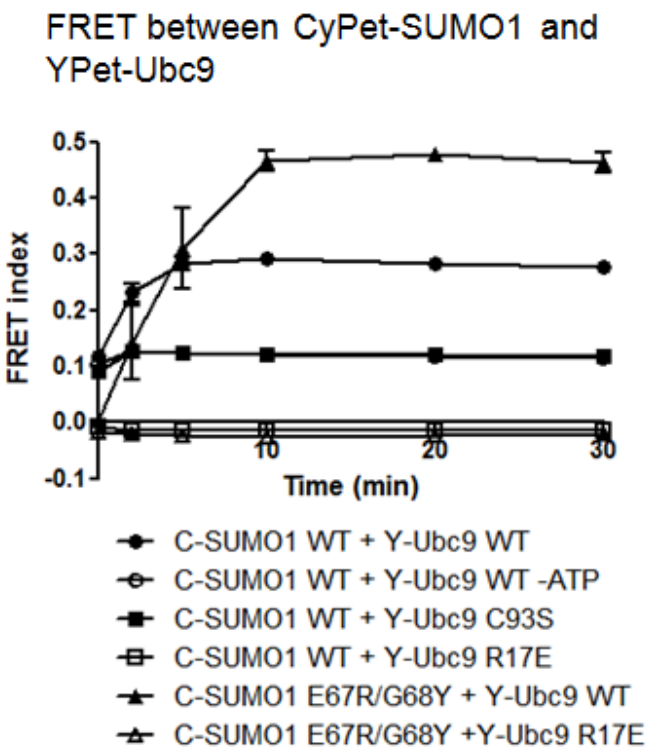

Figure 30. Formation of SUMO-E2 complex is independent of SUMO-E2 non-covalent interaction but cannot stand the lost of both SUMO-E2 and E1-E2 non-covalent interaction. Aos1 and Uba2 were added in all samples and ATP was added at time zero to start the reactions.

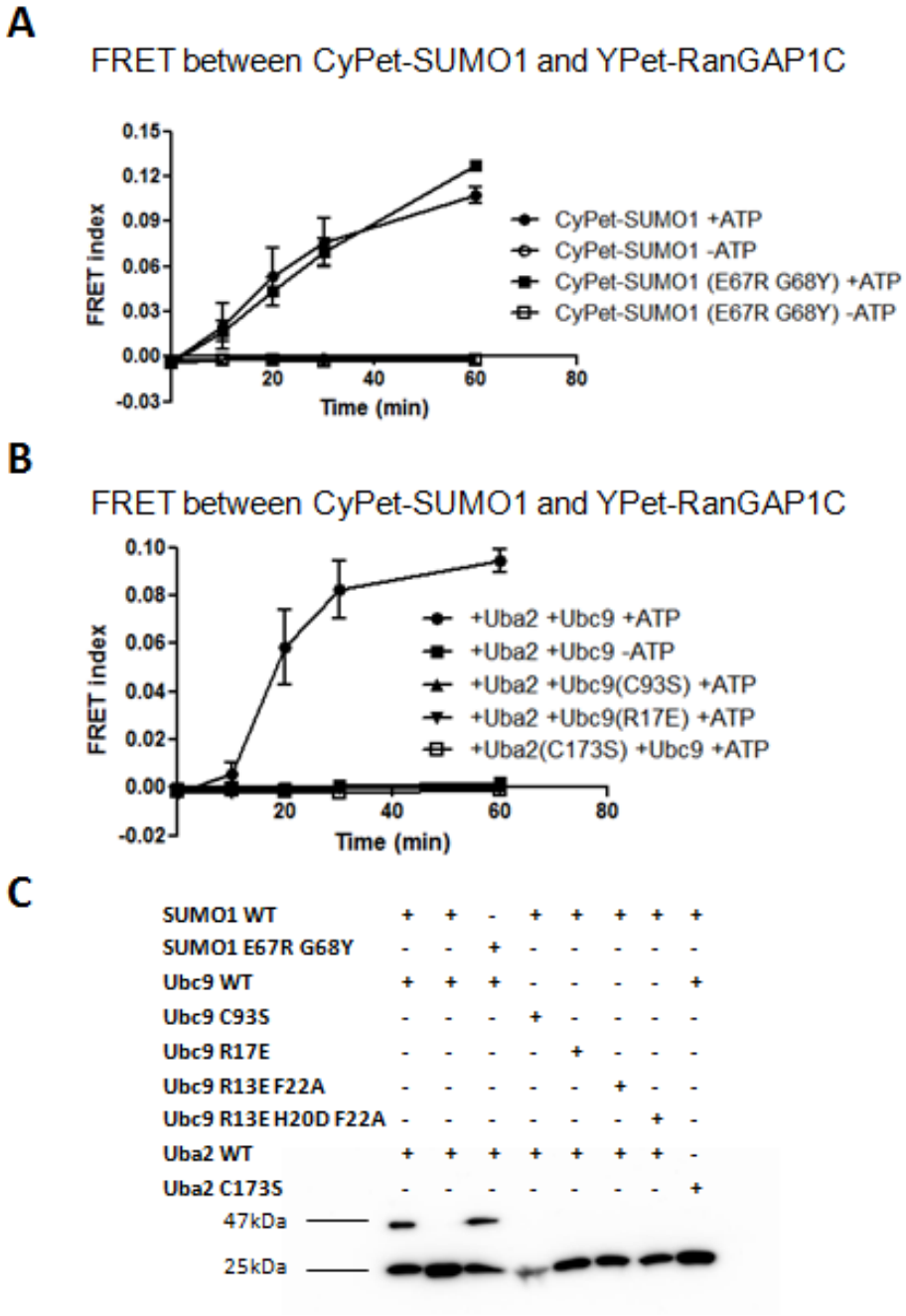

Figure 31. E1-E2 interaction but not SUMO-E2 interaction is required for SUMOylation of RanGAP1C. (A) SUMOylation of RanGAP1 does not require the non-covalent interaction between SUMO1 and Ubc9. (B) SUMOylation of RanGAP1C requires active E1, E2 and interaction between E1 and E2. (C) Western blotting confirms the inability of mutant Ubc9 to mediate the SUMOylation of RanGAP1.

Mapping the target of SUMOylation inhibitor ST025091 by FRET assay

A compound named ST025091 has been identified as small chemical inhibitors of SUMOylation, as described in chapter 3. Because the high-throughput screening platform used to identify this compound adopts a multi-step SUMOylation reaction in the assay, it cannot give detailed information about the target of the inhibitor. I would like to use the FRET-based assay developed in this chapter to figure out if ST025091 can inhibit the formation of SUMO1-E1 complex or SUMO1-E2 complex, or the final transfer of SUMO1 from Ubc9 to RanGAP1C. In the experiments, the FRET index between CyPet-SUMO1 and YPet-Uba2 or YPet-Ubc9 or YPet-RanGAP1C was monitored as described above. ST025091 was added to a concentration of 50 μM and its effect on FRET index increase was determined. As shown in figure 32, ST025091 significantly inhibited the increase of FRET index between all protein pairs. This suggests that ST025091 inhibits SUMOylation by at least inhibiting the formation of SUMO1-E1 complex, but whether it targets Aos1-mediated SUMO1 activation or thioester bond formation between activated SUMO1 and Uba2 is still unclear yet.

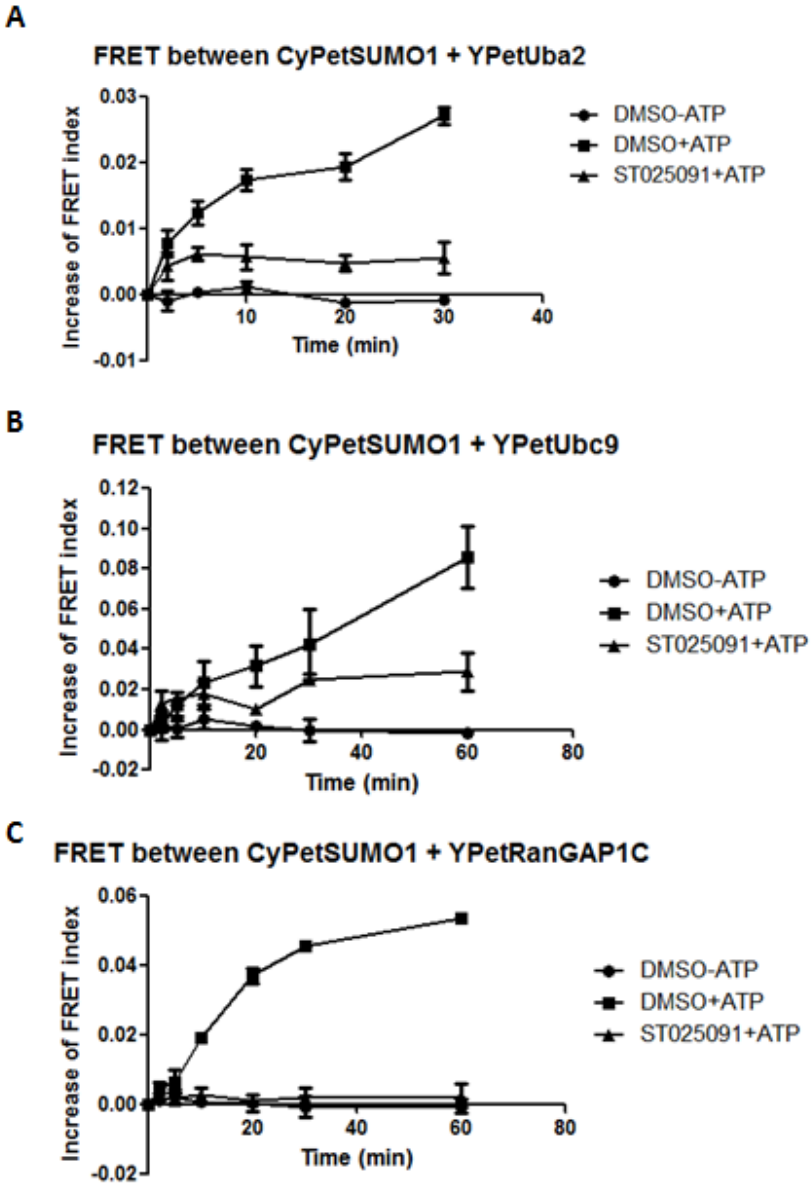

Figure 32. Effect of ST025091 on the formation of different protein complexes involved in SUMOylation. (A) ST025091 inhibits the increase of FRET between CyPetSUMO1 and YPet-Uba2 in the presence of Aos1. (B) ST025091 inhibits the increase of FRET between CyPetSUMO1 and YPet-Ubc9 in the presence of Aos1 and Uba2. (C) ST025091 inhibits the increase of FRET between CyPetSUMO1 and YPet-RanGAP1C in the presence of Aos1, Uba2 and Ubc9.

Discussion

In this chapter, I developed a FRET-based assay to detect the formation of intermediate protein complex in the SUMOylation cascade. This method is based on high-efficient FRET between protein pairs and can monitor the proceeding of SUMOylation reaction in real-time manner. The formation of SUMO-E1 and SUMO-E2 complex during SUMOylation can be detected as an increase of FRET index between fluorescent-tagged protein pairs. The advantage of using FRET index to determine the strength of FRET signal is that it not only eliminates the interference of the direction emission of unquenched CyPet and YPet at the same wavelength, but also considers possible changes in the total fluorescence of YPet. After prolonged exposure to excitation light, YPet might be photo-bleached, which leads to decreased total fluorescence and FRET emission. Calculating the ratio of FRET emission to total fluorescence solves this issue. Therefore FRET index should serve as a good standard to monitor the relative strength of FRET signal in a given system. However, FRET index of protein pairs with dramatically different conformations cannot be compared due to large changes in FRET efficiencies.

While the increase and decrease rate of FRET index can be determined from the assay, it should be considered as a qualitative assay rather than a quantitative assay for the measurement of enzymes kinetics. First, even with the same enzyme, different purified batches often have varied activities, which will lead to different rates of FRET changes in the assay. Second, modification with fluorescent proteins may affect the activity of the enzyme, so the reaction rate of CyPet-SUMO1 + YPet-Aos1 + Uba2 and CyPet-SUMO1 + Aos1 + YPet-Uba2 is likely to be different. One good example of how this FRET-based assay can be used is demonstrated at the end of this chapter, where this FRET-based assay was used to analyze the target of a SUMOylation inhibitor. In this application, the effects of different compounds on FRET index were compared on a given FRET pair, therefore avoiding the issues discussed above.

When this FRET assay is used to detect the formation of SUMO1-Aos1 and SUMO-Uba2 complex, fast decrease of the FRET index was observed after it reached the peak in five to twenty minutes. The exact nature of this phenomenon is still unclear, although there are several hints to the fact. Adding ATP to the mixture of CyPet-SUMO1 and YPet-Uba2 which already reacted and showed FRET increase could not rescue the FRET signal. Furthermore, mutating the active cysteine residue of Uba2 largely abolished the decrease of the FRET index. Based on the crystal structure of the SUMO-E1 intermediate analogue (16), SUMO1 is activated by ATP hydrolysis and bound non-covalently to the binding pocket of Aos1. The complex of SUMO1-Aos1-Uba2 then undergoes a large conformational change so that the C-terminal glycine residue of SUMO1 gets close to the catalytic cysteine residue of Uba2. The two residues then form a thioester bond and SUMO1 will leave the binding pocket of Aos1. Therefore, one possible explanation of the FRET decrease observed between SUMO1 and Aos1/Uba2 is that the FRET signal reflects the status of active SUMO1 binding to the pocket of Aos1. The presence of wide type Uba2 will make SUMO1 get out of the binding pocket and reduces FRET but mutant Uba2 will not have the same effect. Although still a hypothesis, this demonstrates a good example of how this FRET assay can provide insights of the dynamic interactions of proteins in biological process.

CONCLUSIONS

In this dissertation, I have developed several FRET-based assays to study the protein-protein interactions in the SUMO pathway, which is an important protein post-translational modification. FRET is achieved by modifying the N-terminus of target proteins with a pair of engineered fluorescent proteins. Non-covalent interaction or covalent conjugation of fluorescent-tagged proteins will be then detected by changes of FRET. I first used FRET to quantitatively determine the dissociation constant of a well-studied protein pair, SUMO1 and Ubc9. The fluorescence spectrum was carefully analyzed to separate FRET emission from other direct emissions, and novel mathematical algorithms were developed to depict the relationship between protein concentration and FRET emission. The method was tested under different conditions and validated by traditional biochemical methods. It also offers great advantages to previous FRET-based K_d measurement assays. I further apply this FRET technique into high-throughput screening assays to look for small chemical inhibitors which either disrupts the non-covalent protein interactions or inhibits the SUMOylation of substrate proteins. These high-throughput screening assays provide fast and reliable method for the identification of compounds targeting the SUMO pathway. Several screening attempts also discovered the first synthetic small chemical inhibitor of SUMOylation, which is currently under further investigation in our lab. Finally, the principle of FRET was used to develop the first assay for the real-time detection of transient covalent interaction between proteins involved in the SUMO pathway. The formations of SUMO-E1 and SUMO-E2 complex during the SUMOylation reaction were detected, and their dependence on different enzymes was confirmed by using wide type or mutant form of enzymes in the assay. The target of the SUMOylation inhibitor identified from the screening was also successfully revealed using this FRET-based method. Overall the work described in this dissertation provides novel powerful tools for the study of non-covalent and covalent protein-

protein interactions in the SUMO pathway, and can be hopefully expanded to the research of other protein modifiers such as ubiquitin and ubiquitin-like proteins.

REFERENCES

1. Chang C & Stewart RC (1998) The two-component system. Regulation of diverse signaling pathways in prokaryotes and eukaryotes. *Plant Physiol* 117(3):723-731.
2. Barford D, Das AK, & Egloff MP (1998) The structure and mechanism of protein phosphatases: insights into catalysis and regulation. *Annu Rev Biophys Biomol Struct* 27:133-164.
3. Sadoul K, Boyault C, Pabion M, & Khochbin S (2008) Regulation of protein turnover by acetyltransferases and deacetylases. *Biochimie* 90(2):306-312.
4. Grewal SI & Rice JC (2004) Regulation of heterochromatin by histone methylation and small RNAs. *Curr Opin Cell Biol* 16(3):230-238.
5. Hershko A & Ciechanover A (1998) The ubiquitin system. *Annu Rev Biochem* 67:425-479.
6. Johnson ES (2004) Protein modification by SUMO. *Annu Rev Biochem* 73:355-382.
7. Shen Z, Pardington-Purtymun PE, Comeaux JC, Moyzis RK, & Chen DJ (1996) UBL1, a human ubiquitin-like protein associating with human RAD51/RAD52 proteins. *Genomics* 36(2):271-279.
8. Boddy MN, Howe K, Etkin LD, Solomon E, & Freemont PS (1996) PIC 1, a novel ubiquitin-like protein which interacts with the PML component of a multiprotein complex that is disrupted in acute promyelocytic leukaemia. *Oncogene* 13(5):971-982.
9. Matunis MJ, Coutavas E, & Blobel G (1996) A novel ubiquitin-like modification modulates the partitioning of the Ran-GTPase-activating protein RanGAP1 between the cytosol and the nuclear pore complex. *J Cell Biol* 135(6 Pt 1):1457-1470.
10. Mahajan R, Delphin C, Guan T, Gerace L, & Melchior F (1997) A small ubiquitin-related polypeptide involved in targeting RanGAP1 to nuclear pore complex protein RanBP2. *Cell* 88(1):97-107.
11. Mannen H, Tseng HM, Cho CL, & Li SS (1996) Cloning and expression of human homolog HSMT3 to yeast SMT3 suppressor of MIF2 mutations in a centromere protein gene. *Biochem Biophys Res Commun* 222(1):178-180.
12. Chen A, Mannen H, & Li SS (1998) Characterization of mouse ubiquitin-like SMT3A and SMT3B cDNAs and gene/pseudogenes. *Biochem Mol Biol Int* 46(6):1161-1174.
13. Guo D*, et al.* (2004) A functional variant of SUMO4, a new I kappa B alpha modifier, is associated with type 1 diabetes. *Nat Genet* 36(8):837-841.
14. Wang Y & Dasso M (2009) SUMOylation and deSUMOylation at a glance. *J Cell Sci* 122(Pt 23):4249-4252.
15. Gill G (2004) SUMO and ubiquitin in the nucleus: different functions, similar mechanisms? *Genes Dev* 18(17):2046-2059.
16. Olsen SK, Capili AD, Lu X, Tan DS, & Lima CD (2010) Active site remodelling accompanies thioester bond formation in the SUMO E1. *Nature* 463(7283):906-912.
17. Mukhopadhyay D & Dasso M (2007) Modification in reverse: the SUMO proteases. *Trends Biochem Sci* 32(6):286-295.
18. Johnson ES & Gupta AA (2001) An E3-like factor that promotes SUMO conjugation to the yeast septins. *Cell* 106(6):735-744.
19. Kagey MH, Melhuish TA, & Wotton D (2003) The polycomb protein Pc2 is a SUMO E3. *Cell* 113(1):127-137.
20. Meulmeester E, Kunze M, Hsiao HH, Urlaub H, & Melchior F (2008) Mechanism and consequences for paralog-specific sumoylation of ubiquitin-specific protease 25. *Mol Cell* 30(5):610-619.

21. Mikolajczyk J, *et al.* (2007) Small ubiquitin-related modifier (SUMO)-specific proteases: profiling the specificities and activities of human SENPs. *J Biol Chem* 282(36):26217-26224.
22. Schmidt D & Muller S (2002) Members of the PIAS family act as SUMO ligases for c-Jun and p53 and repress p53 activity. *Proc Natl Acad Sci U S A* 99(5):2872-2877.
23. Ungureanu D, Vanhatupa S, Gronholm J, Palvimo JJ, & Silvennoinen O (2005) SUMO-1 conjugation selectively modulates STAT1-mediated gene responses. *Blood* 106(1):224-226.
24. Yang SH, Jaffray E, Hay RT, & Sharrocks AD (2003) Dynamic interplay of the SUMO and ERK pathways in regulating Elk-1 transcriptional activity. *Mol Cell* 12(1):63-74.
25. Yang Y, *et al.* (2011) Inhibition of androgen receptor activity by histone deacetylase 4 through receptor SUMOylation. *Oncogene* 30(19):2207-2218.
26. Verger A, Perdomo J, & Crossley M (2003) Modification with SUMO. A role in transcriptional regulation. *EMBO Rep* 4(2):137-142.
27. Maul GG, Negorev D, Bell P, & Ishov AM (2000) Review: properties and assembly mechanisms of ND10, PML bodies, or PODs. *J Struct Biol* 129(2-3):278-287.
28. Carbia-Nagashima A, *et al.* (2007) RSUME, a small RWD-containing protein, enhances SUMO conjugation and stabilizes HIF-1alpha during hypoxia. *Cell* 131(2):309-323.
29. Sarge KD & Park-Sarge OK (2009) Sumoylation and human disease pathogenesis. *Trends Biochem Sci* 34(4):200-205.
30. McDoniels-Silvers AL, Nimri CF, Stoner GD, Lubet RA, & You M (2002) Differential gene expression in human lung adenocarcinomas and squamous cell carcinomas. *Clin Cancer Res* 8(4):1127-1138.
31. Mo YY, Yu Y, Theodosiou E, Ee PL, & Beck WT (2005) A role for Ubc9 in tumorigenesis. *Oncogene* 24(16):2677-2683.
32. Wang L & Banerjee S (2004) Differential PIAS3 expression in human malignancy. *Oncol Rep* 11(6):1319-1324.
33. Cheng J, Bawa T, Lee P, Gong L, & Yeh ET (2006) Role of desumoylation in the development of prostate cancer. *Neoplasia* 8(8):667-676.
34. Steffan JS, *et al.* (2004) SUMO modification of Huntingtin and Huntington's disease pathology. *Science* 304(5667):100-104.
35. Dorval V & Fraser PE (2006) Small ubiquitin-like modifier (SUMO) modification of natively unfolded proteins tau and alpha-synuclein. *J Biol Chem* 281(15):9919-9924.
36. Li Y, *et al.* (2003) Positive and negative regulation of APP amyloidogenesis by sumoylation. *Proc Natl Acad Sci U S A* 100(1):259-264.
37. Jakobs PM, *et al.* (2001) Novel lamin A/C mutations in two families with dilated cardiomyopathy and conduction system disease. *J Card Fail* 7(3):249-256.
38. Bohren KM, Nadkarni V, Song JH, Gabbay KH, & Owerbach D (2004) A M55V polymorphism in a novel SUMO gene (SUMO-4) differentially activates heat shock transcription factors and is associated with susceptibility to type I diabetes mellitus. *J Biol Chem* 279(26):27233-27238.
39. Nacerddine K, *et al.* (2005) The SUMO pathway is essential for nuclear integrity and chromosome segregation in mice. *Dev Cell* 9(6):769-779.
40. Alkuraya FS, *et al.* (2006) SUMO1 haploinsufficiency leads to cleft lip and palate. *Science* 313(5794):1751.
41. Liu B, *et al.* (2004) PIAS1 selectively inhibits interferon-inducible genes and is important in innate immunity. *Nat Immunol* 5(9):891-898.

42. Fukuda I*, et al.* (2009) Ginkgolic acid inhibits protein SUMOylation by blocking formation of the E1-SUMO intermediate. *Chem Biol* 16(2):133-140.
43. Fukuda I*, et al.* (2009) Kerriamycin B inhibits protein SUMOylation. *J Antibiot (Tokyo)* 62(4):221-224.
44. Förster T (1948) Zwischenmolekulare Energiewanderung und Fluoreszenz. *Ann. Physik* 437(55).
45. Bücher H, Drexhage, K. H., Fleck, M., Kuhn, H., Möbius, D., Schäfer, F. P., Sondermann, J., Sperling, W., Tillmann, P., and Wiegand, J. (1967) *Mol. Cryst.* 2(199).
46. Stryer L & Haugland RP (1967) Energy transfer: a spectroscopic ruler. *Proc Natl Acad Sci U S A* 58(2):719-726.
47. Haugland RP, Yguerabide J, & Stryer L (1969) Dependence of the kinetics of singlet-singlet energy transfer on spectral overlap. *Proc Natl Acad Sci U S A* 63(1):23-30.
48. Stryer L (1978) Fluorescence energy transfer as a spectroscopic ruler. *Annu Rev Biochem* 47:819-846.
49. dos Remedios CG & Moens PD (1995) Fluorescence resonance energy transfer spectroscopy is a reliable "ruler" for measuring structural changes in proteins. Dispelling the problem of the unknown orientation factor. *J Struct Biol* 115(2):175-185.
50. Szollosi J, Damjanovich S, & Matyus L (1998) Application of fluorescence resonance energy transfer in the clinical laboratory: routine and research. *Cytometry* 34(4):159-179.
51. Majoul I, Straub M, Duden R, Hell SW, & Soling HD (2002) Fluorescence resonance energy transfer analysis of protein-protein interactions in single living cells by multifocal multiphoton microscopy. *J Biotechnol* 82(3):267-277.
52. Lu S & Wang Y (2010) Fluorescence resonance energy transfer biosensors for cancer detection and evaluation of drug efficacy. *Clin Cancer Res* 16(15):3822-3824.
53. Solly K*, et al.* (2008) Miniaturization and HTS of a FRET-based membrane potential assay for K(ir) channel inhibitors. *Assay Drug Dev Technol* 6(2):225-234.
54. Appiah KK*, et al.* (2011) A High-Throughput Screen for Receptor Protein Tyrosine Phosphatase-{gamma} Selective Inhibitors. *J Biomol Screen*.
55. Gilson MK & Zhou HX (2007) Calculation of protein-ligand binding affinities. *Annu Rev Biophys Biomol Struct* 36:21-42.
56. Homola J (2008) Surface plasmon resonance sensors for detection of chemical and biological species. *Chem Rev* 108(2):462-493.
57. Boozer C, Kim G, Cong S, Guan H, & Londergan T (2006) Looking towards label-free biomolecular interaction analysis in a high-throughput format: a review of new surface plasmon resonance technologies. *Curr Opin Biotechnol* 17(4):400-405.
58. Freire E, van Osdol WW, Mayorga OL, & Sanchez-Ruiz JM (1990) Calorimetrically determined dynamics of complex unfolding transitions in proteins. *Annu Rev Biophys Biophys Chem* 19:159-188.
59. Perozzo R, Folkers G, & Scapozza L (2004) Thermodynamics of protein-ligand interactions: history, presence, and future aspects. *J Recept Signal Transduct Res* 24(1-2):1-52.
60. Seeman P, Corbett R, & Van Tol HH (1997) Atypical neuroleptics have low affinity for dopamine D2 receptors or are selective for D4 receptors. *Neuropsychopharmacology* 16(2):93-110; discussion 111-135.
61. Martin SF, Tatham MH, Hay RT, & Samuel ID (2008) Quantitative analysis of multi-protein interactions using FRET: application to the SUMO pathway. *Protein Sci* 17(4):777-784.

62. Knipscheer P, van Dijk WJ, Olsen JV, Mann M, & Sixma TK (2007) Noncovalent interaction between Ubc9 and SUMO promotes SUMO chain formation. *EMBO J* 26(11):2797-2807.
63. Tatham MH*, et al.* (2003) Role of an N-terminal site of Ubc9 in SUMO-1, -2, and -3 binding and conjugation. *Biochemistry* 42(33):9959-9969.
64. Nguyen AW & Daugherty PS (2005) Evolutionary optimization of fluorescent proteins for intracellular FRET. *Nat Biotechnol* 23(3):355-360.
65. Aslan K, Lakowicz JR, & Geddes CD (2005) Plasmon light scattering in biology and medicine: new sensing approaches, visions and perspectives. *Curr Opin Chem Biol* 9(5):538-544.
66. Smith EA & Corn RM (2003) Surface plasmon resonance imaging as a tool to monitor biomolecular interactions in an array based format. *Appl Spectrosc* 57(11):320A-332A.
67. Motulski H & Christopoulos A (2003) Fitting models to biological data using linear and nonlinear regression: A practical guide to curve fitting. *GraphPad Software, Inc., San Diego, CA*.
68. Linman MJ, Abbas A, & Cheng Q (2010) Interface design and multiplexed analysis with surface plasmon resonance (SPR) spectroscopy and SPR imaging. *Analyst* 135(11):2759-2767.
69. Berg T (2008) Small-molecule inhibitors of protein-protein interactions. *Curr Opin Drug Discov Devel* 11(5):666-674.
70. Yin H & Hamilton AD (2005) Strategies for targeting protein-protein interactions with synthetic agents. *Angew Chem Int Ed Engl* 44(27):4130-4163.
71. Arkin MR & Wells JA (2004) Small-molecule inhibitors of protein-protein interactions: progressing towards the dream. *Nat Rev Drug Discov* 3(4):301-317.
72. Blazer LL & Neubig RR (2009) Small molecule protein-protein interaction inhibitors as CNS therapeutic agents: current progress and future hurdles. *Neuropsychopharmacology* 34(1):126-141.
73. Vassilev LT*, et al.* (2004) In vivo activation of the p53 pathway by small-molecule antagonists of MDM2. *Science* 303(5659):844-848.
74. Cavalli A*, et al.* (2007) A small molecule targeting the multifactorial nature of Alzheimer's disease. *Angew Chem Int Ed Engl* 46(20):3689-3692.
75. Chan SL*, et al.* (2003) Identification of chelerythrine as an inhibitor of BclXL function. *J Biol Chem* 278(23):20453-20456.
76. Yunus AA & Lima CD (2009) Structure of the Siz/PIAS SUMO E3 ligase Siz1 and determinants required for SUMO modification of PCNA. *Mol Cell* 35(5):669-682.
77. Tang Z, Hecker CM, Scheschonka A, & Betz H (2008) Protein interactions in the sumoylation cascade: lessons from X-ray structures. *FEBS J* 275(12):3003-3015.
78. Elrouby N & Coupland G (2010) Proteome-wide screens for small ubiquitin-like modifier (SUMO) substrates identify Arabidopsis proteins implicated in diverse biological processes. *Proc Natl Acad Sci U S A* 107(40):17415-17420.
79. Kroetz MB & Hochstrasser M (2009) Identification of SUMO-interacting proteins by yeast two-hybrid analysis. *Methods Mol Biol* 497:107-120.
80. Reverter D & Lima CD (2005) Insights into E3 ligase activity revealed by a SUMO-RanGAP1-Ubc9-Nup358 complex. *Nature* 435(7042):687-692.
81. Windecker H & Ulrich HD (2008) Architecture and assembly of poly-SUMO chains on PCNA in Saccharomyces cerevisiae. *J Mol Biol* 376(1):221-231.
82. Yang M, Hsu CT, Ting CY, Liu LF, & Hwang J (2006) Assembly of a polymeric chain of SUMO1 on human topoisomerase I in vitro. *J Biol Chem* 281(12):8264-8274.

83. Carlson CB, Horton RA, & Vogel KW (2009) A toolbox approach to high-throughput TR-FRET-based SUMOylation and DeSUMOylation assays. *Assay Drug Dev Technol* 7(4):348-355.
84. Zhang JH, Chung TD, & Oldenburg KR (1999) A Simple Statistical Parameter for Use in Evaluation and Validation of High Throughput Screening Assays. *J Biomol Screen* 4(2):67-73.
85. Piston DW & Kremers GJ (2007) Fluorescent protein FRET: the good, the bad and the ugly. *Trends Biochem Sci* 32(9):407-414.
86. Giepmans BN, Adams SR, Ellisman MH, & Tsien RY (2006) The fluorescent toolbox for assessing protein location and function. *Science* 312(5771):217-224.
87. Zhang J, Campbell RE, Ting AY, & Tsien RY (2002) Creating new fluorescent probes for cell biology. *Nat Rev Mol Cell Biol* 3(12):906-918.
88. Saitoh N*, et al.* (2006) In situ SUMOylation analysis reveals a modulatory role of RanBP2 in the nuclear rim and PML bodies. *Exp Cell Res* 312(8):1418-1430.
89. Walden H, Podgorski MS, & Schulman BA (2003) Insights into the ubiquitin transfer cascade from the structure of the activating enzyme for NEDD8. *Nature* 422(6929):330-334.
90. Eletr ZM, Huang DT, Duda DM, Schulman BA, & Kuhlman B (2005) E2 conjugating enzymes must disengage from their E1 enzymes before E3-dependent ubiquitin and ubiquitin-like transfer. *Nat Struct Mol Biol* 12(10):933-934.
91. Haas AL, Bright PM, & Jackson VE (1988) Functional diversity among putative E2 isozymes in the mechanism of ubiquitin-histone ligation. *J Biol Chem* 263(26):13268-13275.
92. Walden H*, et al.* (2003) The structure of the APPBP1-UBA3-NEDD8-ATP complex reveals the basis for selective ubiquitin-like protein activation by an E1. *Mol Cell* 12(6):1427-1437.
93. Lois LM & Lima CD (2005) Structures of the SUMO E1 provide mechanistic insights into SUMO activation and E2 recruitment to E1. *EMBO J* 24(3):439-451.
94. Lee I & Schindelin H (2008) Structural insights into E1-catalyzed ubiquitin activation and transfer to conjugating enzymes. *Cell* 134(2):268-278.
95. Huang DT*, et al.* (2007) Basis for a ubiquitin-like protein thioester switch toggling E1-E2 affinity. *Nature* 445(7126):394-398.
96. Lake MW, Wuebbens MM, Rajagopalan KV, & Schindelin H (2001) Mechanism of ubiquitin activation revealed by the structure of a bacterial MoeB-MoaD complex. *Nature* 414(6861):325-329.